Discrimination of multi-photon entangled states using linear optics

Budaraju Sasank
MS16143

A dissertation submitted for the partial fulfilment of BS-MS dual degree in Science

Indian Institute of Science Education and Research Mohali
May 2021

Certificate of Examination

This is to certify that the dissertation titled **"Discrimination of multi-photon entangled states using linear optics"** submitted by Budaraju Sasank (Reg. No. MS16143) for the partial fulfilment of BS-MS dual degree program of the Institute, has been examined by the thesis committee duly appointed by the Institute. The committee finds the work done by the candidate satisfactory and recommends that the report be accepted.

Dr. Manabendra Nath Bera	Dr. Kinjalk Lochan	Dr. Sandeep Kumar Goyal (Supervisor)

Dated: May 4, 2021

Declaration

The work presented in this dissertation has been carried out by me under the guidance of Prof. Sibasish Ghosh at The Institute of Mathematical Sciences (IMSc), Chennai, and Dr. Sandeep Kumar Goyal at the Indian Institute of Science Education and Research Mohali. This work has not been submitted in part or in full for a degree, a diploma, or a fellowship to any other university or institute. Whenever contributions of others are involved, every effort is made to indicate this clearly, with due acknowledgement of collaborative research and discussions. This thesis is a bonafide record of original work done by me and all sources listed within have been detailed in the bibliography.

Budaraju Sasank
(Candidate)

Dated: May 4th, 2021

In my capacity as the supervisor of the candidate's project work, I certify that the above statements by the candidate are true to the best of my knowledge.

Dr. Sandeep Kumar Goyal
(Supervisor)

Acknowledgement

To begin, I would like to sincerely thank Prof. Sibasish Ghosh, who gave me the opportunity to work on this exciting project. His constant patience, support and guidance has helped me greatly to appreciate this field and enjoy every moment of my project. Further, I am deeply indebted to Dr. Sandeep Goyal, who constantly inspired me to think deeply about my project, and supported me at times of confusion and sickness.

I'm very grateful to Akshay Menon for helping with the figures in this text. Discussions with Abhijeet Singh and Ruchira Mishra have helped spark new directions in my project and have motivated me to work hard and constantly search for beauty in physics. I cannot thank them enough for their support.

It would be a crime to not acknowledge the stackexchange pages of Mathematica and LaTeX, without which my project would never have reached this far. Dr. Abhishek Chaudhuri has also constantly supported me through my project and PhD application process, and I'm immensely thankful for all his guidance. I am very fortunate to have found a wonderful set of friends who have stood by me and given me strength through tough times this year. I'm indebted to them for their company and support. Some of them are: Ijaz, Ardra, Shradha, Kausthub, Ruchira, Abhijeet, Anshul, Abhimanyu, Shikhar, Vedang, Vinod, Mayank and Arpan.

Finally, I'm thankful for the infinite love from my brother, parents, and grandparents.

Contents

Abstract

In this thesis, we study the the discrimination of orthogonal multi-photon entangled states using linear optical setups. Beginning with the Bell states, we motivate Bell State Measurements (BSMs) by describing protocols in quantum information theory where they form an integral step. We then review a no-go theorem regarding the possibility of complete BSMs using linear optics, and a result placing a bound on the success probability of discrimination using a restricted linear optical setup containing no ancillaries. We describe and compare various resources proposed in literature that can be used to enhance the success probabilities of BSMs (ancillary entanglement, hyperentanglement, gaussian squeezing, and non-linear optical elements), and study their applications to quantum information protocols.

Next, we study distinguishing between two-photon Non-Maximally Entangled (NME) states and the three-photon GHZ states using ancillary entanglement. For a specific setup with one ancillary entangled pair, we find that the NME states are harder to distinguish than the Bell states. Finally, we place upper bounds on the success probability of GHZ state discrimination using ancillary entanglement as a function of number of photons used, for polarization preserving setups.

Chapter 1

Introduction

This thesis is in the broad field of Linear Optical Quantum Computing (LOQC). This is a paradigm of quantum computing where the information carriers are photons, and quantum gates are implemented through linear optical devices like beam splitters, mirrors and phase shifters. LOQC is an attractive candidate for quantum information processing for several reasons. Firstly, photons are fast and robust carriers of quantum information, and don't decohere quickly. Moreover, linear operations are cost-effective, and easier to implement than non-linear operations. However, the restriction on linear optical gadgets leads to some drawbacks as well. Two-qubit logic gates are harder to implement using LOQC as photons don't interact with each other through linear operations. As a result, universal gates like the CNOT are a challenge to implement. However, in their seminar work in 2001, Knill, Laflamme and Milburn proved that efficient universal quantum computation is possible using only linear optical elements [KLM01], single photons, and projective measurements. Their work has come to be known as the KLM protocol. They showed that a complete set of universal quantum gates can be implemented through LOQC. An effective interaction between the photons is created by the projective measurements at the detectors.

In this thesis, we explore a specific problem in this vast field: discrimination of multi-photon polarization entangled states using linear optics. We explore experimental setups that distinguish between various sets of orthogonal states of photons. The three types of states explored in this thesis are: Bell states, two-photon Non-Maximally Entangled states, and the three-photon GHZ states.

The Bell states are maximally entangled orthogonal states of two qubits. They form a basis for the 4-dimensional (2-qubit) Hilbert space. The Bell states in the polarization degree of freedom are given as

$$\begin{aligned}
\left|\Psi^+\right\rangle &= \frac{1}{\sqrt{2}}\left[h_1^\dagger v_2^\dagger + \ v_1^\dagger h_2^\dagger\right]_{in}|0\rangle \equiv \frac{1}{\sqrt{2}}\left[|HV\rangle + \ |VH\rangle\right] \\
\left|\Psi^-\right\rangle &= \frac{1}{\sqrt{2}}\left[h_1^\dagger v_2^\dagger - \ v_1^\dagger h_2^\dagger\right]_{in}|0\rangle \equiv \frac{1}{\sqrt{2}}\left[|HV\rangle - \ |VH\rangle\right] \\
\left|\Phi^+\right\rangle &= \frac{1}{\sqrt{2}}\left[h_1^\dagger h_2^\dagger + \ v_1^\dagger v_2^\dagger\right]_{in}|0\rangle \equiv \frac{1}{\sqrt{2}}\left[|HH\rangle + \ |VV\rangle\right] \\
\left|\Phi^-\right\rangle &= \frac{1}{\sqrt{2}}\left[h_1^\dagger h_2^\dagger - \ v_1^\dagger v_2^\dagger\right]_{in}|0\rangle \equiv \frac{1}{\sqrt{2}}\left[|HH\rangle - \ |VV\rangle\right]
\end{aligned} \tag{1.1}$$

Here, h and v denote polarization, and the subscripts denote the spatial mode.
A Bell state measurement essentially means measuring in the Bell basis, a process that collapses any

arbitrary state into one of the four Bell states. However, to know which Bell state the collapse has occurred into, we need to be able to distinguish between the Bell states. That is, an experimental apparatus must be able to tell with certainty which of the four Bell states was present. So, a Bell state measurement requires Bell state discrimination.

Discriminating between various orthogonal entangled states using linear optics is the main subject of this thesis. We will investigate experimental setups that try to distinguish between the Bell states and other multi-photon entangled states. To motivate this study, I briefly discuss two quantum information protocols: quantum teleportation and dense coding.

1.1 Teleportation

Quantum teleportation was first proposed by Bennett *et al.* [BBC$^+$93]. It is a process through which one party (we call Alice) can teleport the state of her particle (not the particle itself) to another party (denoted by Bob), without having any prior information about the state to be teleported or the location of Bob's lab. A schematic of the protocol is shown in figure 1.1. Consider a photon in Alice's lab (called photon 1) with an arbitrary polarization state (the subscript 1 is a label for the first photon)

$$|\Psi\rangle_1 = (\alpha\,|H\rangle_1 + \beta\,|V\rangle_1) \tag{1.2}$$

where $\alpha, \beta \in \mathbb{C}$ and satisfy

$$|\alpha|^2 + |\beta|^2 = 1 \tag{1.3}$$

This is the state Alice wishes to teleport to Bob. In order to teleport the state of the above photon, we require a source of maximally entangled states. For photons, the most common method to generate Bell states is through a non-linear process called Spontaneous Parametric Down Conversion (SPDC), where one photon of a higher energy is converted to two photons, conserving energy and momentum. In this process, a beam of UV light is sent through a slab of birefringent crystal (for example, Barium Borate). Most of the light does not undergo down conversion; the efficiency of the SPDC process is usually low. However, if the down conversion process takes place, one can obtain the two photons in an entangled state by selectively placing the detectors. Let us assume that an SPDC source produces two photons (denoted by photons 2 and 3) of the form (where the subscript again denotes the photon numbers)

$$|\Psi\rangle_{23} = \left(\frac{|H\rangle_2\,|V\rangle_3 - |V\rangle_2\,|H\rangle_3}{\sqrt{2}}\right) \tag{1.4}$$

After generating a maximally entangled state, one photon is sent to Alice, and the other is sent to Bob. So, the combined state of the three photons is

$$\begin{aligned} |\Psi\rangle_{123} &= |\Psi\rangle_1 \otimes |\Psi\rangle_{23} \\ &= \frac{1}{\sqrt{2}}\left[\alpha\,|H\rangle_1\,|H\rangle_2\,|V\rangle_3 - \alpha\,|H\rangle_1\,|V\rangle_2\,|H\rangle_3 + \beta\,|V\rangle_1\,|H\rangle_2\,|V\rangle_3 - \beta\,|V\rangle_1\,|V\rangle_2\,|H\rangle_3\right] \end{aligned} \tag{1.5}$$

This three-photon state can be written in a different form, as a combination of the Bell states of the first two photons:

$$\begin{aligned} |\Psi\rangle_{123} = \frac{1}{2}[&\left|\Psi^+\right\rangle_{12}(-\alpha\,|H\rangle_3 + \beta\,|V\rangle_3) - \left|\Psi^-\right\rangle_{12}(\alpha\,|H\rangle_3 + \beta\,|V\rangle_3) \\ &+ \left|\Phi^+\right\rangle_{12}(-\beta\,|H\rangle_3 + \alpha\,|V\rangle_3) + \left|\Phi^-\right\rangle_{12}(\beta\,|H\rangle_3 + \alpha\,|V\rangle_3)] \end{aligned} \tag{1.6}$$

The protocol proceeds as follows. Alice receives two photons, one who's state must be teleported, and

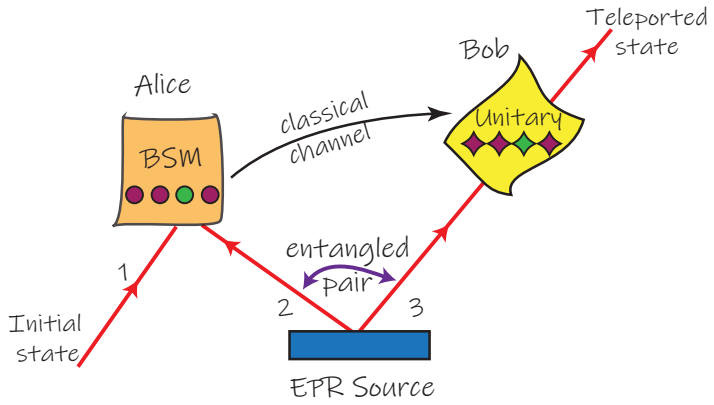

Figure 1.1: General protocol for teleportation [BPM+97]

another photon (photon 2) which is part of a maximally entangled state $|\Psi\rangle_{23}$. Alice now performs a measurement of her two photons onto the Bell basis. That is, she collapses the first two photons into one of the four possible Bell states. From (1.6), we can see that there are four possibilities. If Alice obtains the state $|\Psi^-\rangle_{12}$, the state of Bob's photon is $(\alpha\,|H\rangle_3 + \beta\,|V\rangle_3)$, which is the state that had to be teleported. However, if Alice obtains any of the other Bell states, Bob must perform an appropriate unitary transformation on his photon to retrieve the required state (1.2).

If Alice obtains the state $|\Psi^+\rangle_{12}$, Bob must perform the phase flip operation on his photon. In the computational basis, with $|H\rangle = \begin{bmatrix}1\\0\end{bmatrix}$ and $|V\rangle = \begin{bmatrix}0\\1\end{bmatrix}$ the phase flip gate is given by

$$Z = \begin{bmatrix}1 & 0\\0 & -1\end{bmatrix} \tag{1.7}$$

If $|\Phi^-\rangle_{12}$ is detected, Bob must apply the NOT gate, given by

$$X = \begin{bmatrix}0 & 1\\1 & 0\end{bmatrix} \tag{1.8}$$

Finally, if $|\Phi^+\rangle_{12}$ is detected, Bob must apply the X and the Z gate together

$$XZ = \begin{bmatrix}0 & 1\\1 & 0\end{bmatrix}\begin{bmatrix}1 & 0\\0 & -1\end{bmatrix} = \begin{bmatrix}0 & -1\\1 & 0\end{bmatrix} \tag{1.9}$$

Here is where the importance of Bell state measurements comes in. Alice must be able to tell which Bell state the photons 1 and 2 have collapsed to, and send this information to Bob via a classical channel (like a phone call, say). After receiving one of four messages (that is, two bits of information), Bob will then carry out a unitary rotation of his photon to retrieve the required state (1.2).

So, it is clear that Alice needs to have a device that can discriminate between the Bell states. Ideally, if Alice's Bell state analyzer gives completely exclusive outcomes for all the four Bell states, then in principle, Alice can achieve perfect teleportation of her photon, without ever failing. The first few chapters in this thesis will discuss several Bell state analyzers using linear optical setups.

In the first ever experimental demonstration of teleportation, the device used to distinguish between the Bell states was not perfect; it only had an success probability of 25%. This device was simply a 50-50 (symmetric) beam splitter. How does a beam splitter distinguish between Bell states? Consider

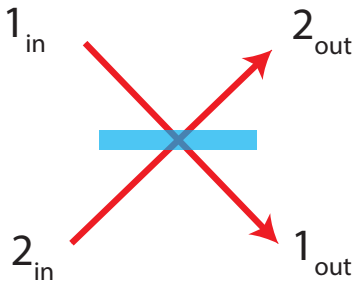

Figure 1.2: A symmetric beam splitter

the beam splitter in figure 1.2. The creation operators corresponding to the input modes are $(a_1^\dagger)_{in}$ and $(a_2^\dagger)_{in}$, and $(a_1^\dagger)_{out}$ and $(a_2^\dagger)_{out}$ for the output modes. Here, $a^\dagger$ can stand for either $h^\dagger$ or $v^\dagger$. A 50-50 beam splitter is characterized by the operator transformations (both the h and v operators transform in the same manner)

$$\begin{pmatrix} a_1^\dagger \\ a_2^\dagger \end{pmatrix}_{in} \rightarrow \frac{1}{\sqrt{2}} \begin{bmatrix} 1 & i \\ i & 1 \end{bmatrix} \begin{pmatrix} a_1^\dagger \\ a_2^\dagger \end{pmatrix}_{out} \qquad a \in \{h, v\} \tag{1.10}$$

If the four Bell states pass through this beam splitter, the final states are given by

$$\begin{aligned} \left|\Psi^+\right\rangle &\equiv \frac{\left[h_1^\dagger v_2^\dagger + v_1^\dagger h_2^\dagger\right]_{in} |0\rangle}{\sqrt{2}} \rightarrow \frac{i\left[h_1^\dagger v_1^\dagger + h_2^\dagger v_2^\dagger\right]_{out} |0\rangle}{\sqrt{2}} \\ \left|\Psi^-\right\rangle &\equiv \frac{\left[h_1^\dagger v_2^\dagger - v_1^\dagger h_2^\dagger\right]_{in} |0\rangle}{\sqrt{2}} \rightarrow \frac{\left[h_1^\dagger v_2^\dagger - v_1^\dagger h_2^\dagger\right]_{out} |0\rangle}{\sqrt{2}} \\ \left|\Phi^\pm\right\rangle &\equiv \frac{\left[h_1^\dagger h_2^\dagger \pm v_1^\dagger v_2^\dagger\right]_{in} |0\rangle}{\sqrt{2}} \rightarrow \frac{i\left[h_1^{\dagger 2} + h_2^{\dagger 2} \pm v_1^{\dagger 2} \pm v_2^{\dagger 2}\right]_{out} |0\rangle}{2\sqrt{2}} \end{aligned} \tag{1.11}$$

Can the final states be distinguished from each other? Firstly, note that the outcomes for $|\Psi^+\rangle$ and $|\Psi^-\rangle$ are different from each other, and are distinct from those for $|\Phi^\pm\rangle$. For $|\Psi^+\rangle$, both the photons are detected on the same side of the beam splitter (either 1 or 2). This is true for the $|\Phi^\pm\rangle$ states as well, but in that case both photons of the same polarization are detected at the same detector. Clearly, there is no way to tell $|\Phi^+\rangle$ apart from $|\Phi^-\rangle$ using the outcomes at the detectors. However, if there is a detection on **both sides** of the beam splitter, then we can tell for sure that the Bell state must've been $|\Psi^-\rangle$, as it is the only state containing terms with both subscripts 1 and 2. Therefore, a symmetric beam splitter can identify two out of the four states, $|\Psi^+\rangle$ and $|\Psi^-\rangle$. In the teleportation experiment, only those cases where a detection on both sides of the beam splitter was seen were considered to identify the Bell state $|\Psi^-\rangle$. The probability of Bob retreiving the correct state for his photon, and achieving accurate teleportation was thus 25%.

1.2 Superdense Coding

Another central application of Bell state analysis is the superdense coding protocol. This is a process through which two classical bits of information can be sent from one party to another, using a single qubit of communication. This process was proposed by Bennett and Wiesner [BW92], and first experimentally realized by Mattle *et al.* [MWKZ96]. Consider a pair of photons. The collective polarization state of this pair lies in a four-dimensional Hilbert space, with one possible basis being: $|HH\rangle, |HV\rangle, |VH\rangle$, and $|VV\rangle$. Since these four states are orthogonal, one can encode each of these

states to be a distinct message, and thus four messages can be communicated by manipulating both the photons (i.e., two bits of information).

However, information can be stored in superpositions of states as well. If we instead choose the four Bell states as our basis:

$$\begin{aligned}
\left|\Psi^+\right\rangle &= \frac{1}{\sqrt{2}}\left[|HV\rangle + |VH\rangle\right] \\
\left|\Psi^-\right\rangle &= \frac{1}{\sqrt{2}}\left[|HV\rangle - |VH\rangle\right] \\
\left|\Phi^+\right\rangle &= \frac{1}{\sqrt{2}}\left[|HH\rangle + |VV\rangle\right] \\
\left|\Phi^-\right\rangle &= \frac{1}{\sqrt{2}}\left[|HH\rangle - |VV\rangle\right]
\end{aligned} \tag{1.12}$$

These states too span a four-dimensional space, and can thus encode 2 bits of information. However, since they are entangled, operations on only one particle can convert any of the above states into any other. For example, let Alice and Bob share the state $|\Psi^+\rangle$, Bob has the first photon and Alice has the second. Bob can perform the following four operations that will convert their state into the four Bell states.

1. Identity operation: $\begin{bmatrix} 1 & 0 \\ 0 & 1 \end{bmatrix} \implies |\Psi^+\rangle \to |\Psi^+\rangle$
2. Polarization flip: $\begin{bmatrix} 0 & 1 \\ 1 & 0 \end{bmatrix} \implies |\Psi^+\rangle \to |\Phi^+\rangle$
3. Polarization dependent phase flip: $\begin{bmatrix} 1 & 0 \\ 0 & -1 \end{bmatrix} \implies |\Psi^+\rangle \to |\Psi^-\rangle$
4. Performing operations 2 and 3 together $\begin{bmatrix} 0 & -1 \\ 1 & 0 \end{bmatrix} \implies |\Psi^+\rangle \to |\Phi^-\rangle$

The protocol of dense coding goes as follows. Firstly, Bob and Alice share a Bell pair between them. Then, Bob performs any of the above four operations on his photon, encoding one of four messages. Then, he physically transfers his photon to Alice. Now, Alice has two photons at her disposal. By finding out which Bell state the two photons are in, Alice can retrieve one of four messages. Thus, Bob has effectively communicated 2 bits of information using operations on only one photon.

In the first experimental demonstration of dense coding [MWKZ96], the Bell state analyzer was simply a beam splitter, just as in the case of teleportation. As we have seen, the four Bell states incident on a symmetric beam splitter yield three distinct type of outcomes (for $|\Psi^+\rangle$, $|\Psi^-\rangle$, and $|\Phi^\pm\rangle$). This means that using linear optics, the best we can do is transmit 3 messages using operations on one photon. This channel capacity of $\log_2 3 = 1.585$ bits per photon is termed dense coding. Later in this thesis, I will discuss attemps to increase the channel capacity beyond this threshold.

Thus, we have seen that Bell state measurements are a vital part of teleportation and dense coding. They are also required for many other quantum information tasks, like quantum communication, cryptography, key distribution and entanglement swapping. Therefore, it is worth exploring various ways in which BSMs are carried out. Further, distinguishing between the three-photon GHZ states is also important in the generalization of the above protocols for multipartite systems. Therefore, studying the discrimination of these multi-photon states could be useful for these protocols. In this

thesis, we also explore distinguishing between Non-Maximally Entangled (NME) states. This question is also worthwhile to study, as these states have also been used for key distribution [XLG01] and quantum communication [LDL$^+$06]. Moreover, if one is not provided with maximally entangled states but has a lesser resource, it is worth exploring how useful these states are for various protocols.

The thesis is arranged as follows. Chapter 2 presents some initial work in this area that placed bounds on the success probability of Bell state measurements for a general class of linear optical setups. In chapter 3, we discuss several methods to surpass the bounds placed by chapter 2 for BSMs. In chapters 4 and 5, we discuss distinguishing between Non-Maximally Entangled states and the GHZ states respectively. We mainly explore the resource of ancillary entanglement to distinguish between the states. Finally, we conclude our results in chapter 6.

Chapter 2

Bounds on success probability of BSMs for linear optical setups

Bell state measurements using general linear optical setups were first discussed in the seminal paper by Lütkenhaus, N., J. Calsamiglia, and K-A. Suominen [LCS99]. The problem they were trying to address was the following: if we restrict our apparatus to contain only linear elements, can the set of orthogonal Bell states be completely distinguished? Consequently, can perfect teleporation be achieved? By linear optical setups, we mean that the set of creation operators of the input modes must be mapped to the creation operators of the output modes via a unitary matrix. Reck et al. proposed a method through which any such $N \times N$ unitary mapping of the spatial modes can be realized using only beam splitters and phase shifters, and the total number of gadgets required scales quadratically with N [RZBB94].

To answer this question, one must study the evolution of the Bell states through the most general linear setup. This analysis was done in the paper [LCS99], and is discussed here. In this chapter, a different notation is used for the Bell states for convenience of calculation. They will be represented by

$$\begin{aligned}
\left|\Psi^1\right\rangle &= \frac{1}{\sqrt{2}}\left(a_1^\dagger a_3^\dagger + a_2^\dagger a_4^\dagger\right)|0\rangle \\
\left|\Psi^2\right\rangle &= \frac{1}{\sqrt{2}}\left(a_1^\dagger a_3^\dagger - a_2^\dagger a_4^\dagger\right)|0\rangle \\
\left|\Psi^3\right\rangle &= \frac{1}{\sqrt{2}}\left(a_1^\dagger a_4^\dagger + a_2^\dagger a_3^\dagger\right)|0\rangle \\
\left|\Psi^4\right\rangle &= \frac{1}{\sqrt{2}}\left(a_1^\dagger a_4^\dagger - a_2^\dagger a_3^\dagger\right)|0\rangle
\end{aligned} \tag{2.1}$$

Here, $a_1^\dagger$ and $a_2^\dagger$ denote creation operators corresponding to two orthogonal polarizations (say H and V) of the first photon, and $a_3^\dagger, a_4^\dagger$ similarily for the second photon. To relate this with our earlier notation, here $\left|\Psi^1\right\rangle$ would correspond to $\frac{1}{\sqrt{2}}(|HH\rangle + |VV\rangle)$.

The authors considered a general setup shown in figure 2.1. The photons in the Bell states are combined (using beam splitters) with some number of additional photons $(D-4)$, and evolved through a unitary matrix U_1. The auxiliary photons can be in any state with a fixed photon number. After this evolution, one particular mode k_1 is picked and measured (we assume ideal photon number resolving detectors). Conditional measurements are allowed, meaning that based on the result obtained at k_1,

some number of additional auxiliary photons can be added and the photons can be evolved through a second unitary U_2 (which depends on the outcome at k_1). This procedure can be repeated any number of times, before the photons finally reach ideal detectors. The authors investigated the orthogonality of these final states after passing through this setup. Let us begin by studying the first

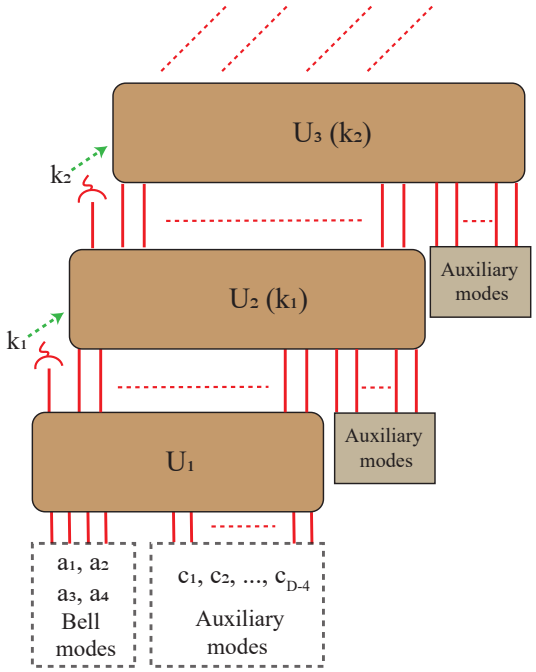

Figure 2.1: General setup for BSM [LCS99]

step of this setup, pictured in figure 2.3. The Bell states are combined with auxiliary photons and are evolved through a unitary U. Then, one mode at the output (d) is picked and measured, collapsing the rest of the modes into one of four possible conditional states, depending on the input Bell state. It turns out that studying this step alone is sufficient to rule out a perfect Bell state analyzer using linear elements, as the conditional states can be non-orthogonal.

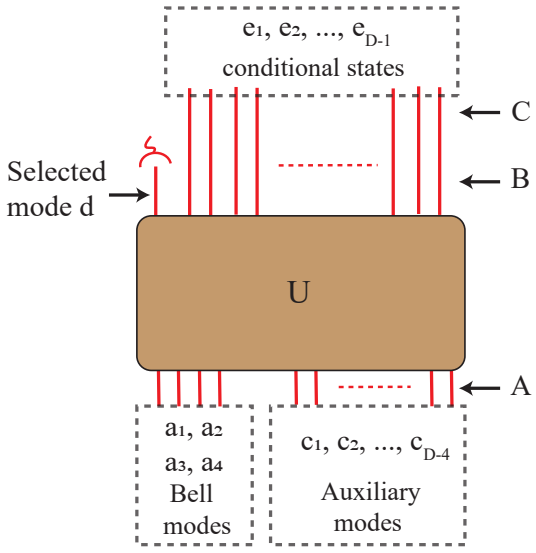

Figure 2.2: First step of the protocol [LCS99]

Let the intial state of the system (at A) be

$$\left|\Psi^{i,\text{total}}\right\rangle = P_{\text{aux}}(c_j^\dagger) P_{\Psi^i}(a_1^\dagger, a_2^\dagger, a_3^\dagger, a_4^\dagger)\left|0\right\rangle \tag{2.2}$$

Here $i = 1, 2, 3, 4$ represents the four Bell states, and $P_{\text{aux}}, P_{\Psi^i}$ are polynomials of the creation operators for the auxillary modes and the Bell states respectively. P_{aux} is an arbitrary polynomial with $(D-4)$ number of modes. The only condition that is assumed on this polynomial is that the auxillary input state has definite photon number. Now, we already know the polynomials P_{Ψ^i}. From (2.1), they are given by

$$\begin{aligned}
P_{\Psi^1} &= \frac{1}{\sqrt{2}}\left(a_1^\dagger a_3^\dagger + a_2^\dagger a_4^\dagger\right) \\
P_{\Psi^2} &= \frac{1}{\sqrt{2}}\left(a_1^\dagger a_3^\dagger - a_2^\dagger a_4^\dagger\right) \\
P_{\Psi^3} &= \frac{1}{\sqrt{2}}\left(a_1^\dagger a_4^\dagger + a_2^\dagger a_3^\dagger\right) \\
P_{\Psi^4} &= \frac{1}{\sqrt{2}}\left(a_1^\dagger a_4^\dagger - a_2^\dagger a_3^\dagger\right)
\end{aligned} \tag{2.3}$$

Now, the state (2.2) passes through an arbitrary unitary operation, where the creation operators of the input state $a_1^\dagger, a_2^\dagger, \ldots, c_{D-4}^\dagger$ are mapped to the output operators $d^\dagger, e_1^\dagger, \ldots, e_{D-1}^\dagger$ through the matrix U. So, at stage B (before the mode d is measured) the state can be written as a polynomial of the output operators. These polynomials depend on U, and in general will be different from those in (2.2). So, they are represented with a tilde.

$$\left|\Psi^{i,\text{total}}\right\rangle = \widetilde{P_{\text{aux}}}(d^\dagger, e_k^\dagger)\widetilde{P_{\Psi^i}}(d^\dagger, e_k^\dagger)\left|0\right\rangle \tag{2.4}$$

We now expand the above polynmials as a power series in $d^\dagger$:

$$\begin{aligned}
\widetilde{P_{\text{aux}}}(d^\dagger, e_k^\dagger) &= (d^\dagger)^{N_{\text{aux}}}\widetilde{Q_{\text{aux}}}(e_k^\dagger) + ... \\
\widetilde{P_{\Psi^i}}(d^\dagger, e_k^\dagger) &= (d^\dagger)^{N_{\text{Bell}}}\widetilde{Q_{\Psi^i}}(e_k^\dagger) + ...
\end{aligned} \tag{2.5}$$

In the above, N_{aux} is order of $d^\dagger$ in $\widetilde{P_{\text{aux}}}$. So, the term written has the highest power of $d^\dagger$ in $\widetilde{P_{\text{aux}}}$, and all further terms have lesser powers of $d^\dagger$, and are just represented by dots. The notation for the $\widetilde{P_{\Psi^i}}$ equation however, is a little different. N_{Bell} is **not** the order of $d^\dagger$ in $\widetilde{P_{\Psi^i}}$. It is rather the maximum order of $d^\dagger$ in all the four polynomials $\widetilde{P_{\Psi^i}}$, $i = 1, 2, 3, 4$. Note that as a consequence, it is possible that one of the polynomials $\widetilde{Q_{\Psi^i}}$ might be 0. Thus, N_{Bell} is independent of i.
So, rewriting equation (2.4), we have

$$\left|\Psi^{i,\text{total}}\right\rangle = \left((d^\dagger)^{N_{\text{aux}}}\widetilde{Q_{\text{aux}}}(e_k^\dagger) + ...\right)\left((d^\dagger)^{N_{\text{Bell}}}\widetilde{Q_{\Psi^i}}(e_k^\dagger) + ...\right)\left|0\right\rangle \tag{2.6}$$

Once both terms are multiplied, we will obtain a polynomial of degree $N_{\text{aux}} + N_{\text{Bell}}$ in d. As per our setup, we now measure the number of photons at the d mode. The number of photons detected will be in between 0 and $N_{\text{aux}} + N_{\text{Bell}}$. We would like to analyze the conditional states of the other photons in the remaining modes once a detection takes place at d.

Let us say that the mode d detects some n_d number of photons. Then, the state of the remaining photons can be determined from (2.6), by simply picking those terms which accompany $(d^\dagger)^{n_d}$. We will obtain four such conditional states for the Bell states (i.e, for $i = 1, 2, 3, 4$). If there is even

one detection scenario where these conditional states are not orthogonal, this implies that the four states $\left|\Psi_i^{\text{total}}\right\rangle$ cannot be distinguished from each other with unit probability, and the unitary U fails as a perfect Bell analyzer.

The main result of the paper was the following: there is always atleast one detection event at d after which the conditional states of the remaining modes are non-orthogonal, **irrespective** of the unitary U used. This means that no matter how the Bell states are evolved through the setup, there is always a possibility that they can't be distinguished with certainity. As a consequence, one can never create a perfect Bell state analyzer using the general scheme in figure 2.1.

We will now prove the above claim. We don't have to analyze all possible photon number detections at d as we only require one example where the conditional states are non-orthogonal. Consider the case where d detects $N = N_{\text{aux}} + N_{\text{Bell}}$ photons. The state of remaining modes is then

$$\left|\Phi^{i,\text{total}}\right\rangle = \widetilde{Q_{\text{aux}}}(e_k^\dagger)\widetilde{Q_{\Psi^i}}(e_k^\dagger)\left|0\right\rangle \tag{2.7}$$

Are these states orthogonal? Taking the inner product of conditional states for two different Bell state inputs, we have

$$\begin{aligned}
\left\langle\Phi^{i,\text{total}}\middle|\Phi^{j,\text{total}}\right\rangle &= \langle 0|\,\widetilde{Q_{\Psi^i}}^\dagger\widetilde{Q_{\text{aux}}}^\dagger\widetilde{Q_{\text{aux}}}\widetilde{Q_{\Psi^j}}\,|0\rangle &(2.8)\\
&= \langle 0|\,\widetilde{Q_{\text{aux}}}^\dagger\widetilde{Q_{\text{aux}}}\widetilde{Q_{\Psi^i}}^\dagger\widetilde{Q_{\Psi^j}}\,|0\rangle &(2.9)\\
&= \sum_{\bar{n}}\langle 0|\,\widetilde{Q_{\text{aux}}}^\dagger\widetilde{Q_{\text{aux}}}\,|\bar{n}\rangle\,\langle\bar{n}|\,\widetilde{Q_{\Psi^i}}^\dagger\widetilde{Q_{\Psi^j}}\,|0\rangle &(2.10)
\end{aligned}$$

Pushing the $\widetilde{Q_{\Psi^i}}^\dagger$ across the $\widetilde{Q_{\text{aux}}}$ operators is allowed since creation operators corresponding to different modes commute. In the final step, we've introduced the identity operator of all the modes. Here $\bar{n} = (n_1, n_2, \ldots, n_D)$ and $|\bar{n}\rangle$ signifies a general product state of all the D modes.

$$\mathbb{1} = \left(\sum_{n=0}^{\infty}|n\rangle\langle n|\right)^{\otimes D} = \sum_{\bar{n}}^{\infty}|\bar{n}\rangle\langle\bar{n}| \tag{2.11}$$

Now, we make some observations. Since $P_{\Psi^i}\left|0\right\rangle$ is a two photon state, so must be $\widetilde{P_{\Psi^i}}\left|0\right\rangle$. This implies (from (2.5)) that $\widetilde{Q_{\Psi^j}}\left|0\right\rangle$ must have photon number $2 - N_{\text{Bell}}$. Clearly then, the inner product $\langle\bar{n}|\,\widetilde{Q_{\Psi^i}}^\dagger\widetilde{Q_{\Psi^j}}\,|0\rangle$ can only be non-zero if $\bar{n} = \bar{0}$. Therefore, the inner product simplifies to

$$\boxed{\left\langle\Phi^{i,\text{total}}\middle|\Phi^{j,\text{total}}\right\rangle = \langle 0|\,\widetilde{Q_{\text{aux}}}^\dagger\widetilde{Q_{\text{aux}}}\,|0\rangle\,\langle 0|\,\widetilde{Q_{\Psi^i}}^\dagger\widetilde{Q_{\Psi^j}}\,|0\rangle} \tag{2.12}$$

Since $\widetilde{Q_{\text{aux}}}$is not zero, the first term in the above expression is a non-zero quantity. The states $\left|\Phi^{i,\text{total}}\right\rangle$ and $\left|\Phi^{j,\text{total}}\right\rangle$ can only be orthogonal if $\widetilde{Q_{\Psi^i}}\left|0\right\rangle$ and $\widetilde{Q_{\Psi^j}}\left|0\right\rangle$ are orthogonal. So, auxiliary photons' contribution cannot make nonorthogonal states orthogonal. This leads us to the crucial conclusion that in the case of d detecting $N_{\text{aux}} + N_{\text{Bell}}$ photons, ancillary photons are of no use at all for perfect state discrimination. (Note: we are not saying that ancillary photons are not a useful resource for state discrimination. In fact, two chapters in this thesis investigate ancillary entanglement for distinguishing between other kinds of states. What we are saying is that there is always atleast one scenario when ancillary photons cannot help us achieve a **perfect** state discrimination.)

Since additional photons are not of any use, we will henceforth assume that the auxiliary modes

$c_1, c_2, \ldots, c_{D-4}$ are in the vacuum state. Let us then specifically study the cases where d detects 1 and 2 photons. Consider an input state which is some linear combination of the four Bell states

$$|\Psi\rangle = \frac{1}{\sqrt{2}}\left[\mu_1\left(a_1^\dagger a_3^\dagger + a_2^\dagger a_4^\dagger\right) + \mu_2\left(a_1^\dagger a_3^\dagger - a_2^\dagger a_4^\dagger\right) + \mu_3\left(a_1^\dagger a_4^\dagger + a_2^\dagger a_3^\dagger\right) + \mu_4\left(a_1^\dagger a_4^\dagger - a_2^\dagger a_3^\dagger\right)\right]|0\rangle \tag{2.13}$$

To write this state in a compact form, we introduce the following symmetric matrix

$$M = 2^{-3/2}\begin{pmatrix} 0 & 0 & \mu_1+\mu_2 & \mu_3+\mu_4 & \ldots & 0 \\ 0 & 0 & \mu_3-\mu_4 & \mu_1-\mu_2 & \ldots & 0 \\ \mu_1+\mu_2 & \mu_3-\mu_4 & 0 & 0 & \ldots & 0 \\ \mu_3+\mu_4 & \mu_1-\mu_2 & 0 & 0 & \ldots & 0 \\ 0 & 0 & 0 & 0 & \ldots & 0 \\ \vdots & \vdots & \vdots & \vdots & \ldots & \vdots \end{pmatrix} \tag{2.14}$$

Using this matrix, (2.13) can be written as

$$|\Psi\rangle = (a_1^\dagger, a_2^\dagger, \ldots, c_{D-4}^\dagger)M(a_1^\dagger, a_2^\dagger, \ldots, c_{D-4}^\dagger)^T|0\rangle \tag{2.15}$$

The state above is transformed by the unitary U (of dimension D × D), which acts on the creation operators as:

$$(a_1^\dagger, a_2^\dagger, \ldots, c_{D-4}^\dagger)^T \to U(d^\dagger, e_1^\dagger, \ldots, e_{D-1}^\dagger)^T \tag{2.16}$$

So, the final state is

$$\begin{aligned} |\Psi\rangle &= (d^\dagger, e_1^\dagger, \ldots, e_{D-1}^\dagger)U^T M U(d^\dagger, e_1^\dagger, \ldots, e_{D-1}^\dagger)^T|0\rangle \\ &\equiv (d^\dagger, e_1^\dagger, \ldots, e_{D-1}^\dagger)\tilde{M}(d^\dagger, e_1^\dagger, \ldots, e_{D-1}^\dagger)^T|0\rangle \end{aligned} \tag{2.17}$$

where $\tilde{M} = U^T M U$. Let us now study the possibilty of a two-photon detection at the d mode. Clearly, the matrix element of $\tilde{M}$ that contributes to this outcome is $\tilde{M}_{11}$, the coefficient of the $d^{\dagger 2}$ term. Taking the first column of U to be $(a, b, c, d, \ldots)^T$, this element can be calculated out to be

$$\tilde{M}_{11} = \frac{1}{\sqrt{2}}\left[\mu_1(ac+bd) + \mu_2(ac-bd) + \mu_3(ad+bc) + \mu_4(ad-bc)\right] \tag{2.18}$$

If the two photon outcome must unambiguously identify one Bell state, then only one Bell state must contribute to the above expression. That is, three of the four coefficients of μ in the above equation must be 0. However, it can be seen that if three coefficients are 0 (which implies either $a = b = 0$, or $c = d = 0$), the fourth one is also forced to be 0. So, a perfect Bell state analyzer can never detect two photons in the d mode. In the following, we will assume the first column of U to be $(a, b, 0, \ldots)^T$. One can also use $(0, 0, c, d\ldots)^T$, and it gives the same result.

We are left to analyze the case of single photon detection in detector d. For this calculation, we represent the matrix U as

$$U = \begin{bmatrix} a & \vec{a_R} \\ b & \vec{b_R} \\ 0 & \vec{c_R} \\ 0 & \vec{d_R} \\ \vdots & \vdots \end{bmatrix} \tag{2.19}$$

where the vectors $\vec{a_R}, \vec{b_R}, \ldots$ are row vectors of dimension $1 \times (D-1)$. After a single photon detection in mode d, the conditional state of the other photon can be obtained from (2.17). Only the first row (or column) of $\tilde{M}$ will contribute to the state. Denoting the first row by $\vec{v_1}$, we have for the (unnormalized) conditional state $|\Phi\rangle$

$$|\Phi\rangle = \vec{v_1}(d^\dagger, e_1^\dagger, \ldots, e_{D-1}^\dagger)^T |0\rangle \tag{2.20}$$

Now, $\vec{v_1}$ can also be explicitly calculated using $\tilde{M} = U^T M U$. Using the form of U in (2.19) and the matrix M in (2.14), we get

$$\vec{v_1} = \frac{1}{2\sqrt{2}} \left(0, \mu_1(a\vec{c_R} + b\vec{d_R}) + \mu_2(a\vec{c_R} - b\vec{d_R}) + \mu_3(b\vec{c_R} + a\vec{d_R}) - \mu_4(b\vec{c_R} - a\vec{d_R})\right) \tag{2.21}$$

In (2.20), we can now directly obtain conditional states for the four Bell states by setting three of the four μ's to zero, and the remaining μ to 1. These turn out to be

$$\begin{aligned}
|\Phi_1\rangle &= \left(a\vec{c_R} + b\vec{d_R}\right)\left(e_1^\dagger, e_2^\dagger, \ldots, e_{D-1}^\dagger\right)^T |0\rangle \\
|\Phi_2\rangle &= \left(a\vec{c_R} - b\vec{d_R}\right)\left(e_1^\dagger, e_2^\dagger, \ldots, e_{D-1}^\dagger\right)^T |0\rangle \\
|\Phi_3\rangle &= \left(a\vec{d_R} + b\vec{c_R}\right)\left(e_1^\dagger, e_2^\dagger, \ldots, e_{D-1}^\dagger\right)^T |0\rangle \\
|\Phi_4\rangle &= \left(a\vec{d_R} - b\vec{c_R}\right)\left(e_1^\dagger, e_2^\dagger, \ldots, e_{D-1}^\dagger\right)^T |0\rangle
\end{aligned} \tag{2.22}$$

We finally must check the orthogonalilty of these states. For perfect state discrimination, the states corresponding to different Bell states must be orthogonal. Let's check this, by first calculating the inner product of $|\Phi_1\rangle$ and $|\Phi_2\rangle$. Below, we also define the two vectors $\vec{e^\dagger} = \left(e_1^\dagger, e_2^\dagger, \ldots, e_{D-1}^\dagger\right)$ and $\vec{e} = (e_1, e_2, \ldots, e_{D-1})$ to express the above conditional states as a dot product of the row vectors of U and $\vec{e^\dagger}$.

$$\begin{aligned}
|\Phi_1\rangle &= \left(a\vec{c_R} + b\vec{d_R}\right) \cdot \vec{e^\dagger} |0\rangle \\
|\Phi_2\rangle &= \left(a\vec{c_R} - b\vec{d_R}\right) \cdot \vec{e^\dagger} |0\rangle \\
\implies \langle\Phi_1|\Phi_2\rangle &= \langle 0| \left(a^* \vec{c_R}^* \cdot \vec{e} + b^* \vec{d_R}^* \cdot \vec{e}\right)\left(a\vec{c_R} \cdot \vec{e^\dagger} - b\vec{d_R} \cdot \vec{e^\dagger}\right) |0\rangle \\
&= |a|^2 |\vec{c_R}|^2 - |b|^2 |\vec{d_R}|^2 - a^* b \vec{c_R}^* \cdot \vec{d_R} + a b^* \vec{c_R} \cdot \vec{d_R}^*
\end{aligned} \tag{2.23}$$

Note however that since different rows of U must be orthogonal, we must have $\vec{c_R} \cdot \vec{d_R}^* = \vec{c_R}^* \cdot \vec{d_R} = 0$. So, the inner product simplifies to

$$\langle\Phi_1|\Phi_2\rangle = |a|^2 |\vec{c_R}|^2 - |b|^2 |\vec{d_R}|^2 \tag{2.24}$$

Similarily, one can calculate all $\binom{4}{2} = 6$ possible overlaps between the $|\Phi\rangle$ states. These are given below.

$$\begin{aligned}
\langle\Phi_1|\Phi_2\rangle &= |a|^2 |\vec{c_R}|^2 - |b|^2 |\vec{d_R}|^2 \\
\langle\Phi_3|\Phi_4\rangle &= -|b|^2 |\vec{c_R}|^2 + |a|^2 |\vec{d_R}|^2
\end{aligned} \tag{2.25}$$

$$\begin{aligned}
\langle\Phi_1|\Phi_3\rangle &= a^* b |\vec{c_R}|^2 + b^* a |\vec{d_R}|^2 \\
\langle\Phi_1|\Phi_4\rangle &= -a^* b |\vec{c_R}|^2 + b^* a |\vec{d_R}|^2 \\
\langle\Phi_2|\Phi_3\rangle &= a^* b |\vec{c_R}|^2 - b^* a |\vec{d_R}|^2 \\
\langle\Phi_2|\Phi_4\rangle &= -a^* b |\vec{c_R}|^2 - b^* a |\vec{d_R}|^2
\end{aligned} \tag{2.26}$$

We now set all the above six quantities to zero. From (2.26), we simply get

$$\begin{aligned} a^* b |c_R|^2 &= 0 \\ b^* a |d_R|^2 &= 0 \end{aligned} \tag{2.27}$$

Further, adding and subtracting the two equations in (2.25), we get

$$\begin{aligned} \left(|a|^2 - |b|^2\right)\left(|c_R|^2 + |d_R|^2\right) &= 0 \\ \left(|a|^2 + |b|^2\right)\left(|c_R|^2 - |d_R|^2\right) &= 0 \end{aligned} \tag{2.28}$$

Since $|a|^2 + |b|^2 \neq 0$, we must have $|c_R|^2 = |d_R|^2$. The above constraints now simplify to

$$\begin{aligned} 2\left(|a|^2 - |b|^2\right)|c_R|^2 &= 0 \\ |c_R|^2 &= |d_R|^2 \\ a^* b |c_R|^2 &= 0 \end{aligned} \tag{2.29}$$

All the above conditions can be satisfied only if the vectors c_R and d_R are null vectors. This is not allowed, as it would make U non-unitary (see (2.19), the condition $U^\dagger U = \mathbb{1}$ cannot be satisfied). We have seen that irrespective of the number of photons detected in d, the conditional states are not orthogonal and thus cannot be distinguished with certainty. So, we reach the following conclusion:

No experimental setup using only linear elements can implement a perfect Bell state analyzer

The natural question to ask now is, if a 100% success probability is not possible, what is the highest success that can be achieved? Using linear optical elements, how many Bell states can be distinguished from each other? Calsamiglia and Lütkenhaus carried forward their previous result and placed a bound on the success probability of BSMs using linear optics [CL01]. Specifically, they considered a restricted setup, with no ancillary photons and no conditional measurements (see figure 2.3). Their analysis is presented below.

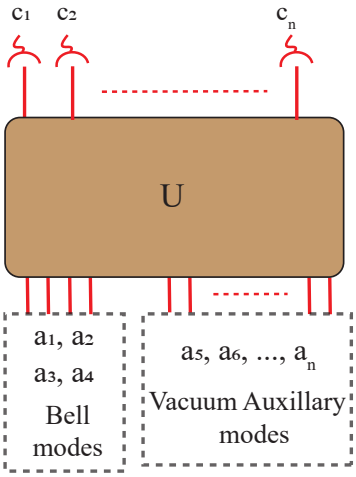

Figure 2.3: A restricted setup: no ancillary photons, and no conditional measurements [CL01]

A different notation is used for the ancillary modes in this paper to make the calculations easier,

as we will see. Recall that the Bell states as before, are given by

$$\begin{aligned}
\left|\Psi^1\right\rangle &= \frac{1}{\sqrt{2}}\left(a_1^\dagger a_3^\dagger + a_2^\dagger a_4^\dagger\right)|0\rangle \\
\left|\Psi^2\right\rangle &= \frac{1}{\sqrt{2}}\left(a_1^\dagger a_3^\dagger - a_2^\dagger a_4^\dagger\right)|0\rangle \\
\left|\Psi^3\right\rangle &= \frac{1}{\sqrt{2}}\left(a_1^\dagger a_4^\dagger + a_2^\dagger a_3^\dagger\right)|0\rangle \\
\left|\Psi^4\right\rangle &= \frac{1}{\sqrt{2}}\left(a_1^\dagger a_4^\dagger - a_2^\dagger a_3^\dagger\right)|0\rangle
\end{aligned} \tag{2.30}$$

The remaining (n-4) modes in the setup have no photons in them. So, the action of the setup is to spread out the two photons of the Bell state across n output modes. The setup is characterized by an arbitrary unitary operation U. The operators $c_1^\dagger, ..., c_n^\dagger$ are creation operators corresponding to the n output modes. Lastly, there are photon detectors at every output mode to measure the number of photons.

Setting aside Bell states for the moment, we begin our analysis with the most general two-photon input state $\left|\Psi^{in}\right\rangle$, formed as a combination of all possible terms with two creation operators (since we don't use any ancillary photons):

$$\left|\Psi^{in}\right\rangle = \sum_{i,j=1}^{n} N_{ij} a_i^\dagger a_j^\dagger |0\rangle \tag{2.31}$$

The coefficients of these terms are represented by N_{ij}, which are arbitrary complex numbers that satisfy the normalization condition $\left\langle\Psi^{in}\middle|\Psi^{in}\right\rangle = 1$. Now, let us define vector $\vec{a}$ to be

$$\vec{a} = \begin{pmatrix} a_1^\dagger \\ a_2^\dagger \\ \vdots \\ a_n^\dagger \end{pmatrix} \tag{2.32}$$

Using this definition, the equation (2.31) can compactly be written in matrix form as:

$$\left|\Psi^{in}\right\rangle = \sum_{i,j=1}^{n} N_{ij} a_i^\dagger a_j^\dagger |0\rangle = \vec{a}^T \; N \; \vec{a}\,|0\rangle \tag{2.33}$$

Here, we have defined N to be the $n \times n$ matrix with the elements N_{ij}. The input state is entirely characterized by this matrix N. Now, since the creation operators corresponding to two different modes commute, we can write

$$\left|\Psi^{in}\right\rangle = \sum_{i,j=1}^{n} N_{ij} a_i^\dagger a_j^\dagger |0\rangle = \sum_{i,j=1}^{n} N_{ij} a_j^\dagger a_i^\dagger |0\rangle \tag{2.34}$$

Since both i and j independently take values from 1 to n, we can interchange indices to obtain

$$\begin{aligned}
\sum_{i,j=1}^{n} N_{ij} a_i^\dagger a_j^\dagger |0\rangle = \sum_{i,j=1}^{n} N_{ij} a_j^\dagger a_i^\dagger |0\rangle &= \sum_{i,j=1}^{n} N_{ji} a_i^\dagger a_j^\dagger |0\rangle \\
\implies N_{ij} = N_{ji} \qquad \forall i, j = 1, ..., n &
\end{aligned} \tag{2.35}$$

Therefore, N must be a symmetric matrix. Now, to write the output state, we require the transformation of the creation operators through the setup. This is given by

$$c_i^\dagger = \sum_{j=1}^{n} U_{ij}^\dagger a_j^\dagger \tag{2.36}$$

Inverting this equation and writing it in matrix form simply gives

$$\vec{a} = U\vec{c} \tag{2.37}$$

Using this relation, we can out write $\left|\Psi^{in}\right\rangle$ terms of the output operators as

$$\left|\Psi^{in}\right\rangle = \vec{a}^T\ N\ \vec{a}\,|0\rangle = \vec{c}^T\ U^T N U\ \vec{c}|0\rangle \equiv \vec{c}^T M\ \vec{c}|0\rangle \tag{2.38}$$

where we have defined $M = U^T N U$ (a relation we saw in the previous proof as well). We can see that (2.38) has the same form as (2.33). Here, the matrix M completely characterizes the output state in terms of the $c^\dagger$ operators. By definition, M is also symmetric since

$$M^T = \left(U^T N U\right)^T = U^T N^T U = U^T N U = M \tag{2.39}$$

Till this point, our analysis holds for any arbitrary input state. Let us now consider specifically the Bell states (2.30). Each of these states would have a different N matrix that characterizes it. The matrix corresponding to the state $|\Psi^\mu\rangle$ will be denoted as N^μ, $\mu = 1, 2, 3, 4$. For these states in particular, the N matrix happens to take a simple form:

$$N^\mu = \frac{1}{2\sqrt{2}} \left(\begin{array}{c|c} W^\mu & 0_{4\times(n-4)} \\ \hline 0_{(n-4)\times 4} & 0_{(n-4)\times(n-4)} \end{array}\right) \tag{2.40}$$

The matrix is divided into four blocks, three of which are completely filled with zeroes ($0_{a\times b}$ represents a zero matrix of dimension $a \times b$). This is because (2.30) makes use of only the operators $a_1^\dagger, a_2^\dagger, a_3^\dagger$ and $a_4^\dagger$ and none of the auxiliary modes. To ensure that none of these auxiliary modes are picked up in the matrix multiplication of (2.33), these three blocks must be 0.
Now, the W matrix in the above is defined as:

$$W^\mu = \begin{pmatrix} 0 & 0 & \delta_{\mu1} + \delta_{\mu2} & \delta_{\mu3} + \delta_{\mu4} \\ 0 & 0 & \delta_{\mu3} - \delta_{\mu4} & \delta_{\mu1} - \delta_{\mu2} \\ \delta_{\mu1} + \delta_{\mu2} & \delta_{\mu3} - \delta_{\mu4} & 0 & 0 \\ \delta_{\mu3} + \delta_{\mu4} & \delta_{\mu1} - \delta_{\mu2} & 0 & 0 \end{pmatrix} \tag{2.41}$$

Note that W^μ is symmetric, leading to a symmetric N^μ, as demanded by (2.35). Moreover, it is straightforward to check that all the four W^μ's are unitary. To justify the equations (2.40) and (2.41), let us work out an example for one of the Bell states.
Taking $\mu = 1$, we have the W matrix to be

$$W^1 = \begin{pmatrix} 0 & 0 & 1 & 0 \\ 0 & 0 & 0 & 1 \\ 1 & 0 & 0 & 0 \\ 0 & 1 & 0 & 0 \end{pmatrix} \tag{2.42}$$

Now, the state corresponding to this N (from (2.33)) is given by

$$|\Psi\rangle = \begin{pmatrix} a_1^\dagger & a_2^\dagger & \dots & a_n^\dagger \end{pmatrix} N^1 \begin{pmatrix} a_1^\dagger \\ a_2^\dagger \\ \vdots \\ a_n^\dagger \end{pmatrix} |0\rangle \tag{2.43}$$

Since only the 4×4 block W contributes to the matrix multiplication, the above equation reduces to

$$\begin{aligned} |\Psi\rangle &= \frac{1}{2\sqrt{2}} \begin{pmatrix} a_1^\dagger & a_2^\dagger & a_3^\dagger & a_4^\dagger \end{pmatrix} W^1 \begin{pmatrix} a_1^\dagger \\ a_2^\dagger \\ a_3^\dagger \\ a_4^\dagger \end{pmatrix} |0\rangle \\ &= \frac{1}{2\sqrt{2}} \begin{pmatrix} a_1^\dagger & a_2^\dagger & a_3^\dagger & a_4^\dagger \end{pmatrix} \begin{pmatrix} 0 & 0 & 1 & 0 \\ 0 & 0 & 0 & 1 \\ 1 & 0 & 0 & 0 \\ 0 & 1 & 0 & 0 \end{pmatrix} \begin{pmatrix} a_1^\dagger \\ a_2^\dagger \\ a_3^\dagger \\ a_4^\dagger \end{pmatrix} |0\rangle \\ &= \frac{1}{2\sqrt{2}} \begin{pmatrix} a_1^\dagger & a_2^\dagger & a_3^\dagger & a_4^\dagger \end{pmatrix} \begin{pmatrix} a_3^\dagger \\ a_4^\dagger \\ a_1^\dagger \\ a_2^\dagger \end{pmatrix} |0\rangle \\ &= \frac{1}{\sqrt{2}} \left(a_1^\dagger a_3^\dagger + a_2^\dagger a_4^\dagger \right) |0\rangle = \left| \Psi^1 \right\rangle \end{aligned} \tag{2.44}$$

So, we obtain the state $\left|\Psi^1\right\rangle$ as required. The equation (2.41) similarily gives the correct W matrices corresponding to the states $\left|\Psi^2\right\rangle, \left|\Psi^3\right\rangle$ and $\left|\Psi^4\right\rangle$.

Moving forward, the output M matrix corresponding to each of the bell states will be called M^μ, and is given by

$$M^\mu = U^T N^\mu U \tag{2.45}$$

Again, since only the first 4×4 block is non-zero, the above equation gets simplified. To see how, we first partition out U in the following manner:

$$U = \left(\begin{array}{c|c} U_{4\times 4} & U_{4\times(n-4)} \\ \hline U_{(n-4)\times 4} & U_{(n-4)\times(n-4)} \end{array} \right) = \left(\begin{array}{c|c} U_1 & U_2 \\ \hline U_3 & U_4 \end{array} \right) \tag{2.46}$$

Note that U_1, U_2, U_3 and U_4 have different dimensions. We can expand out the equation (2.45) using

the above block representation of U,

$$
\begin{aligned}
M^\mu &= \frac{1}{2\sqrt{2}} U^T \left(\begin{array}{c|c} W^\mu & 0_{4\times(n-4)} \\ \hline 0_{(n-4)\times 4} & 0_{(n-4)\times(n-4)} \end{array}\right) U \\
&= \frac{1}{2\sqrt{2}} \left(\begin{array}{c|c} U_1 & U_2 \\ \hline U_3 & U_4 \end{array}\right)^T \left(\begin{array}{c|c} W^\mu & 0_{4\times(n-4)} \\ \hline 0_{(n-4)\times 4} & 0_{(n-4)\times(n-4)} \end{array}\right) \left(\begin{array}{c|c} U_1 & U_2 \\ \hline U_3 & U_4 \end{array}\right) \\
&= \frac{1}{2\sqrt{2}} \left(\begin{array}{c|c} U_1^T & U_3^T \\ \hline U_2^T & U_4^T \end{array}\right) \left(\begin{array}{c|c} W^\mu & 0_{4\times(n-4)} \\ \hline 0_{(n-4)\times 4} & 0_{(n-4)\times(n-4)} \end{array}\right) \left(\begin{array}{c|c} U_1 & U_2 \\ \hline U_3 & U_4 \end{array}\right) \\
&= \frac{1}{2\sqrt{2}} \left(\begin{array}{c|c} U_1^T & U_3^T \\ \hline U_2^T & U_4^T \end{array}\right) \left(\begin{array}{c|c} W^\mu U_1 & W^\mu U_2 \\ \hline 0_{(n-4)\times 4} & 0_{(n-4)\times(n-4)} \end{array}\right) \\
&= \frac{1}{2\sqrt{2}} \left(\begin{array}{c|c} U_1^T W^\mu U_1 & U_1^T W^\mu U_2 \\ \hline U_2^T W^\mu U_1 & U_2^T W^\mu U_2 \end{array}\right)
\end{aligned}
\tag{2.47}
$$

So, we can see that U_3 and U_4 do not contribute to M^μ. Further, the last matrix can be written as

$$
\begin{aligned}
M^\mu &= \frac{1}{2\sqrt{2}} \begin{pmatrix} U_1^T \\ \hline U_2^T \end{pmatrix} \left(W^\mu U_1 \,\middle|\, W^\mu U_2 \right) \\
&= \frac{1}{2\sqrt{2}} \begin{pmatrix} U_1^T \\ \hline U_2^T \end{pmatrix} W^\mu \left(U_1 \,\middle|\, U_2 \right) \\
&\equiv \frac{1}{2\sqrt{2}} U_{tr}^T W^\mu U_{tr}
\end{aligned}
\tag{2.48}
$$

where we define U_{tr} to be the matrix comprising of the first four rows of U

$$
U_{tr} = \left(U_1 \,\middle|\, U_2 \right) = \left(U_{4\times 4} \,\middle|\, U_{4\times(n-4)} \right) \tag{2.49}
$$

Thus, we have shown that only the first four rows of U contribute to the matrix M^μ for the Bell states. With this result, we are now ready to begin our study of discriminating between the four Bell states. We proceed along the same lines as the previous paper. We pick one particular output mode, measure the number of photons and then study the conditional states of the other modes. Our goal is to search for those detector outcomes which can unambiguously identify a particular Bell state.
Let us begin with a two-photon detection at some mode c_i. The question we ask is, can such an outcome arise due to only one Bell state? The probability of a two photon detection at c_i due to the Bell state $|\Psi^\mu\rangle$ is clearly

$$
P_i^\mu[2] = |\langle 2_i|\Psi^\mu\rangle|^2 \tag{2.50}
$$

where the state $|2_i\rangle$ is given by

$$
|2_i\rangle = \frac{1}{\sqrt{2}} c_i^{\dagger 2} |0\rangle \tag{2.51}
$$

We can write $|\Psi^\mu\rangle$ using (2.38), obtaining

$$
\begin{aligned}
\langle 2_i|\Psi^\mu\rangle &= \frac{1}{\sqrt{2}} \langle 0|\, c_i^2 \;\vec{c}^T M^\mu \;\vec{c}\,|0\rangle \\
&= \frac{1}{\sqrt{2}} \sum_{j,k=1}^{n} \langle 0|\, c_i^2 \; M_{jk}^\mu c_j^\dagger c_k^\dagger \,|0\rangle
\end{aligned}
\tag{2.52}
$$

Clearly, the only non-zero term in the above summation is the one with $j = k = i$, leading to

$$\langle 2_i|\Psi^\mu\rangle = \frac{1}{\sqrt{2}}\langle 0|\, c_i^2\ M_{ii}^\mu c_i^{\dagger 2}\,|0\rangle = \sqrt{2}M_{ii}^\mu \tag{2.53}$$

As expected, it is the diagonal element of M that is responsible for two photons appearing in the same mode. The probability of a two-photon detection at mode i is then just

$$P_i^\mu[2] = 2|M_{ii}^\mu|^2 \tag{2.54}$$

Our next task is to evaluate M_{ii}^μ, and we do this by expanding (2.48).

$$(M^\mu)_{ii} = \frac{1}{2\sqrt{2}}(U_{tr}^T W^\mu U_{tr})_{ii} = \frac{1}{2\sqrt{2}}\sum_{\alpha,\beta=1}^{4}(U_{tr}^T)_{i\alpha}(W^\mu)_{\alpha\beta}(U_{tr})_{\beta i} \tag{2.55}$$

Using the explicit form of W^μ from (2.41), we can expand this matrix product to get

$$\begin{aligned}(M^\mu)_{ii} = \sqrt{2}[&\delta_{\mu,1}(U_{1i}U_{3i} + U_{2i}U_{4i}) + \delta_{\mu,2}(U_{1i}U_{3i} - U_{2i}U_{4i})\\ &+\delta_{\mu,3}(U_{1i}U_{4i} + U_{2i}U_{3i}) + \delta_{\mu,4}(U_{1i}U_{4i} - U_{2i}U_{3i})]\end{aligned} \tag{2.56}$$

Now, the two-photon outcome can be unambiguous if and only if a single Bell state contributes to the above probability. If three of the above four coefficients of the delta functions are 0, then only one delta term remains, and this situation would imply that the two-photon outcome arises only because of one Bell state. However, looking at the coefficients in (2.56), it is evident that if three coefficients are 0, then the fourth coefficient is forced to be 0 as well. For example, if the first three coefficients are 0,

$$\begin{aligned}U_{1i}U_{3i} + U_{2i}U_{4i} &= 0\\ U_{1i}U_{3i} - U_{2i}U_{4i} &= 0\\ U_{1i}U_{4i} + U_{2i}U_{3i} &= 0\end{aligned} \tag{2.57}$$

The first two equations imply that $U_{1i}U_{3i} = U_{2i}U_{4i} = 0$. Further, the third equation says that $U_{1i}U_{4i} = -U_{2i}U_{3i}$. It is easy to see that these three equations put together imply that $U_{1i}U_{4i} = U_{2i}U_{3i} = 0$, and thus $U_{1i}U_{4i} - U_{2i}U_{3i} = 0$. We conclude that a two-photon outcome at any mode cannot unambiguously identify a Bell state because the probability of this occurrence can never depend only on one Bell state.

So, if we would like unambiguous identification of a Bell state, we must now study the situation where the two photons are detected at different modes. Let's say that one photon is detected at mode i. Then, the conditional state of the other photon is given by (from (2.38), we collect all terms which contain one $c_i^\dagger$)

$$|\Phi_i^\mu\rangle = 2\sum_{j=1,j\neq i}^{n} M_{ij}^\mu c_j^\dagger\,|0\rangle \tag{2.58}$$

The factor of 2 in the above arises because of the symmetricity of M, $M_{ij} = M_{ji}$. Note that this state in general will not be normalized. The norm of the conditional state will give the probability of obtaining a single photon in mode i. Defining $\vec{m_i}^\mu$ to be the ith column of M^μ, we can rewrite the above as

$$|\Phi_i^\mu\rangle = 2\sum_{j=1,j\neq i}^{n} M_{ij}^\mu c_j^\dagger\,|0\rangle = 2\left((\vec{m_i}^\mu)^T\vec{c} - M_{ii}^\mu c_i^\dagger\right)|0\rangle \tag{2.59}$$

Now, from (2.48), we can extract only the ith column of M^μ. Denoting $\vec{\alpha_i} = (U_{1i}, U_{2i}, U_{3i}, U_{4i})^T$, the ith column of U_{tr}, we get

$$\begin{aligned} M^\mu &= \frac{1}{2\sqrt{2}} U_{tr}^T W^\mu U_{tr} \\ \implies \vec{m_i}^\mu &= \frac{1}{2\sqrt{2}} U_{tr}^T W^\mu \vec{\alpha_i} \equiv \frac{1}{2\sqrt{2}} U_{tr}^T \vec{s_i}^\mu \end{aligned} \tag{2.60}$$

where $\vec{s_i}^\mu = W^\mu \vec{\alpha_i}$ ($\dim(U_{tr}^T) = n \times 4$, $\dim(\vec{s_i}^\mu) = 4 \times 1$) $\implies$ $\dim(\vec{m_i}^\mu) = n \times 1$). Now, for the bell states, the vectors $\vec{s_i}^1, ..., \vec{s_i}^4$ can be explicitly calculated using (2.41). For simple notation, let

$$\vec{\alpha_i} = \begin{pmatrix} a \\ b \\ c \\ d \end{pmatrix} \tag{2.61}$$

Then, the vectors $\vec{s_i}^1, ..., \vec{s_i}^4$ become

$$\begin{aligned} \vec{s_i}^1 &= \begin{pmatrix} c \\ d \\ a \\ b \end{pmatrix} \qquad \vec{s_i}^2 = \begin{pmatrix} c \\ -d \\ a \\ -b \end{pmatrix} \\ \vec{s_i}^3 &= \begin{pmatrix} d \\ c \\ b \\ a \end{pmatrix} \qquad \vec{s_i}^4 = \begin{pmatrix} d \\ -c \\ -b \\ a \end{pmatrix} \end{aligned} \tag{2.62}$$

It turns out that these four vectors are **linearly dependent.** We can see this by confirming that the matrix formed by these four vectors has 0 determinant.

$$\det \begin{pmatrix} c & c & d & d \\ d & -d & c & -c \\ a & a & b & -b \\ b & -b & a & a \end{pmatrix} = 0 \tag{2.63}$$

This linear dependence implies that

$$\sum_{\mu=1}^{4} b_\mu \vec{s_i}^\mu = 0 \text{ with at least one } b_\mu \neq 0 \tag{2.64}$$

However, we also know that none of the vectors are zero (recall that W^μ is unitary):

$$|\vec{s_i}^\mu|^2 = |W^\mu \vec{\alpha_i}|^2 = \vec{\alpha_i}^{*T} W^{\mu\dagger} W^\mu \vec{\alpha_i} = |\vec{\alpha_i}|^2 \tag{2.65}$$

$\vec{\alpha_i}$ is a non-zero vector, so it's magnitude (and therefore $\vec{s_i}^\mu$'s magnitude) must be non-zero. Thus, all the $\vec{s_i}^\mu$'s are non-zero vectors, with the same magnitude. Because of this additional condition, we must have

$$\sum_{\mu=1}^{4} b_\mu \vec{s_i}^\mu = 0 \text{ with at least two } b_\mu \neq 0 \tag{2.66}$$

Crucially, because of the linearity of equations (2.59) and (2.60), we can extend this linear dependence

to the conditional states themselves:

$$\sum_{\mu=1}^{4} b_\mu \left|\Phi_i\right\rangle^\mu = 0 \text{ with at least two } b_\mu \neq 0 \tag{2.67}$$

Thus, we have shown that upon a single-photon detection at mode i, the conditional states of the other photon corresponding to the four Bell states are linearly dependent, irrespective of the particular unitary mapping U. It is well known that an orthogonal set of states can be completely identified via a projection measurement. But if one has to discriminate between non-orthogonal states, this is not possible with a 100% success probability. We can correctly identify a state in some cases, but there is always a non-zero probability of getting an ambiguous measurement outcome - one that could have occurred due to multiple states. Nevertheless, we can discriminate between linearly independent states probabilistically without any error, i.e., and we'll never obtain a misleading outcome. However, discriminating between states from a linearly dependent set is not possible without error, even probabilistically. No measurement can identify a particular state with certainty.

So, if we are given a set of linearly dependent states like in (2.67), the best we can do is to distinguish between a subset of states that are linearly independent of the others, with some non-zero probability. Since the minimum number of vectors from the set $[\vec{s_i}^1, ..., \vec{s_i}^4]$ that are dependent is also 2, this implies that the maximum number of states which may be unambiguously discriminated from each other is 2. We proceed now with calculating the maximum probability of this discrimination. The overlap between two different conditional states is (from (2.59))

$$\langle \Phi_i^\eta | \Phi_i^\mu \rangle = 4 \left[(\vec{m_i}^{\eta *})^T (\vec{m_i}^\mu) - M_{ii}^{\eta *} M_{ii}^\mu \right] \tag{2.68}$$

This inner product can be further simplified using (2.60). Note that

$$\begin{aligned} M_{ii}^\mu = \frac{1}{2\sqrt{2}} (U_{tr}^T \vec{s_i}^\mu)_i = \frac{1}{2\sqrt{2}} \sum_{k=1}^{4} (U_{tr}^T)_{ik} (\vec{s_i}^\mu)_k = \frac{1}{2\sqrt{2}} \sum_{k=1}^{4} (U_{tr})_{ki} (\vec{s_i}^\mu)_k \\ = \frac{1}{2\sqrt{2}} \sum_{k=1}^{4} (\alpha_i)_k (\vec{s_i}^\mu)_k = \frac{1}{2\sqrt{2}} (\alpha_i)^T (\vec{s_i}^\mu) \end{aligned} \tag{2.69}$$

Using the same relation to simplify the first expression $(\vec{m_i}^{\eta *})^T (\vec{m_i}^\mu)$ as well, we finally get

$$\langle \Phi_i^\eta | \Phi_i^\mu \rangle = \frac{1}{2} \left[(\vec{s_i}^{\eta *})^T \vec{s_i}^\mu - ((\vec{\alpha_i})^T \vec{s_i}^{\eta *})((\vec{\alpha_i})^T \vec{s_i}^\mu) \right] \tag{2.70}$$

Now, the probability of one photon detection at c_i can be calculated from the above as the norm of the conditional state $|\Phi_i^\mu\rangle$ (since $\vec{s_i}^\mu = W^\mu \vec{\alpha_i}$)

$$P_i^\mu[1] = \langle \Phi_i^\mu | \Phi_i^\mu \rangle = \frac{1}{2} \left(|\vec{\alpha_i}|^2 - \left| \vec{\alpha_i}^T \vec{s_i}^\mu \right|^2 \right) \leq \frac{1}{2} (|\vec{\alpha_i}|^2) \tag{2.71}$$

Let us denote these two states that can be unambiguously distinguished with some non-zero probability by $\mu = a, b$. So, the probability of unambiguous discrimination when mode i is involved is

$$p_i^s \leq \frac{1}{4} \left(P[1]_i^a + P[1]_i^b \right) \leq \frac{1}{4} |\vec{\alpha_i}|^2 \tag{2.72}$$

The $\frac{1}{4}$ is present due to our assumption of a priori equiprobable Bell states. To find the total

probability of unambiguous discrimination, we have to sum over all modes

$$P^s \leq \frac{1}{2}\sum_{i=1}^{n} p_i^s \tag{2.73}$$

An additional 1/2 factor has to be introduced as each mode is counted twice in the above calculation (if one photon is detected in mode i, obviously another photon has to be detected in another mode j). From (2.72),

$$P^s \leq \frac{1}{8}\sum_{i=1}^{n} |\alpha_i|^2 \tag{2.74}$$

But recall that since U is unitary,

$$\sum_{i=1}^{n} |\alpha_i|^2 = \sum_{i=1}^{n}\sum_{j=1}^{4} |U_{ji}|^2 = \sum_{j=1}^{4}\sum_{i=1}^{n} |U_{ji}|^2 = \sum_{j=1}^{4}(1) = 4 \tag{2.75}$$

Therefore, we finally obtain

$$\boxed{P_s \leq 1/2} \tag{2.76}$$

The maximum success probability of unambiguous discrimination between the Bell states, with no ancillary photons and no conditional measurements is 1/2.

We infer that the maximum number of Bell states that can be unambiguously discriminated from each other using such linear optical setups is two. In the previous chapter, we already came across a setup that separates two out of the four Bell states - simply a 50-50 beam splitter. This proof shows that we cannot unambiguously distinguish between more than two Bell states using these setups. The question we discuss in the next chapter is the following: Can one go beyond this 50% limit? If so, how?

Chapter 3

Enhancing the success probability of BSMs beyond 50%

Since Lutkenhaus's results, there have been several attempts to increase the success rate of BSMs beyond 50% using various resources. In this chapter, some of these results will be reviewed. The resources discussed are gaussian squeezing, ancillary entanglement, non-linear optics, and entanglement in multiple degrees of freedom.

3.1 Gaussian Squeezing

The possibility of using squeezing operations to distinguish between the Bell states was proposed in 2013 by Zaidi and Loock [ZvL13]. Before discussing the paper, the concept of squeezing is briefly introduced.

The single-mode squeezing operator is an unitary operator defined as

$$\hat{S}(\xi) = \exp\left[\frac{1}{2}\left(\xi^* \hat{a}^2 - \xi \hat{a}^{\dagger 2}\right)\right] \tag{3.1}$$

where $\xi = re^{i\theta}$ is an arbitrary complex number. The number r can take any real value, and is known as the squeeze parameter. This operator can be better understood by studying its action on vaccuum, which would result in

$$\hat{S}(\xi)\,|0\rangle \equiv |\xi\rangle = \frac{1}{\sqrt{\cosh \mathrm{r}}} \sum_{m=0}^{\infty} \frac{\sqrt{(2m)!}}{2^m m!} e^{im\theta} (\tanh \mathrm{r})^m\,|2m\rangle \tag{3.2}$$

Squeezing operations can change the number of photons in the state. Therefore, they are **active** linear operations, unlike beam splitters which are passive linear devices. Moreover, the summation only includes the fock states with an even number of photons. Thus, we can conclude (as is clear from (3.1)) that the squeezing adds photons in *pairs*.

Recall the dimensionless quadrature operators

$$\begin{aligned} \hat{X_1} &= \frac{1}{2}(\hat{a} + \hat{a^\dagger}) \\ \hat{X_2} &= \frac{1}{2i}(\hat{a} - \hat{a^\dagger}) \end{aligned} \tag{3.3}$$

They satisfy the uncertainity relation [GKK05]

$$\left\langle (\Delta \hat{X}_1)^2 \right\rangle \left\langle (\Delta \hat{X}_2)^2 \right\rangle \geq \frac{1}{16} \tag{3.4}$$

where $\Delta \hat{X} = \hat{X} - \left\langle \hat{X} \right\rangle$. It is well known that the vaccum state saturates this bound of 1/16, and the variances of both the quadratures are equal. That is,

$$\left\langle (\Delta \hat{X}_1)^2 \right\rangle_{vac} = \left\langle (\Delta \hat{X}_2)^2 \right\rangle_{vac} = \frac{1}{4} \tag{3.5}$$

However, for the squeezed vaccum state, the variances in the quadratures are not equal. Using the Baker-Hausdorf formula, it can be shown that [GKK05]

$$\begin{aligned} \left\langle (\Delta \hat{X}_1)^2 \right\rangle_{vac} &= \frac{1}{4} \left[\cosh^2 r + \sinh^2 r - 2 \sinh r \cosh r \cos\theta \right] \\ \left\langle (\Delta \hat{X}_2)^2 \right\rangle_{vac} &= \frac{1}{4} \left[\cosh^2 r + \sinh^2 r + 2 \sinh r \cosh r \cos\theta \right] \end{aligned} \tag{3.6}$$

which if $\theta = 0$ become

$$\begin{aligned} \left\langle (\Delta \hat{X}_1)^2 \right\rangle_{vac} &= \frac{1}{4} \left[\cosh r - \sinh r \right]^2 = \frac{1}{4} e^{-2r} \\ \left\langle (\Delta \hat{X}_1)^2 \right\rangle_{vac} &= \frac{1}{4} \left[\cosh r + \sinh r \right]^2 = \frac{1}{4} e^{2r} \end{aligned} \tag{3.7}$$

Therefore, in a squeezed vacuum state, the variance along one quadrature is made larger, and the other is reduced. This means that we gain more knowledge about one of the quadratures but lose out on the other. The direction along which this 'squeezing' takes place is given by θ, and the parameter r measures the amount of squeezing. (For $\theta = 0$, the squeezing occurs along the X_1 quadrature, and for $\theta = \pi$ it occurs around X_2.)

With this background, we now discuss the results of the paper [ZvL13]. The apparatus proposed is shown in figure 3.1. It comprises of a 50-50 beam splitter B, two polarizing beam splitters P_1, P_2 (which transmit horizontally polarized and reflect vertically polarized photons), and four single-mode squeezers, all of which are assumed to have the same squeezing parameter r. After passing through

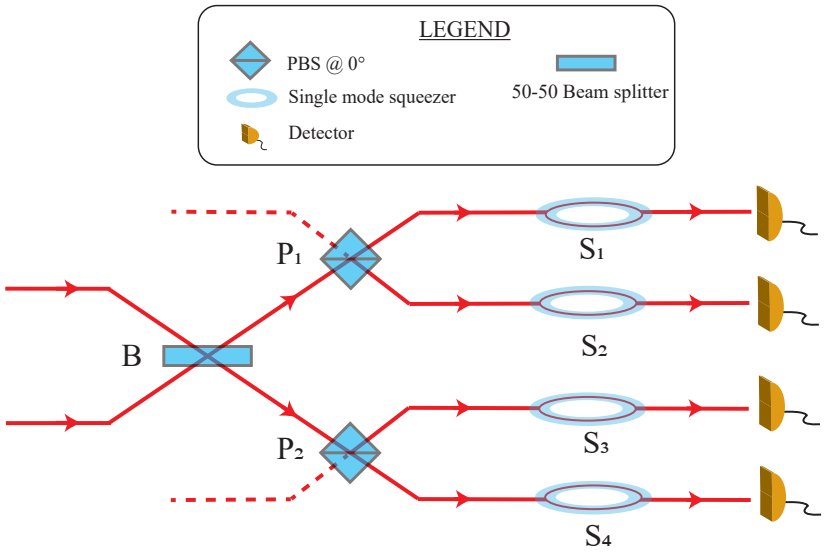

Figure 3.1: BSM apparatus with single-mode squeezers [ZvL13]

the spatial and polarizing beam splitters, the transformation of the Bell states is discussed below (the

effect of a 50-50 beam splitter on the Bell states was given in (1.11)).

$$\left|\Psi^+\right\rangle \xrightarrow{\text{50-50 BS}} \frac{i}{\sqrt{2}}\left[h_1^\dagger v_1^\dagger + h_2^\dagger v_2^\dagger\right]_{out}|0\rangle \tag{3.8}$$

$h_1^\dagger v_1^\dagger|0\rangle$ denotes two photons moving upwards after crossing the beam splitter. Now, when they enter P_1, the horizontally polarized photon is transmitted towards S_1, and the vertically polarized photon is reflected towards S_2. Since S_3 and S_4 don't receive any photons in this case, the resultant state after passing through the polarizing beam splitter will be denoted by the ket $|1100\rangle$, where the numbers in the ket represent the number of photons passing through each of the 4 modes that contain S_1, S_2, S_3 and S_4. Similarily, $h_2^\dagger v_2^\dagger|0\rangle$ denotes two photons that would pass through P_2, and lead to the state represented as $|0011\rangle$. Thus, the evolution of the state $|\Psi^+\rangle$ until the squeezers is given by:

$$\left|\Psi^+\right\rangle \xrightarrow{\text{50-50 BS}} \frac{i}{\sqrt{2}}\left[h_1^\dagger v_1^\dagger + h_2^\dagger v_2^\dagger\right]_{out}|0\rangle \xrightarrow{\text{PBSs}} \frac{i}{\sqrt{2}}\left(|1100\rangle + |0011\rangle\right) \tag{3.9}$$

Similarily, the other states evolve as:

$$\begin{aligned}\left|\Psi^-\right\rangle &\xrightarrow{\text{50-50 BS}} \frac{1}{\sqrt{2}}\left[h_1^\dagger v_2^\dagger - v_1^\dagger h_2^\dagger\right]_{out}|0\rangle \xrightarrow{\text{PBSs}} \frac{1}{\sqrt{2}}\left(|1010\rangle + |0101\rangle\right)\\ \left|\Phi^\pm\right\rangle &\xrightarrow{\text{50-50 BS}} \frac{i}{2\sqrt{2}}\left[h_1^{\dagger 2} + h_2^{\dagger 2} \pm v_1^{\dagger 2} \pm v_2^{\dagger 2}\right]_{out}|0\rangle \xrightarrow{\text{PBSs}} \frac{i}{\sqrt{2}}\left(|2000\rangle + |0002\rangle \pm |0200\rangle \pm |0020\rangle\right)\end{aligned} \tag{3.10}$$

If we are equipped with perfect photon number resolving detectors, then at this stage, we can discriminate perfectly between the states $|\Psi^+\rangle$ and $|\Psi^-\rangle$, but not within $|\Phi^\pm\rangle$. So, the success probability is 50% at this point, as expected.

Crucially, it turns out that the $|\Psi^\pm\rangle$ states will remain perfectly distinguishable **even after squeezing**. The main reason for this is the fact that photons are added in pairs. This implies that, for example, the state $|1010\rangle$ after squeezing will lead to infinitely many terms, all of which must have the form |odd,even,odd,even⟩. This kind of term is unique to $|\Psi^-\rangle$; it cannot arise due to $|\Psi^+\rangle$ or $|\Phi^\pm\rangle$. Similarly, after the state $|\Psi^+\rangle$ is squeezed, we will obtain two types of terms: |odd,odd,even,even⟩ or |even,even,odd,edd⟩. Both of these types of terms can only be obtained due to $|\Psi^+\rangle$. For this reason, we retain the distinguishability of $|\Psi^+\rangle$ and $|\Psi^-\rangle$ after squeezing.

Now, we are left to study the distinguishability of $|\Phi^\pm\rangle$. Before squeezing, both these states gave degenerate outcomes. Now, note that all the four terms in $|\Phi^\pm\rangle$ clearly will give rise to only |even,even,even,even⟩ after squeezing. Therefore, there might be some terms present in $|\Phi^+\rangle$ but not in $|\Phi^-\rangle$ (and vice versa) due to cancellation across the ± sign. This might lead to some unambiguous discrimination of these both states. Indeed, this is exactly what happens. To calculate the final states of $|\Phi^\pm\rangle$ after applying squeezing operations on all spatial modes (with the same squeezing parameter $\xi = r$), we make use the following relations:

$$\begin{aligned}\hat{S}(r)|0\rangle &= \sqrt{\text{sech}r}\exp\left(-\tanh r\ a^{\dagger 2}/2\right)|0\rangle\\ \hat{S}(r)|1\rangle &= (\text{sech}r)^{3/2}\exp\left(-\tanh r\ a^{\dagger 2}/2\right)|1\rangle\\ \hat{S}(r)|2\rangle &= \sqrt{\text{sech}r/2}\,\tanh r\exp\left(-\tanh r\ a^{\dagger 2}/2\right)|0\rangle + (\text{sech}r)^{5/2}\exp\left(-\tanh r\ a^{\dagger 2}/2\right)|2\rangle\end{aligned} \tag{3.11}$$

We can now use the above identities in (3.10) to expand the states $|\Phi^\pm\rangle$. Below, we ignore higher photon-number terms for the moment and only write the result up to two-photon terms.

$$\left|\Phi^{\pm}\right\rangle \rightarrow \frac{\alpha^{\pm}}{\sqrt{2}}\left|0000\right\rangle - \frac{1}{2}\left(\alpha^{\pm}\text{tanh}r - \text{sech}^4 r\right)\left(\left|2000\right\rangle + \left|0002\right\rangle\right) - \frac{1}{2}\left(\alpha^{\pm}\text{tanh}r \mp \text{sech}^4 r\right)\left(\left|0200\right\rangle + \left|0020\right\rangle\right) \tag{3.12}$$

where $\alpha^{\pm}$ is defined as

$$\alpha^{\pm} = (1 \pm 1)\tanh r \,\text{sech}^2 r \tag{3.13}$$

The first thing to note is that the vacuum output $|0000\rangle$ is unique to $|\Phi^+\rangle$ (since $\alpha^- = 0$), thus giving a success probability of greater than 50% for **any** non-zero value of squeezing. So, squeezing indeed helps distinguish between the $|\Phi^{\pm}\rangle$ states. Further, if $r = 0.6585$, then $\alpha^+\text{tanh}r - \text{sech}^4 r = 0$ and the two photon terms become completely unambiguous: they vanish for $|\Phi^+\rangle$, but remain for $|\Phi^-\rangle$. This does not mean that $|\Phi^+\rangle \rightarrow |0000\rangle$, as the above expression does not display higher order terms, many of which remain even after the above condition is imposed.

Through numerical computations involving higher-order terms, the authors confirmed that $r = 0.6585$ leads to the best success probability of unambiguous discrimination between $|\Phi^+\rangle$ and $|\Phi^-\rangle$. To find the success probability, both states are expanded to a particular order, and $r = 0.6585$ is imposed. Then, the terms that become unique for $|\Phi^+\rangle$ and $|\Phi^-\rangle$ are collected. The sum of the absolute squared of the coefficients of all the unique terms for $|\Phi^+\rangle$ gives the probability of identifying the state as $|\Phi^+\rangle$ and not any other state. This computation was performed for both states, and the sum was found to be 0.3748 for $|\Phi^+\rangle$ and 0.1975 for $|\Phi^-\rangle$. Thus the total unambiguous success probability (for initial equiprobable Bell states) becomes

$$\boxed{P = \frac{1}{4}\left(1 + 1 + 0.3748 + 0.1975\right) = 0.643 \equiv 64.3\%} \tag{3.14}$$

An arbitrary two-mode squeezing setup can be decomposed into a multiport linear interferometer, followed by single mode squeezers, and finally another multiport linear interferometer [Bra05]. The authors investigated such setups with two-mode squeezers as well but found that the success probability was bounded by 62.5%.

In a recent work, Saikat Guha and Thomas Kilmer showed that the 64.3% success probability is actually not experimentally attainable [KG19]. It is a point result, for a very specific value of r, $r = 0.6585$. The slightest change in r drops the success probability to around 59%. They showed that a more feasible, experimentally achievable bound is actually around 59.6%.

3.2 Ancillary Entanglement

We now discuss another approach to increase success probability: using additional ancillary entangled photons. This was proposed by W.P. Grice in 2011 [Gri11]. We're already aware that a setup consisting solely of a 50-50 beam splitter yields a success rate of 50%.

$$\begin{aligned}
\left|\Psi^+\right\rangle &\equiv \frac{\left[h_1^\dagger v_2^\dagger + v_1^\dagger h_2^\dagger\right]_{in}\left|0\right\rangle}{\sqrt{2}} \rightarrow \frac{\left[h_1^\dagger v_1^\dagger + h_2^\dagger v_2^\dagger\right]_{out}\left|0\right\rangle}{\sqrt{2}} \\
\left|\Psi^-\right\rangle &\equiv \frac{\left[h_1^\dagger v_2^\dagger - v_1^\dagger h_2^\dagger\right]_{in}\left|0\right\rangle}{\sqrt{2}} \rightarrow \frac{\left[h_1^\dagger v_2^\dagger - v_1^\dagger h_2^\dagger\right]_{out}\left|0\right\rangle}{\sqrt{2}} \\
\left|\Phi^{\pm}\right\rangle &\equiv \frac{\left[h_1^\dagger h_2^\dagger \pm v_1^\dagger v_2^\dagger\right]_{in}\left|0\right\rangle}{\sqrt{2}} \rightarrow \frac{\left[h_1^{\dagger 2} + h_2^{\dagger 2} \pm v_1^{\dagger 2} \pm v_2^{\dagger 2}\right]_{out}\left|0\right\rangle}{2\sqrt{2}}
\end{aligned} \tag{3.15}$$

Let n_h and n_v denote the number of horizontal and vertically polarized photons in the detectors, and $n_{[1]}$ the number of photons that reach detector 1. From (3.15), it is clear that n_h and n_v are odd for $|\Psi^{\pm}\rangle$ and even for $|\Phi^{\pm}\rangle$. Moreover, $n_{[1]}$ is even for $|\Psi^{+}\rangle$ but odd for $|\Psi^{-}\rangle$.

In order to break the degeneracy between the $|\Phi^{\pm}\rangle$ states, Grice uses an ancillary photon pair of the same form as $|\Phi^{+}\rangle$, denoted by $|\gamma_1\rangle$.

$$|\gamma_1\rangle \equiv \frac{1}{\sqrt{2}}\left[h_3^\dagger h_4^\dagger + v_3^\dagger v_4^\dagger\right]_{in}|0\rangle \tag{3.16}$$

The setup analysed is given in figure 3.2 The transformation of the creation operators due to this

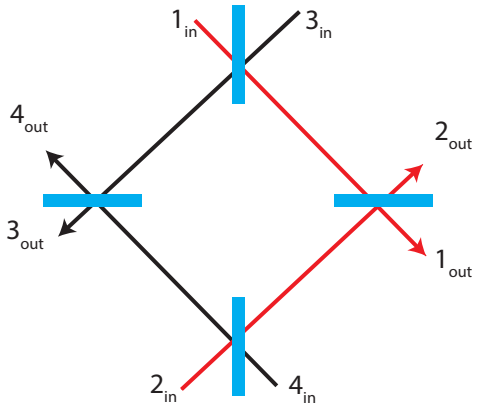

Figure 3.2: Setup with two ancillary photons (passed through the modes 3 and 4), beam splitters are 50-50

setup is given by

$$\begin{pmatrix} a_1^\dagger \\ a_2^\dagger \\ a_3^\dagger \\ a_4^\dagger \end{pmatrix}_{in} \rightarrow \frac{1}{2}\begin{bmatrix} 1 & i & i & -1 \\ i & 1 & -1 & i \\ i & -1 & 1 & i \\ -1 & i & i & 1 \end{bmatrix} \begin{pmatrix} a_1^\dagger \\ a_2^\dagger \\ a_3^\dagger \\ a_4^\dagger \end{pmatrix}_{out} \qquad (a = \{h, v\}) \tag{3.17}$$

Our input states are now

$$|\Psi^{\pm}\rangle|\gamma_1\rangle \equiv \frac{1}{2}\left[\left(h_1^\dagger v_2^\dagger \pm v_1^\dagger h_2^\dagger\right)\left(h_3^\dagger h_4^\dagger + v_3^\dagger v_4^\dagger\right)\right]_{in}|0\rangle \tag{3.18}$$

$$|\Phi^{\pm}\rangle|\gamma_1\rangle \equiv \frac{1}{2}\left[\left(h_1^\dagger h_2^\dagger \pm v_1^\dagger v_2^\dagger\right)\left(h_3^\dagger h_4^\dagger + v_3^\dagger v_4^\dagger\right)\right]_{in}|0\rangle \tag{3.19}$$

The task at hand is to check if the introduction of an ancillary pair helps us better distinguish between the above states. To find the final states, we have to write each of the input operators in (3.18) and (3.19) in terms of the output operators using (3.17).

Note that n_h and n_v are odd for $|\Psi^{\pm}\rangle|\gamma_1\rangle$, and even for $|\Phi^{\pm}\rangle|\gamma_1\rangle$. Since the setup only mixes spatial modes and not polarization, the final states written in terms of the output operators also retain this nature. There will certainly be a large number of terms, but for all of them, n_h and n_v will stay odd (for $|\Psi^{\pm}\rangle|\gamma_1\rangle$) or even ($|\Phi^{\pm}\rangle|\gamma_1\rangle$). So, $|\Psi^{\pm}\rangle|\gamma_1\rangle$ and $|\Phi^{\pm}\rangle|\gamma_1\rangle$ can always be distinguished using the detector outcomes.

Next, we ask if $|\Psi^{+}\rangle|\gamma_1\rangle$ can be discerned from $|\Psi^{-}\rangle|\gamma_1\rangle$. A simple but rather tedious calcula-

tion is involved here, and is discussed below. Beginning with $|\Psi^+\rangle|\gamma_1\rangle$, the term $\left(h_1^\dagger v_2^\dagger + v_1^\dagger h_2^\dagger\right)$ evolves as (from (3.17)):

$$\begin{gathered}\frac{1}{2}\left[\left(h_1^\dagger v_2^\dagger + v_1^\dagger h_2^\dagger\right)\right] \\ \downarrow \\ \frac{1}{8}\left[(h_1^\dagger + ih_2^\dagger + ih_3^\dagger - h_4^\dagger)(iv_1^\dagger + v_2^\dagger - v_3^\dagger + iv_4^\dagger) + (v_1^\dagger + iv_2^\dagger + iv_3^\dagger - v_4^\dagger)(ih_1^\dagger + h_2^\dagger - h_3^\dagger + ih_4^\dagger)\right] \\ = \frac{1}{4}\left[ih_1^\dagger v_1^\dagger - h_1^\dagger v_3^\dagger + ih_2^\dagger v_2^\dagger - h_2^\dagger v_4^\dagger - h_3^\dagger v_1^\dagger - h_4^\dagger v_2^\dagger - ih_3^\dagger v_3^\dagger - ih_4^\dagger v_4^\dagger\right]\end{gathered} \tag{3.20}$$

Further, the second term $\left(h_3^\dagger h_4^\dagger + v_3^\dagger v_4^\dagger\right)$ (that represents the ancillary $|\gamma_1\rangle$) evolves into

$$\begin{gathered}\left[\left(h_3^\dagger h_4^\dagger + v_3^\dagger v_4^\dagger\right)\right] \\ \downarrow \\ \frac{1}{4}\left[(ih_1^\dagger - h_2^\dagger + h_3^\dagger + ih_4^\dagger)(-h_1^\dagger + ih_2^\dagger + ih_3^\dagger + h_4^\dagger) + (iv_1^\dagger - v_2^\dagger + v_3^\dagger + iv_4^\dagger)(-v_1^\dagger + iv_2^\dagger + iv_3^\dagger + v_4^\dagger)\right] \\ = \frac{1}{4}\left[(-ih_1^{\dagger 2} - ih_2^{\dagger 2} + ih_3^{\dagger 2} + ih_4^{\dagger 2} - 2h_1^\dagger h_3^\dagger - 2h_2^\dagger h_4^\dagger) + (-iv_1^{\dagger 2} - iv_2^{\dagger 2} + iv_3^{\dagger 2} + iv_4^{\dagger 2} - 2v_1^\dagger v_3^\dagger - 2v_2^\dagger v_4^\dagger)\right]\end{gathered} \tag{3.21}$$

To obtain the final state, one must multiply the final expressions of both (3.20) and (3.21). Instead of doing that, we make the following observation. Let us define $n_{[1,3]} \equiv n_1 + n_3$. Now, each term in (3.20) and (3.21) have $n_{[1,3]} = 0, 2$. So, $n_{[1,3]}$ is even for all terms in (3.20) and (3.21). Thus, when (3.20) and (3.21) are multiplied, it is clear that for all the resulting terms, $n_{[1,3]}$ will be an **even** number.

Now, we consider the state $|\Psi^-\rangle|\gamma_1\rangle$. We have already looked at the terms arising from $|\gamma_1\rangle$, let us expand the term $\left(h_1^\dagger v_2^\dagger - v_1^\dagger h_2^\dagger\right)$.

$$\begin{gathered}\frac{1}{2}\left[\left(h_1^\dagger v_2^\dagger - v_1^\dagger h_2^\dagger\right)\right] \\ \downarrow \\ \frac{1}{8}\left[(h_1^\dagger + ih_2^\dagger + ih_3^\dagger - h_4^\dagger)(iv_1^\dagger + v_2^\dagger - v_3^\dagger + iv_4^\dagger) - (v_1^\dagger + iv_2^\dagger + iv_3^\dagger - v_4^\dagger)(ih_1^\dagger + h_2^\dagger - h_3^\dagger + ih_4^\dagger)\right] \\ = \frac{1}{4}\left[h_1^\dagger v_2^\dagger - h_2^\dagger v_1^\dagger - ih_2^\dagger v_3^\dagger - h_3^\dagger v_4^\dagger + h_4^\dagger v_3^\dagger + ih_3^\dagger v_2^\dagger - ih_4^\dagger v_1^\dagger + ih_1^\dagger v_4^\dagger\right]\end{gathered} \tag{3.22}$$

Notice that here however, for all terms in (3.22), $n_{[1,3]} = 1$. So, when (3.22) is multiplied with $|\gamma_1\rangle$, all terms that result would have an **odd** value of $n_{[1,3]}$. Therefore, by measuring the number of photons that reach detectors 1 and 3, we can distinguish between the states $|\Psi^+\rangle|\gamma_1\rangle$ and $|\Psi^-\rangle|\gamma_1\rangle$.

The above conclusions imply that ancillary entanglement is not doing any harm, as we are not losing what we had before: the perfect distinguishability of $|\Psi^\pm\rangle$ from $|\Phi^\pm\rangle$, and $|\Psi^+\rangle$ from $|\Psi^-\rangle$.

The power of the ancillary photons becomes evident when we expand the states $|\Phi^\pm\rangle|\gamma_1\rangle$:

$$\begin{aligned}|\Phi^\pm\rangle|\gamma_1\rangle &\equiv \frac{1}{2}\left[\left(h_1^\dagger h_2^\dagger \pm v_1^\dagger v_2^\dagger\right)\left(h_3^\dagger h_4^\dagger + v_3^\dagger v_4^\dagger\right)\right]_{in}|0\rangle \\ &= \frac{1}{2}\left[\left(h_1^\dagger h_2^\dagger h_3^\dagger h_4^\dagger \pm v_1^\dagger v_2^\dagger v_3^\dagger v_4^\dagger + h_1^\dagger h_2^\dagger v_3^\dagger v_4^\dagger \pm v_1^\dagger v_2^\dagger h_3^\dagger h_4^\dagger\right)\right]_{in}|0\rangle\end{aligned} \tag{3.23}$$

In this case, the output terms can either have an equal number (two) of horizontal and vertically

polarized photons or all photons with the same polarization. Both these possibilities are equally likely. When all photons have the same polarization, we cannot tell if the initial state was $|\Phi^+\rangle$ or $|\Phi^-\rangle$; the terms corresponding to $n_h = 4, n_v = 0$ and $n_h = 0, n_v = 4$ are all common to both states. However, we can make a distinction in the other case when $n_h = n_v = 2$. Below, only the terms belonging to $|\Phi^+\rangle$ and $|\Phi^-\rangle$ with $n_h = n_v = 2$ are shown.

$$\begin{aligned}|\Phi^+\rangle \longrightarrow [&h_1^{\dagger 2}v_1^{\dagger 2} + h_1^{\dagger 2}v_2^{\dagger 2} - h_1^{\dagger 2}v_3^{\dagger 2} - h_1^{\dagger 2}v_4^{\dagger 2} + h_2^{\dagger 2}v_1^{\dagger 2} + h_1^{\dagger 2}v_2^{\dagger 2} - h_1^{\dagger 2}v_3^{\dagger 2} - h_2^{\dagger 2}v_4^{\dagger 2} - h_3^{\dagger 2}v_1^{\dagger 2} - h_1^{\dagger 2}v_2^{\dagger 2} + h_3^{\dagger 2}v_3^{\dagger 2} \\ &+h_3^{\dagger 2}v_4^{\dagger 2} - h_4^{\dagger 2}v_1^{\dagger 2} - h_4^{\dagger 2}v_2^{\dagger 2} + h_4^{\dagger 2}v_3^{\dagger 2} + h_4^{\dagger 2}v_4^{\dagger 2} + 2h_1^{\dagger}h_3^{\dagger}v_1^{\dagger}v_3^{\dagger} + 2h_2^{\dagger}h_4^{\dagger}v_1^{\dagger}v_3^{\dagger} + 2h_2^{\dagger}h_4^{\dagger}v_2^{\dagger}v_4^{\dagger} + 2h_1^{\dagger}h_3^{\dagger}v_2^{\dagger}v_4^{\dagger}]\end{aligned} \tag{3.24}$$

$$\begin{aligned}|\Phi^-\rangle \longrightarrow i[&-h_1^{\dagger 2}v_1^{\dagger}v_3^{\dagger} - h_1^{\dagger 2}v_2^{\dagger}v_4^{\dagger} - h_2^{\dagger 2}v_1^{\dagger}v_3^{\dagger} - h_2^{\dagger 2}v_2^{\dagger}v_4^{\dagger} + h_3^{\dagger 2}v_1^{\dagger}v_3^{\dagger} + h_3^{\dagger 2}v_2^{\dagger}v_4^{\dagger} + h_4^{\dagger 2}v_1^{\dagger}v_3^{\dagger} + h_4^{\dagger 2}v_2^{\dagger}v_4^{\dagger} \\ &h_1^{\dagger}h_3^{\dagger}v_1^{\dagger 2} + h_1^{\dagger}h_3^{\dagger}v_2^{\dagger 2} - h_1^{\dagger}h_3^{\dagger}v_3^{\dagger 2} - h_1^{\dagger}h_3^{\dagger}v_4^{\dagger 2} + h_2^{\dagger}h_4^{\dagger}v_1^{\dagger 2} + h_2^{\dagger}h_4^{\dagger}v_2^{\dagger 2} - h_2^{\dagger}h_4^{\dagger}v_3^{\dagger 2} - h_2^{\dagger}h_4^{\dagger}v_4^{\dagger 2}]\end{aligned} \tag{3.25}$$

A close look at equations (3.24) and (3.25) reveals that $n_{[1,2]}$ is even for $|\phi^+\rangle|\gamma_1\rangle$ and odd for $|\phi^-\rangle|\gamma_1\rangle$. This means that $|\phi^+\rangle$ and $|\phi^+\rangle$ can indeed be distinguished from each other (50% of the time), a result that could not be obtained without ancillary photons. Thus, we obtain a success probability of

$$\boxed{P = \frac{1}{4}\left(1 + 1 + \frac{1}{2} + \frac{1}{2}\right) = \frac{3}{4} \equiv 75\%} \tag{3.26}$$

Let us summarize the scheme. We first measure n_h or n_v. If they are odd, the state belongs to $|\Psi^{\pm}\rangle|\gamma_1\rangle$. In this case, we measure $n_{[1,3]}$. If it is odd, the state must be $|\Psi^-\rangle|\gamma_1\rangle$, and if it is even, the state must be $|\Psi^+\rangle|\gamma_1\rangle$.
If n_h or n_v are even, then the state belongs to $|\Phi^{\pm}\rangle|\gamma_1\rangle$. We now check if either n_v or n_h are 0. If so, we cannot tell if the state was $|\Phi^+\rangle|\gamma_1\rangle$ or $|\Phi^-\rangle|\gamma_1\rangle$. If on the other hand, $n_h = n_v = 2$, then we measure $n_{[1,2]}$. If it is even, the state must be $|\Phi^+\rangle|\gamma_1\rangle$ and if it is odd, the state is $|\Phi^-\rangle|\gamma_1\rangle$.

We have seen that one pair of ancillary photons yields a success probability of 75%. Intuitively then, we can expect that additional ancillary can be of more help. This is indeed the case. Grice also generalized the above setup to include n pairs of ancillary photons and found that adding $2^N - 2$ photons yields a success rate of $1 - 1/2^N$. Thus, we can achieve arbitrarily complete Bell state measurements using linear optics by using Grice's method.
However, an important caveat must be stated here. To go beyond 75% with this setup, we require 4-photon entangled, 8-photon entangled states, and so on.

$$\begin{aligned}|\gamma_1\rangle &= \frac{1}{\sqrt{2}}\left[h_3^{\dagger}h_4^{\dagger} + v_3^{\dagger}v_4^{\dagger}\right]_{in}|0\rangle \\ |\gamma_2\rangle &= \frac{1}{\sqrt{2}}\left[h_5^{\dagger}h_6^{\dagger}h_7^{\dagger}h_8^{\dagger} + v_5^{\dagger}v_6^{\dagger}v_7^{\dagger}v_8^{\dagger}\right]_{in}|0\rangle \\ &\vdots\end{aligned}$$

States like $|\gamma_2\rangle$ and beyond are challenging to produce in a lab. Therefore, this method might be impractical from an experimental perspective (to reach probabilities higher than 75%).

3.3 Non-linear Optics

Taking a short digression from linear optics, we discuss an experimental result of Kim, Kulik, and Shih [KKS01] (2001) where a **complete** BSM and teleportation was achieved using non-linear optical elements. A schematic of their apparatus is shown in figure 3.3.

A non-linear medium is one where the polarization response of the medium does not vary linearly with the applied electric field. The polarization density $P(t)$ of a dielectric medium in general varies as

$$\vec{P}(t) = \epsilon_0 \left(\chi^{(1)} \vec{E}(t) + \chi^{(2)} \vec{E}^2(t) + \chi^{(3)} \vec{E}^3(t) + \dots \right) \tag{3.27}$$

In the above, $\chi^{(n)}$ is an (n+1)th order tensor. These are known as the susceptibility tensors and are material dependent. For a linear process, all the tensors $\chi^{(n)}$ beyond $n = 1$ are zero. Some examples of non-linear processes are SPDC, the Kerr effect, and four-wave mixing. The specific non-linear process used in this paper is known as Sum Frequency Generation (SFG). This is a second-order nonlinear phenomena ($\chi^{(2)} \neq 0$), where two photons (of frequencies ω_1 and ω_2) combine together, get annihilated and create one photon of higher energy (ω_3). This process is parametric, which means that the state of the medium is unchanged due to the interaction. Therefore, the energy and momentum of the optical field are conserved. Energy conservation implies:

$$\hbar\omega_1 + \hbar\omega_2 = \hbar\omega_3 \tag{3.28}$$

Efficient SFG demands that a phase matching condition must also be satisfied (momentum conservation)

$$\hbar\kappa_1 + \hbar\kappa_2 \approx \hbar\kappa_3 \tag{3.29}$$

Another property of a second-order non-linear process is that it cannot occur in centrosymmetric media. The light has to interact with matter that is asymmetric (for instance, on a material's surface). For this reason, the SFG process can be used as a spectroscopic tool to study surfaces [VT05].

In a uniaxial crystal (like Barium Borate), all directions except one are equivalent and have the same refractive index. The unique direction which has a different refractive index is called the optic axis of the crystal. So, the crystal can be rotated about this axis without changing its optical properties. The difference between these two refractive indices is called the birefringence of the crystal. A ray of light that travels along the optic axis and having polarization perpendicular to the optic axis is called an ordinary ray. This ray would experience the same refractive index due to the material, irrespective of its polarization.

Consider a ray propagating along a direction different from the optic axis. The polarization of this ray can be resolved into two components; one which lies in the plane perpendicular to the optic axis and another perpendicular to this direction. A ray with the former polarization behaves like an ordinary ray. However, the second ray has a polarization component along the optic axis and experiences a direction-dependent refractive index. This ray is termed the extraordinary ray. Thus, in general, a ray of light passing through a birefringent crystal splits up into two rays, an ordinary ray, and an extraordinary ray. This causes the process of double refraction.

There are different types of SFG depending on the polarizations of the incoming and outgoing photons and the optic axis of the crystal. Some common types are:

- Type-0 : Two photons with extraordinary polarization w.r.t the crystal are converted to a photon with extraordinary polarization.
- Type-I : Two photons with ordinary polarization w.r.t the crystal are converted to a photon with extraordinary polarization.

- Type-II : Two photons with orthogonal polarization w.r.t the crystal are converted to a photon with extraordinary polarization.

In this paper, the Type-I and the Type-II SFG are used. The SPDC source creates two photons 2

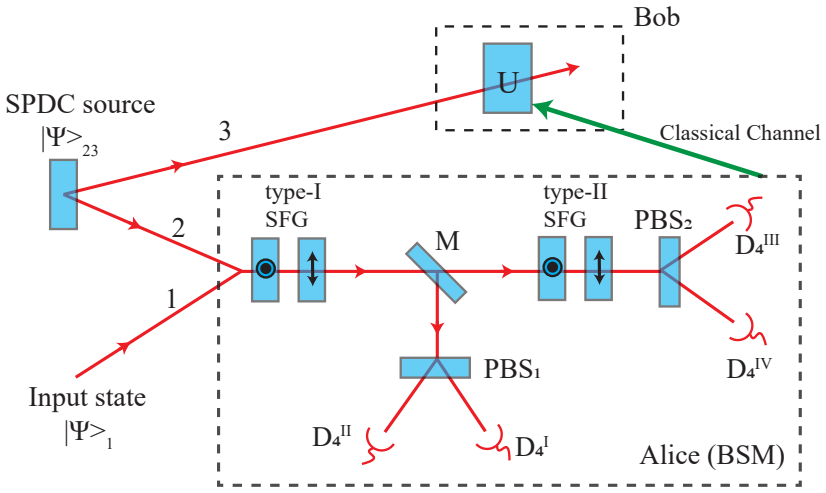

Figure 3.3: Non-linear BSM setup [KKS01]

and 3 in an entangled state (assumed to be $|\Phi^-\rangle$ in this calculation). The photon we wish to teleport (photon 1) is sent to Alice's lab along with photon 2. Both the photons pass through two SFG crystals of each type. The symbols on the SFG devices denote the optic axis of the crystal. The concentric circles represent a crystal with optic axis along the horizontal, and the arrow represents a crystal with optic axis vertical. Therefore, as per our discussion above, the action of the four SFG crystals in the setup, in order, are described by

$$|V_1V_2\rangle \to |H_4\rangle$$
$$|H_1H_2\rangle \to |V_4\rangle$$

$$|H_1V_2\rangle \to |H_4\rangle$$
$$|V_1H_2\rangle \to |V_4\rangle$$

where the photon created by the SFG process is denoted with the subscript 4. Those photons that undergo SFG are reflected by a wavelength selective dichroic mirror onto polarizing beam splitters oriented at 45°, and finally reach the detectors $D_4^I, D_4^{II}, D_4^{III}, D_4^{IV}$.

Let us study the effect of this process on the teleportation protocol. If we'd like to teleport the state

$$|\Psi_1\rangle = \alpha\,|H_1\rangle + \beta\,|V_1\rangle \tag{3.30}$$

using the entangled pair

$$|\Psi_{23}\rangle = \frac{1}{\sqrt{2}}\left(|H_2H_3\rangle - |V_2V_3\rangle\right) \tag{3.31}$$

The complete state of the three photons prior to measurement is then

$$|\Psi_{123}\rangle = \frac{\alpha}{\sqrt{2}}\left(|H_1H_2H_3\rangle - |H_1V_2V_3\rangle\right) + \frac{\beta}{\sqrt{2}}\left(|V_1H_2H_3\rangle - |V_1V_2V_3\rangle\right) \tag{3.32}$$

The Type-I SFG acts on the first and the fourth term in (3.32), and the dichroic mirror reflects the result towards G1. So, the final state corresponding to these terms is

$$\begin{aligned} |\Psi_{43}\rangle &= \alpha\,|V_4H_3\rangle - \beta\,|H_4V_3\rangle \\ &= \frac{1}{\sqrt{2}}\left[|45^\circ{}_4\rangle\,(\alpha\,|H\rangle_3 - \beta\,|V\rangle_3) + |135^\circ{}_4\rangle\,(\alpha\,|H\rangle_3 + \beta\,|V\rangle_3)\right] \end{aligned} \tag{3.33}$$

where, the states $|45^\circ{}_4\rangle$ and $|135^\circ{}_4\rangle$ are defined as

$$\begin{aligned} |45^\circ{}_4\rangle &= \frac{1}{\sqrt{2}}(-\,|H_4\rangle + |V_4\rangle) \\ |135^\circ{}_4\rangle &= \frac{1}{\sqrt{2}}(|H_4\rangle + |V_4\rangle) \end{aligned} \tag{3.34}$$

Similarily, the Type-II SFG acts on the second and third terms, and the resulting photon state at G2 is

$$|\Psi_{43}\rangle = \frac{1}{\sqrt{2}}\left[|45^\circ{}_4\rangle\,(-\alpha\,|H\rangle_3 + \beta\,|V\rangle_3) + |135^\circ{}_4\rangle\,(-\alpha\,|H\rangle_3 - \beta\,|V\rangle_3)\right] \tag{3.35}$$

Based on which of the four detectors $D_4^I, D_4^{II}, D_4^{III}, D_4^{IV}$ clicks, a rotation can be performed on the 3rd photon, and the required state (3.30) can be retrieved. Thus, a **complete** Bell state measurement can be performed using this process.

Even though a complete BSM has been achieved, this does not demonstrate perfect teleportation. This is because non-linear processes are very inefficient ($\sim 10^{-6}$), and we can never tell if a photon sent into the setup will actually undergo the SFG process or not. Thus, this protocol will be unreliable if a single arbitrary state has to be teleported.

3.4 Entanglement in two degrees of freedom

The last resource we will discuss is possibly the most important one in the context of linear optics. Can we distinguish between the Bell states if they are also entangled in another degree of freedom? This question was first answered by P. Kwait and Harald Weinfurter in 1998 [KW98]. They showed that equipped with additional entanglement, **perfect** discrimination of these states is possible. Entanglement in multiple degrees of freedom is often termed 'hyperentanglement'. One of the schemes in [KW98] is discussed here.
Consider the states below, which are entangled in both polarization and momentum/path degrees of freedom.

$$\begin{aligned} \left|\Psi^\pm\right\rangle &= \frac{1}{2}\left[(a_H^\dagger b_V^\dagger \pm a_V^\dagger b_H^\dagger) + (c_H^\dagger d_V^\dagger \pm c_V^\dagger d_H^\dagger)\right]|0\rangle \\ \left|\Phi^\pm\right\rangle &= \frac{1}{2}\left[(a_H^\dagger b_H^\dagger \pm a_V^\dagger b_V^\dagger) + (c_H^\dagger d_H^\dagger \pm c_V^\dagger d_V^\dagger)\right]|0\rangle \end{aligned} \tag{3.36}$$

The proposed setup to distinguish between these states is shown in figure 3.4. The states in (3.36) pass through a beam splitter, and then two polarizing beam splitters oriented at 0°, and four polarizing beam splitters oriented at 45°, before being detected at photon-number resolving detectors. The transformations of the creation operators across this setup are given by the following relations.

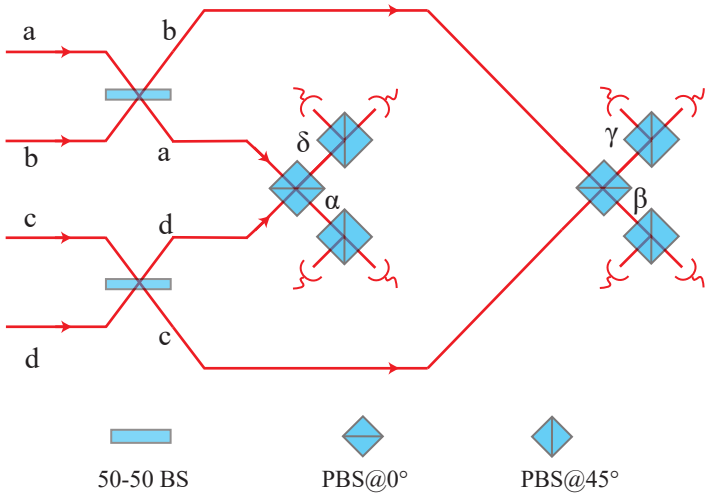

Figure 3.4: Bell state analysis using polarization-momentum hyperentanglement [KW98]

Through the 50-50 beam splitter:

$$\begin{aligned} a^\dagger &\to \frac{1}{\sqrt{2}}\left(a^\dagger + ib^\dagger\right) & b^\dagger &\to \frac{1}{\sqrt{2}}\left(ia^\dagger + b^\dagger\right) \\ c^\dagger &\to \frac{1}{\sqrt{2}}\left(c^\dagger + id^\dagger\right) & d^\dagger &\to \frac{1}{\sqrt{2}}\left(ic^\dagger + d^\dagger\right) \end{aligned} \tag{3.37}$$

Since a beam splitter preserves polarization of photons, the relations above are equally valid for creation operators corresponding to H and V. Now, the polarizing beam splitter oriented at 0°transmits horizontally polarized photons, and reflects vertically polarized photons. So its action is given by

$$\begin{aligned} a_H^\dagger &\to \alpha_H^\dagger & a_V^\dagger &\to \delta_V^\dagger \\ b_H^\dagger &\to \beta_H^\dagger & b_V^\dagger &\to \gamma_V^\dagger \\ c_H^\dagger &\to \gamma_H^\dagger & c_V^\dagger &\to \beta_V^\dagger \\ d_H^\dagger &\to \delta_H^\dagger & d_V^\dagger &\to \alpha_V^\dagger \end{aligned} \tag{3.38}$$

Finally, the action of the polarizing beam splitter oriented at 45°is ($X \to \alpha, \beta, \gamma, \delta$):

$$\begin{aligned} X_H^\dagger &\to \frac{1}{\sqrt{2}}\left(X_{45}^\dagger + X_{-45}^\dagger\right) \\ X_V^\dagger &\to \frac{1}{\sqrt{2}}\left(X_{45}^\dagger - X_{-45}^\dagger\right) \end{aligned} \tag{3.39}$$

Our task now is to use the relations in (3.37), (3.38), and (3.39) to evolve the states (3.36), and analyse the possible outcomes. The case of $|\Psi^+\rangle$ is dealt with in detail below.

$$
\begin{aligned}
|\Psi^+\rangle &= \frac{1}{2}\left[(a_H^\dagger b_V^\dagger + a_V^\dagger b_H^\dagger) + (c_H^\dagger d_V^\dagger + c_V^\dagger d_H^\dagger)\right]|0\rangle \xrightarrow{\text{50-50 BS}} \\
&\frac{1}{4}\left[(a_H^\dagger + ib_H^\dagger)(ia_V^\dagger + b_V^\dagger) + (a_V^\dagger + ib_V^\dagger)(ia_H^\dagger + b_H^\dagger) + (c_H^\dagger + id_H^\dagger)(ic_V^\dagger + d_V^\dagger) + (c_V^\dagger + id_V^\dagger)(ic_H^\dagger + d_H^\dagger)\right] \\
&= \frac{1}{2}\left[(ia_H^\dagger a_V^\dagger + ib_H^\dagger b_V^\dagger) + (ic_H^\dagger c_V^\dagger + id_H^\dagger d_V^\dagger)\right]|0\rangle \\
&\xrightarrow{\text{PBS @ 0°}} \frac{1}{2}\left[(i\alpha_H^\dagger \delta_V^\dagger + i\beta_H^\dagger \gamma_V^\dagger) + (i\gamma_H^\dagger \beta_V^\dagger + i\delta_H^\dagger \alpha_V^\dagger)\right]|0\rangle \\
&\xrightarrow{\text{PBS @ 45°}} \frac{i}{4}[(\alpha_{45}^\dagger + \alpha_{-45}^\dagger)(\delta_{45}^\dagger - \delta_{-45}^\dagger) + (\beta_{45}^\dagger + \beta_{-45}^\dagger)(\gamma_{45}^\dagger - \gamma_{-45}^\dagger) \\
&+(\gamma_{45}^\dagger + \gamma_{-45}^\dagger)(\beta_{45}^\dagger - \beta_{-45}^\dagger) + (\delta_{45}^\dagger + \delta_{-45}^\dagger)(\alpha_{45}^\dagger - \alpha_{-45}^\dagger)]\,|0\rangle \\
&= \frac{1}{2}\left[\alpha_{45}^\dagger \delta_{45}^\dagger - \alpha_{-45}^\dagger \delta_{-45}^\dagger + \beta_{45}^\dagger \gamma_{45}^\dagger - \beta_{-45}^\dagger \gamma_{-45}^\dagger\right]|0\rangle
\end{aligned}
\tag{3.40}
$$

A similar calculation can be done for the other Bell states as well. The final result for all the states is shown below.

$$
\begin{aligned}
|\Psi^+\rangle &\to \frac{1}{2}\left[\alpha_{45}^\dagger \delta_{45}^\dagger - \alpha_{-45}^\dagger \delta_{-45}^\dagger + \beta_{45}^\dagger \gamma_{45}^\dagger - \beta_{-45}^\dagger \gamma_{-45}^\dagger\right]|0\rangle \\
|\Psi^-\rangle &\to \frac{1}{2}\left[\alpha_{45}^\dagger \gamma_{45}^\dagger - \alpha_{-45}^\dagger \gamma_{-45}^\dagger - \beta_{45}^\dagger \delta_{45}^\dagger + \beta_{-45}^\dagger \delta_{-45}^\dagger\right]|0\rangle \\
|\Phi^+\rangle &\to \frac{1}{2}\Big[\alpha_{45}^\dagger \alpha_{45}^\dagger - \alpha_{-45}^\dagger \alpha_{-45}^\dagger + \beta_{45}^\dagger \beta_{45}^\dagger - \beta_{-45}^\dagger \beta_{-45}^\dagger + \\
&\qquad \gamma_{45}^\dagger \gamma_{45}^\dagger - \gamma_{-45}^\dagger \gamma_{-45}^\dagger + \delta_{45}^\dagger \delta_{45}^\dagger - \delta_{-45}^\dagger \delta_{-45}^\dagger\Big]|0\rangle \\
|\Phi^+\rangle &\to \frac{-i}{2}\left[\alpha_{45}^\dagger \alpha_{-45}^\dagger + \beta_{45}^\dagger \beta_{-45}^\dagger + \gamma_{45}^\dagger \gamma_{-45}^\dagger + \delta_{45}^\dagger \delta_{-45}^\dagger\right]|0\rangle
\end{aligned}
\tag{3.41}
$$

A close look at the above equations confirms that every possible outcome above occurs uniquely for only one state. This means that no matter what outcome appears at the detectors, we can always trace that outcome uniquely back to one of the four states. Thus, the hyperentangled Bell states can be perfectly distinguished from each other, and this linear optical setup can perform perfect discrimination of the four states in (3.36). The reason we achieve a 100% success here can be attributed to an increase in the number of possible outcomes at the detectors. Since the paper of Kwait and Weinfurter, several other schemes have been proposed and experimentally demonstrated for Bell state analysis using other degrees of freedom of photons [WPM03] [SHKW06] [BVMDM07]. In particular, the paper by Walborn *et al.* [WPM03] improved upon the above setup; their protocol doesn't require photon-number resolving detectors and does not even require two-photon interference. The paper [SHKW06] demonstrated a complete BSM using polarization and time-energy hyperentanglement.

Hyperentangled Bell state analysis has also been demonstrated using the polarization, and Orbital Angular Momentum (OAM) degrees of freedom [KLL+19] [BWK08]. Aside from an angular momentum possessed due to circular polarization (the spin angular momentum), photon beams can also possess angular momentum due to the spatial distribution of the electric field of the beam. This is referred to as the orbital angular momentum. Beams with electric fields of the form $E(\vec{r}, \phi) = \vec{E_0}(r)e^{im\phi}$ (cylindrical coordinates in the plane perpendicular to the direction of propagation) have a well defined angular momentum, and each photon in this beam has a quantized angular momentum of $m\hbar$. The Laguerre-Gaussian modes are cylindrically symmetric solutions of the electric field for the wave equation in the paraxial approximation. These have the same form as above, but with $\vec{E_0}(r)$ being a

generalized Laguerre polynomial. Any beam of light can be decomposed into the basis of LG modes of various mode numbers m. The states $|\pm 1\rangle$ below denote LG modes which carry angular momentum of $\pm\hbar$. The OAM Bell states used here are defined as

$$\begin{aligned}
\left|\Psi^+\right\rangle^{oam} &= \frac{|1\rangle\,|-1\rangle + |-1\rangle\,|1\rangle}{\sqrt{2}} \\
\left|\Psi^-\right\rangle^{oam} &= \frac{|1\rangle\,|-1\rangle - |-1\rangle\,|1\rangle}{\sqrt{2}} \\
\left|\Phi^+\right\rangle^{oam} &= \frac{|1\rangle\,|1\rangle + |-1\rangle\,|-1\rangle}{\sqrt{2}} \\
\left|\Phi^-\right\rangle^{oam} &= \frac{|1\rangle\,|1\rangle - |-1\rangle\,|-1\rangle}{\sqrt{2}}
\end{aligned} \tag{3.42}$$

The paper [KLL+19] proposed a protocol to completely distinguish between the states (the superscripts pol and oam denote Bell states in polarization and orbital angular momentum respectively)

$$\begin{aligned}
|\Theta_1\rangle &= \left|\Psi^+\right\rangle^{pol} \left|\Psi^+\right\rangle^{oam} \\
|\Theta_2\rangle &= \left|\Psi^+\right\rangle^{pol} \left|\Psi^-\right\rangle^{oam} \\
|\Theta_3\rangle &= \left|\Psi^+\right\rangle^{pol} \left|\Phi^+\right\rangle^{oam} \\
|\Theta_4\rangle &= \left|\Psi^+\right\rangle^{pol} \left|\Phi^-\right\rangle^{oam}
\end{aligned} \tag{3.43}$$

The states in (3.42) can be produced using an SPDC process, and this entanglement in the OAM degree of freedom was first experimentally demonstrated by Mair *et al.* in 2001 [MVWZ01]. Just as how wave-plates are used to change the polarization of light, converting between states of different OAMs is usually carried out using computer-generated diffraction gratings with fork dislocations.

The paper [BWK08] on the other hand, proposed a setup to distinguish between the states with fixed OAM and varying polarization: $|\Psi^\pm\rangle^{pol}\,|\Psi^+\rangle^{oam}$ and $|\Phi^\pm\rangle^{pol}\,|\Psi^+\rangle^{oam}$. The central idea of both these papers was the same, which is to develop a setup that distinguishes between the single photon states defined as

$$\begin{aligned}
|\Psi_1\rangle &= \frac{|-1\rangle\,|H\rangle + |1\rangle\,|V\rangle}{\sqrt{2}} \\
|\Psi_2\rangle &= \frac{|-1\rangle\,|H\rangle - |1\rangle\,|V\rangle}{\sqrt{2}} \\
|\Psi_3\rangle &= \frac{|-1\rangle\,|V\rangle + |1\rangle\,|H\rangle}{\sqrt{2}} \\
|\Psi_4\rangle &= \frac{|-1\rangle\,|V\rangle - |1\rangle\,|H\rangle}{\sqrt{2}}
\end{aligned} \tag{3.44}$$

It so happens that the four states $|\Theta_i\rangle$ in (3.43) can be written as **unique** combinations of the $|\Psi\rangle$ states above.

$$\begin{aligned}
|\Theta_1\rangle &= \frac{1}{2}\left(|\Psi_1\rangle_1\,|\Psi_1\rangle_2 - |\Psi_2\rangle_1\,|\Psi_2\rangle_2 + |\Psi_3\rangle_1\,|\Psi_3\rangle_2 - |\Psi_4\rangle_1\,|\Psi_4\rangle_2\right) \\
|\Theta_2\rangle &= \frac{1}{2}\left(|\Psi_2\rangle_1\,|\Psi_1\rangle_2 - |\Psi_1\rangle_1\,|\Psi_2\rangle_2 + |\Psi_4\rangle_1\,|\Psi_3\rangle_2 - |\Psi_3\rangle_1\,|\Psi_4\rangle_2\right) \\
|\Theta_3\rangle &= \frac{1}{2}\left(|\Psi_3\rangle_1\,|\Psi_1\rangle_2 + |\Psi_4\rangle_1\,|\Psi_2\rangle_2 + |\Psi_1\rangle_1\,|\Psi_3\rangle_2 + |\Psi_2\rangle_1\,|\Psi_4\rangle_2\right) \\
|\Theta_4\rangle &= \frac{1}{2}\left(|\Psi_4\rangle_1\,|\Psi_1\rangle_2 + |\Psi_3\rangle_1\,|\Psi_2\rangle_2 + |\Psi_2\rangle_1\,|\Psi_3\rangle_2 + |\Psi_1\rangle_1\,|\Psi_4\rangle_2\right)
\end{aligned} \tag{3.45}$$

where the subscripts outside the ket denote the photon number. Clearly, we can see no overlap between the outcomes of any two $|\Theta\rangle$ states. Therefore, if a setup can distinguish between the four states (3.44), then one could use two copies of this setup for both photons, and perform perfect discrimination of the states (3.45). The setup of paper [BWK08] is described in detail in section 3.4.2.

Now that we have achieved perfect Bell state analysis using only linear optics, it is worth studying the applications of this result. Can this help us in the quantum information protocols discussed in chapter 1? This question is addressed in the following two sections.

3.4.1 Hyperentanglement for teleportation

Although we can perfectly distinguish between Bell states entangled in two degrees of freedom, this **does not** give us the ability to perform deterministic teleportation of an arbitrary state of a photon using linear optics. Why is this so?

Say we want to teleport the OAM state of the photon

$$|\Psi\rangle_1 = |H\rangle_1 \otimes (\alpha\,|1\rangle_1 + \beta\,|-1\rangle_1) \tag{3.46}$$

We are also equipped with a pair of photons (2 and 3) entangled in the OAM degree of freedom. Let their state be

$$|\Psi\rangle_{23} = |H\rangle_2\,|V\rangle_3 \otimes \left(\frac{|1\rangle_2\,|-1\rangle_3 - |-1\rangle_2\,|1\rangle_3}{\sqrt{2}}\right) \tag{3.47}$$

So, the combined state of the three photons is

$$|\Psi\rangle_{123} = |H\rangle_1\,|H\rangle_2\,|V\rangle_3 \otimes \left[(\alpha\,|1\rangle_1 + \beta\,|-1\rangle_1)\left(\frac{|1\rangle_2\,|-1\rangle_3 - |-1\rangle_2\,|1\rangle_3}{\sqrt{2}}\right)\right] \tag{3.48}$$

$$\equiv |H,H,V\rangle \otimes \left[\frac{\alpha\,|1,1,-1\rangle - \alpha\,|1,-1,1\rangle + \beta\,|-1,1,1\rangle - \beta\,|-1,-1,1\rangle}{\sqrt{2}}\right] \tag{3.49}$$

where, $|H,H,V\rangle \equiv |H\rangle_1\,|H\rangle_2\,|V\rangle_3$ and $|1,1,-1\rangle \equiv |1\rangle_1\,|1\rangle_2\,|-1\rangle_3$

The OAM part of the state (3.49) can be rewritten in terms of the OAM bell states of photons 1 and 2, giving

$$\begin{aligned}|\Psi\rangle_{123} = |H,H,V\rangle \otimes [&\left|\Psi^+\right\rangle_{12}^{oam}(-\alpha\,|1\rangle_3 + \beta\,|-1\rangle_3) - \left|\Psi^-\right\rangle_{12}^{oam}(\alpha\,|1\rangle_3 + \beta\,|-1\rangle_3)\\ &+ \left|\Phi^+\right\rangle_{12}^{oam}(-\beta\,|1\rangle_3 + \alpha\,|-1\rangle_3) + \left|\Phi^-\right\rangle_{12}^{oam}(\beta\,|1\rangle_3 + \alpha\,|-1\rangle_3)]\end{aligned} \tag{3.50}$$

where the OAM Bell states are defined as in (3.42). Let us assume that we have a setup that distinguishes between the states in (3.45). For us to benefit from this setup, we must write the states of photon 1 and 2 in (3.50) as jointly entangled in both polarization and OAM degrees of freedom. But clearly, the three photons are a product state in polarization. To convert them into the required entangled state, we must apply a global unitary on the photons 1 and 2 that performs the transformation

$$|H,H\rangle \rightarrow \frac{|H,V\rangle + |V,H\rangle}{\sqrt{2}} \equiv \left|\Psi^+\right\rangle^{pol} \tag{3.51}$$

Assuming this operation can be performed, the state of the three photons becomes

$$\begin{aligned}|\Psi\rangle_{123} = \left|\Psi^+\right\rangle_{12}^{pol} |V\rangle_3 \otimes [\left|\Psi^+\right\rangle_{12}^{oam} (-\alpha\,|1\rangle_3 + \beta\,|-1\rangle_3) - \left|\Psi^-\right\rangle_{12}^{oam} (\alpha\,|1\rangle_3 + \beta\,|-1\rangle_3) \\ + \left|\Phi^+\right\rangle_{12}^{oam} (-\beta\,|1\rangle_3 + \alpha\,|-1\rangle_3) + \left|\Phi^-\right\rangle_{12}^{oam} (\beta\,|1\rangle_3 + \alpha\,|-1\rangle_3)]\end{aligned} \tag{3.52}$$

$$\begin{aligned}\implies |\Psi\rangle_{123} = \left|\Psi^+\right\rangle_{12}^{pol} \left|\Psi^+\right\rangle_{12}^{oam} \otimes |V\rangle_3 (-\alpha\,|1\rangle_3 + \beta\,|-1\rangle_3) - \left|\Psi^+\right\rangle_{12}^{pol} \left|\Psi^-\right\rangle_{12}^{oam} \otimes |V\rangle_3 (\alpha\,|1\rangle_3 + \beta\,|-1\rangle_3) \\ + \left|\Psi^+\right\rangle_{12}^{pol} \left|\Phi^+\right\rangle_{12}^{oam} \otimes |V\rangle_3 (-\beta\,|1\rangle_3 + \alpha\,|-1\rangle_3) + \left|\Psi^+\right\rangle_{12}^{pol} \left|\Phi^-\right\rangle_{12}^{oam} \otimes |V\rangle_3 (\beta\,|1\rangle_3 + \alpha\,|-1\rangle_3)\end{aligned} \tag{3.53}$$

Here, both the polarization and the OAM states of the first two photons are written first, and the state of the 3rd photon is written as a tensor product.
The states of the first two photons in (3.53) are precisely the states entangled in two degrees of freedom $|\Theta\rangle$ as defined earlier. So we finally have

$$\begin{aligned}|\Psi\rangle_{123} = |\Theta_1\rangle_{12} \otimes |V\rangle_3 (-\alpha\,|1\rangle_3 + \beta\,|-1\rangle_3) - |\Theta_2\rangle_{12} \otimes |V\rangle_3 (\alpha\,|1\rangle_3 + \beta\,|-1\rangle_3) \\ + |\Theta_3\rangle_{12} \otimes |V\rangle_3 (-\beta\,|1\rangle_3 + \alpha\,|-1\rangle_3) + |\Theta_4\rangle_{12} \otimes |V\rangle_3 (\beta\,|1\rangle_3 + \alpha\,|-1\rangle_3)\end{aligned} \tag{3.54}$$

Since a setup exists that can distinguish between the $|\Theta\rangle$ states, we can now perform a measurement onto one of the hyperentangled states $|\Theta_i\rangle$, and perform an appropriate rotation to get back the arbitrary state needed. However, the unitary U described in (3.51) is creating polarization entanglement, and it **cannot** be realized with certainty using linear optics. The maximum efficiency of this transformation is 50%. For this reason, entanglement in two degrees of freedom is not a useful resource for teleportation. However, it is a valuable resource for dense coding, and this is discussed next.

3.4.2 Hyperentanglement for dense coding

Since hyperentanglement allows complete state discrimination, dense coding can be performed on hyperentangled photons such that information can be encoded in one degree of freedom (by performing various unitary rotations on the photon in that Hilbert space), and the entangled state in the second Hilbert space is used only to assist in the state discrimination process. Theoretically, this procedure allows for perfect dense coding, with a channel capacity of two bits per photon. Hyperentanglement-assisted dense coding was first described for polarization and OAM modes of photons by Barreiro *et al.* [BWK08], and their apparatus is discussed here. In their protocol, information is encoded in the polarization domain, and perfect discrimination of the states $|\Psi^\pm\rangle^{pol} \otimes |\Psi^+\rangle^{oam}$ and $|\Phi^\pm\rangle^{pol} \otimes |\Psi^+\rangle^{oam}$ is achieved.

The setup shown in figure 3.5 is for a single photon. The photon first passes through a computer-generated hologram which converts the states $|\pm 1\rangle$ into a gaussian ($|0\rangle$) mode in the first diffraction order. Both the $|\pm 1\rangle$ states are deflected in opposite directions by the hologram, and are combined at a polarizing beam splitter @ 0°. Lastly, the photon passes through a set of polarizing beam splitters @ 45°. The effect of the above apparatus is to completely separate the following four single photon

states:

$$\begin{aligned}
\left|\Psi^{+}\right\rangle &= \frac{\left|-1\right\rangle\left|H\right\rangle + \left|1\right\rangle\left|V\right\rangle}{\sqrt{2}} \\
\left|\Psi^{-}\right\rangle &= \frac{\left|-1\right\rangle\left|H\right\rangle - \left|1\right\rangle\left|V\right\rangle}{\sqrt{2}} \\
\left|\Phi^{+}\right\rangle &= \frac{\left|-1\right\rangle\left|V\right\rangle + \left|1\right\rangle\left|H\right\rangle}{\sqrt{2}} \\
\left|\Phi^{-}\right\rangle &= \frac{\left|-1\right\rangle\left|V\right\rangle - \left|1\right\rangle\left|H\right\rangle}{\sqrt{2}}
\end{aligned} \tag{3.55}$$

These states are the same as (3.44), just in another notation. To justify that these four states are completely separated out by the setup in figure 3.5, let us study the evolution of the states in (3.55). When $\left|-1\right\rangle\left|H\right\rangle$ passes through the hologram, the photon is converted into a Gaussian

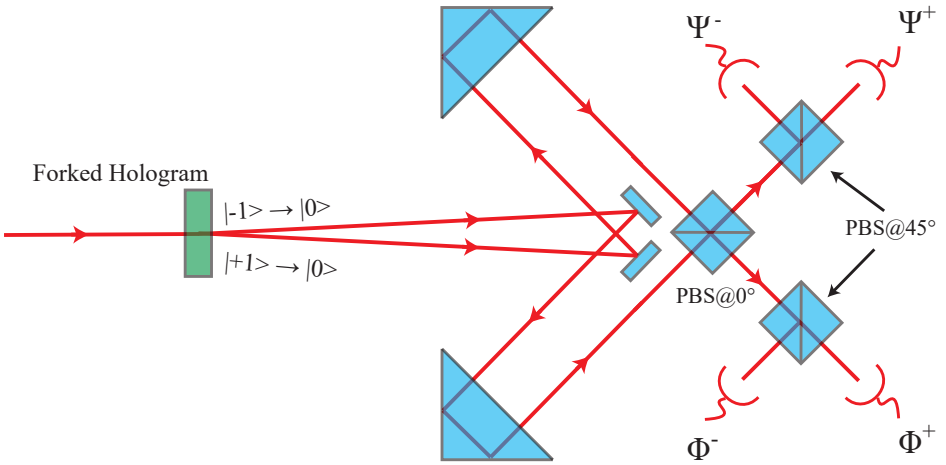

Figure 3.5: Superdense coding with OAM and polarization hyperentanglement ([BWK08])

mode and deflected upwards (according to the diagram, the counterclockwise state is assumed to be $\left|+1\right\rangle$). Then, it passes through the PBS @ 0°, where the photon gets transmitted upwards since it is horizontally polarized. Similarly, the state $\left|1\right\rangle\left|V\right\rangle$ first is deflected downwards by the hologram but again reflected upwards by the polarizing beam splitter since the photon is vertically polarized. So, the evolution of the state $\left|\Psi^{+}\right\rangle$ can be described as

$$\left|\Psi^{+}\right\rangle = \frac{\left|-1\right\rangle\left|H\right\rangle + \left|1\right\rangle\left|V\right\rangle}{\sqrt{2}} \xrightarrow{\text{Hologram and PBS @ 0°}} \left|0\right\rangle \otimes \frac{1}{\sqrt{2}}\left(\left|H\right\rangle + \left|V\right\rangle\right)_{up} \tag{3.56}$$

where the subscript 'up' denotes that the photon is above the polarizing beam splitter. Since each of the four hyperentangled Bell states is a unique combination of these single photon states, passing the states through two identical setups (one for each photon) gives unambiguous outcomes for all states. The same analysis can be performed for the other states to get:

$$\begin{aligned}
\left|\Psi^{+}\right\rangle &= \frac{\left|-1\right\rangle\left|H\right\rangle + \left|1\right\rangle\left|V\right\rangle}{\sqrt{2}} \xrightarrow{\text{Hologram and PBS @ 0°}} \left|0\right\rangle \otimes \frac{1}{\sqrt{2}}\left(\left|H\right\rangle + \left|V\right\rangle\right)_{up} \\
\left|\Psi^{-}\right\rangle &= \frac{\left|-1\right\rangle\left|H\right\rangle - \left|1\right\rangle\left|V\right\rangle}{\sqrt{2}} \xrightarrow{\text{Hologram and PBS @ 0°}} \left|0\right\rangle \otimes \frac{1}{\sqrt{2}}\left(\left|H\right\rangle - \left|V\right\rangle\right)_{up} \\
\left|\Phi^{+}\right\rangle &= \frac{\left|-1\right\rangle\left|V\right\rangle + \left|1\right\rangle\left|H\right\rangle}{\sqrt{2}} \xrightarrow{\text{Hologram and PBS @ 0°}} \left|0\right\rangle \otimes \frac{1}{\sqrt{2}}\left(\left|H\right\rangle + \left|V\right\rangle\right)_{down} \\
\left|\Phi^{-}\right\rangle &= \frac{\left|-1\right\rangle\left|V\right\rangle - \left|1\right\rangle\left|H\right\rangle}{\sqrt{2}} \xrightarrow{\text{Hologram and PBS @ 0°}} \left|0\right\rangle \otimes \frac{1}{\sqrt{2}}\left(\left|H\right\rangle - \left|V\right\rangle\right)_{down}
\end{aligned} \tag{3.57}$$

It is obvious now that these four states can be completely separated out using a PBS @ 45°, as indicated in figure 3.5. Therefore, we have shown that the setup does separate the single-photon states in (3.55). Now, in the previous section, we said that the hyperentangled Bell states (3.45) can be uniquely expressed as combinations of the single photon states. Indeed, this is true here as well:

$$\begin{aligned}\left|\Psi^{\pm}\right\rangle^{pol} \otimes \left|\Psi^{+}\right\rangle^{oam} &= \frac{1}{2}\left(|\Phi_1\rangle^{+} \otimes |\Psi_2\rangle^{\mp} + |\Phi_1\rangle^{-} \otimes |\Psi_2\rangle^{\pm} + |\Psi_1\rangle^{+} \otimes |\Phi_2\rangle^{\pm} + |\Psi_1\rangle^{-} \otimes |\Phi_2\rangle^{\mp}\right) \\ \left|\Phi^{\pm}\right\rangle^{pol} \otimes \left|\Psi^{+}\right\rangle^{oam} &= \frac{1}{2}\left(|\Phi_1\rangle^{+} \otimes |\Phi_2\rangle^{\mp} + |\Phi_1\rangle^{-} \otimes |\Phi_2\rangle^{\pm} + |\Psi_1\rangle^{+} \otimes |\Psi_2\rangle^{\pm} + |\Psi_1\rangle^{-} \otimes |\Psi_2\rangle^{\mp}\right)\end{aligned} \tag{3.58}$$

Therefore, two copies of the apparatus in figure 3.5 can be used to completely separate out the hyperentangled Bell states $|\Psi^{\pm}\rangle^{pol} \otimes |\Psi^{+}\rangle^{oam}$ and $|\Phi^{\pm}\rangle^{pol} \otimes |\Psi^{+}\rangle^{oam}$, and by encoding information in the polarization degree of freedom, one can perform dense coding with the maximum possible channel capacity.

Although theoretically the channel capacity can be 2, the authors of this work were able to achieve a lower channel capacity of 1.630 ± 0.006 due to errors in measurement, input state generation, losses in the components, etc. However, this is still an improvement over the fundamental bound of 1.585 set by linear optics and a single degree of freedom. This illustrates the benefit of BSMs using entanglement in two degrees of freedom. Building on this work, Williams *et al.* were able to achieve a channel capacity of 1.665 ± 0.018 over optical fiber links [WSH17], using time-polarization hyperentanglement.

3.5 Summary

In this chapter, various resources that help enhance the efficiency of Bell measurements beyond 50% were discussed. Gaussian squeezing leads to better discrimination for any non-zero value of the squeezing parameter. However, the maximum success probability is only around 64.3% at the optimal value of $r = 0.6585$. Ancillary entanglement is also a useful resource: The success probability increases to 75% if one pair of ancillary entangled photons are used. Further, using $2^N - 2$ photons yields a success rate of $1 - 1/2^N$, asymptotically approaching perfect discrimination as $N \to \infty$. However, this requires deterministically producing 4-photon entangled, 8-photon entangled states, and so on, which is difficult using today's technology.

Two resources that do enable complete Bell state measurements are non-linear optical methods and entanglement in two degrees of freedom. Although the former can in principle, be used for deterministic teleportation, the efficiencies of today's non-linear devices are too low to achieve this goal. The latter resource cannot help with deterministic teleportation, however can lead to perfect superdense coding (transmitting 2 bits using one photon). Experiments have been carried out to achieve this bound, and current channel capacities lie around 1.63 - 1.66.

Chapter 4

Non-Maximally Entangled (NME) states

A linear optics setup with vacuum ancillae can only discriminate between two of the four bell states. As discussed previously, one way to obtain this discrimination is to pass the states through a 50-50 beam splitter, where they transform as

$$\begin{aligned}
\left|\Psi^{+}\right\rangle &\equiv \frac{\left[h_1^{\dagger}v_2^{\dagger}+v_1^{\dagger}h_2^{\dagger}\right]_{in}|0\rangle}{\sqrt{2}} \rightarrow \frac{\left[h_1^{\dagger}v_1^{\dagger}+h_2^{\dagger}v_2^{\dagger}\right]_{out}|0\rangle}{\sqrt{2}} \\
\left|\Psi^{-}\right\rangle &\equiv \frac{\left[h_1^{\dagger}v_2^{\dagger}-v_1^{\dagger}h_2^{\dagger}\right]_{in}|0\rangle}{\sqrt{2}} \rightarrow \frac{\left[h_1^{\dagger}v_2^{\dagger}-v_1^{\dagger}h_2^{\dagger}\right]_{out}|0\rangle}{\sqrt{2}} \\
\left|\Phi^{\pm}\right\rangle &\equiv \frac{\left[h_1^{\dagger}h_2^{\dagger}\pm v_1^{\dagger}v_2^{\dagger}\right]_{in}|0\rangle}{\sqrt{2}} \rightarrow \frac{\left[h_1^{\dagger 2}+h_2^{\dagger 2}\pm v_1^{\dagger 2}\pm v_2^{\dagger 2}\right]_{out}|0\rangle}{2\sqrt{2}}
\end{aligned} \tag{4.1}$$

The states $|\Psi^{+}\rangle$ and $|\Psi^{-}\rangle$ give different outcomes which are distinct from those shown by $|\Phi^{\pm}\rangle$. However, $|\Phi^{+}\rangle$ cannot be distinguished from $|\Phi^{-}\rangle$ (the detectors cannot differentiate between the $\pm$ coefficients for the states), leading to only a 50% success probability.

The problem we discuss in this chapter is distinguishing between the following orthogonal non-maximally entangled states

$$\begin{aligned}
\left|\widetilde{\Psi^{+}}\right\rangle &= \left[a\ h_1^{\dagger}v_2^{\dagger}+b\ v_1^{\dagger}h_2^{\dagger}\right]_{in}|0\rangle \equiv a\,|HV\rangle + b\ |VH\rangle \\
\left|\widetilde{\Psi^{-}}\right\rangle &= \left[b\ h_1^{\dagger}v_2^{\dagger}-a\ v_1^{\dagger}h_2^{\dagger}\right]_{in}|0\rangle \equiv b\,|HV\rangle - a\ |VH\rangle \\
\left|\widetilde{\Phi^{+}}\right\rangle &= \left[c\ h_1^{\dagger}h_2^{\dagger}+d\ v_1^{\dagger}v_2^{\dagger}\right]_{in}|0\rangle \equiv c\,|HH\rangle + d\ |VV\rangle \\
\left|\widetilde{\Phi^{-}}\right\rangle &= \left[d\ h_1^{\dagger}h_2^{\dagger}-c\ v_1^{\dagger}v_2^{\dagger}\right]_{in}|0\rangle \equiv d\,|HH\rangle - c\ |VV\rangle
\end{aligned} \tag{4.2}$$

where $a, b, c, d \in \mathbb{C}$ and satisfy

$$\begin{aligned}
|a|^2+|b|^2 &= 1 \\
|c|^2+|d|^2 &= 1
\end{aligned} \tag{4.3}$$

Clearly, the states in (4.2) reduce to the Bell states when $a = b = c = d = 1/\sqrt{2}$. The entanglement entropy of these states depends on the coefficients, and is given by:

$$\begin{aligned} S(\left|\widetilde{\Psi^+}\right\rangle) = S(\left|\widetilde{\Psi^-}\right\rangle) &= -\left[|a|^2 \log_2|a|^2 + |b|^2 \log_2|b|^2\right] \\ S(\left|\widetilde{\Phi^+}\right\rangle) = S(\left|\widetilde{\Phi^-}\right\rangle) &= -\left[|c|^2 \log_2|c|^2 + |d|^2 \log_2|d|^2\right] \end{aligned} \tag{4.4}$$

Non-maximally entangled states have found wide application in quantum information processes. Some examples include implementing non-local gates [GR05], probabilistic quantum teleporation [AP02], and key distribution [XLG01]. Moreover, in certain situations, partially entangled states might be a more advantageous resource than the Bell states. For instance, in multiple consecutive teleportations of an arbitrary state, non-maximally states have been shown to provide a larger success probabilty of perfect teleportation [MG08]. These states also enable more feasible experimental tests of Bell inequalities [Ebe93]. Lastly, partially entangled states can be distilled into Bell states [BBPS96] and then utilized for protocols that require maximally entangled states.

Distinguishing between partially entangled states is important to study, as it is a necessary step in some of the protocols listed above. Moreover, in practical scenarios, one might not be equipped with Bell states, but might be provided with a 'weaker' resource, namely partially entangled states. So it is worth finding out how far we can get in discriminating between these states using linear optics.

Before we study the issue of state discrimination, we ask: how are partially entangled states produced? One method is to use postselection; maximally entangled states sent through an asymmetric beam splitter and conditioned on coincidence at either side of the beam splitter lead to non-maximally entangled states [TBMM95]. A simpler method that doesn't rely on postselection was developed by White *et al.* [WJEK99] (see figure 4.1). The setup comprises of two slabs of a birefringent crystal whose optic axes are aligned perpendicularly. They are constructed according to type-I phase matching, which means that a pump photon is converted to two photons, both with polarization orthogonal to that of the pump photon. In the setup in 4.1, if the pump beam is horizontally polarized, only the second crystal undergoes down conversion, resulting in two vertically polarized photons. Similarly, a vertically polarized pump beam results in two horizontally polarized photons from the first crystal.

However, if the pump beam is set to 45°, down conversion is equally likely to occur from either crystal, and a maximally entangled state $\frac{1}{\sqrt{2}}(|HH\rangle + |VV\rangle)$ is produced. Further, tilting the pump beam away from this angle generates a partially entangled state

$$|\Psi\rangle = \frac{1}{\sqrt{1+\epsilon^2}}\left[|HH\rangle + \epsilon\,|VV\rangle\right] \tag{4.5}$$

where $\epsilon = \tan\chi$, χ being the angle the pump beam makes with the vertical. Let us now discuss distinguishing between the states in (4.2). For the maximally entangled states, we saw that two states give unambiguous outcomes after passing through a 50-50 beam splitter. A first guess might be to treat the non-maximally entangled states similarily. When the $\left|\widetilde{\Phi^\pm}\right\rangle$ states from (4.2) are input to a 50-50 beam splitter, the states at the output become (recall (1.10))

$$\begin{aligned} \left|\widetilde{\Phi^+}\right\rangle &\to \frac{\left[c(h_1^{\dagger 2} + h_2^{\dagger 2}) + d(v_1^{\dagger 2} + v_2^{\dagger 2})\right]_{out}|0\rangle}{2} \\ \left|\widetilde{\Phi^-}\right\rangle &\to \frac{\left[d(h_1^{\dagger 2} + h_2^{\dagger 2}) - c(v_1^{\dagger 2} + v_2^{\dagger 2})\right]_{out}|0\rangle}{2} \end{aligned} \tag{4.6}$$

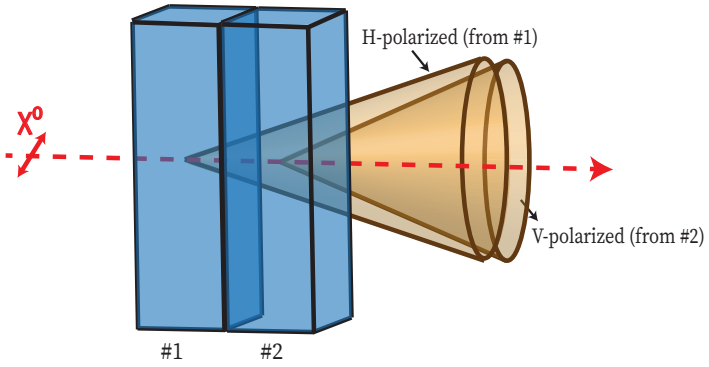

Figure 4.1: Experimental setup to generate partially entangled states (see [WJEK99])

Although the operators' coefficients are different, the set of operators (and thus, detector outcomes) are the same for both states. Therefore, these states cannot be distinguished from each other unless either c or d was 0 (which would imply that our initial states were not entangled). Further, the $\left|\widetilde{\Psi^{\pm}}\right\rangle$ transform as

$$\begin{aligned}\left|\widetilde{\Psi^{+}}\right\rangle &\to \frac{1}{2}\left[ih_1^\dagger v_1^\dagger(b+a)+v_1^\dagger h_2^\dagger(b-a)+h_1^\dagger v_2^\dagger(a-b)+ih_2^\dagger v_2^\dagger(b+a)\right]_{out}|0\rangle \\ \left|\widetilde{\Psi^{-}}\right\rangle &\to \frac{1}{2}\left[ih_1^\dagger v_1^\dagger(b-a)-v_1^\dagger h_2^\dagger(b+a)+h_1^\dagger v_2^\dagger(b+a)+ih_2^\dagger v_2^\dagger(b-a)\right]_{out}|0\rangle\end{aligned} \tag{4.7}$$

Here too, we cannot distinguish between these states in general. The special case of Bell states is also evident here. When $b = a = \frac{1}{\sqrt{2}}$, the terms that cancel for $\left|\widetilde{\Psi^{+}}\right\rangle$ remain for $\left|\widetilde{\Psi^{-}}\right\rangle$ and vice versa. As a result, perfect discrimination is possible, and the result is given in (4.1). If only a 50-50 beam splitter was our setup, we could distinguish between the Bell states with 50% probability, but we have no chance of distinguishing between non-maximally entangled states.

Motivated from the paper of Grice [Gri11], we can ask: Will using ancillary maximally entangled states help us distinguish between the non-maximally entangled states?

4.1 Ancillary Bell states

To understand the effect of ancillary bell states, it's important to notice that the expression for the output state $\left|\widetilde{\Psi^{-}}\right\rangle$ can be obtained from that of $\left|\widetilde{\Psi^{+}}\right\rangle$ by just replacing a with b, and b with $-a$. Similarily, the output state for $\left|\widetilde{\Phi^{-}}\right\rangle$ can be constructed from $\left|\widetilde{\Phi^{+}}\right\rangle$ by making the substitutions: $c \to d, d \to -c$ (This can be seen to be true from (4.6) and (4.7)). This occurs because of the initial construction of the states, to make them orthogonal.

From here, it must be clear that any number of ancillary maximally entangled pairs will **not** help in distinguishing between the states in (4.2). This is because the state of the ancillary photons does not have any dependence on a or b. So, no matter how complicated the final state is, the state for $\left|\widetilde{\Psi^{-}}\right\rangle$ (or $\left|\widetilde{\Phi^{-}}\right\rangle$) can always be obtained from the state of $\left|\widetilde{\Psi^{+}}\right\rangle$ (or $\left|\widetilde{\Phi^{+}}\right\rangle$) by just replacing a with b (c with d), and b with $-a$ (d with $-c$). So, all the terms for these two states will be identical; only the coefficients for some states will be different. Thus, the non-maximally entangled states cannot be distinguished from each other even after using any number of ancillary maximally entangled pairs.

4.2 Ancillary Non-maximally entangled states

Naturally, the next question to ask is what if we use additional *non-maximally entangled* states? If the ancillary states also have a dependence on a, b, c, d, then the above argument does not hold, and there is some chance of distinguishing between the states in (4.2).
In this section, we investigate this problem. Let us begin with an ancillary photon pair of the form

$$|\widetilde{\gamma_1}\rangle = \left(e\ h_3^\dagger h_4^\dagger + f\ v_3^\dagger v_4^\dagger\right)_{in} |0\rangle \tag{4.8}$$

where e and f are arbitrary complex numbers that satisfy the normalization condition

$$|e|^2 + |f|^2 = 1 \tag{4.9}$$

So, our task is to distinguish between the states

$$\begin{aligned} \left|\widetilde{\Psi^+}\right\rangle |\widetilde{\gamma_1}\rangle &= \left[(a\ h_1^\dagger v_2^\dagger + b\ v_1^\dagger h_2^\dagger)(e\ h_3^\dagger h_4^\dagger + f\ v_3^\dagger v_4^\dagger)\right]_{in} |0\rangle \\ \left|\widetilde{\Psi^-}\right\rangle |\widetilde{\gamma_1}\rangle &= \left[(b\ h_1^\dagger v_2^\dagger - a\ v_1^\dagger h_2^\dagger)(e\ h_3^\dagger h_4^\dagger + f\ v_3^\dagger v_4^\dagger)\right]_{in} |0\rangle \end{aligned} \tag{4.10}$$

$$\begin{aligned} \left|\widetilde{\Phi^+}\right\rangle |\widetilde{\gamma_1}\rangle &= \left[(c\ h_1^\dagger h_2^\dagger + d\ v_1^\dagger v_2^\dagger)(e\ h_3^\dagger h_4^\dagger + f\ v_3^\dagger v_4^\dagger)\right]_{in} |0\rangle \\ \left|\widetilde{\Phi^-}\right\rangle |\widetilde{\gamma_1}\rangle &= \left[(d\ h_1^\dagger h_2^\dagger - c\ v_1^\dagger v_2^\dagger)(e\ h_3^\dagger h_4^\dagger + f\ v_3^\dagger v_4^\dagger)\right]_{in} |0\rangle \end{aligned} \tag{4.11}$$

Further. we will investigate the evolution of the above states through a specific setup, the one proposed by Grice [Gri11](pictured below). In this setup, the input and output creation operators are related by

$$\begin{pmatrix} a_1^\dagger \\ a_2^\dagger \\ a_3^\dagger \\ a_4^\dagger \end{pmatrix}_{in} \rightarrow \frac{1}{2} \begin{bmatrix} 1 & i & i & -1 \\ i & 1 & -1 & i \\ i & -1 & 1 & i \\ -1 & i & i & 1 \end{bmatrix} \begin{pmatrix} a_1^\dagger \\ a_2^\dagger \\ a_3^\dagger \\ a_4^\dagger \end{pmatrix}_{out} \quad (a = \{h, v\}) \tag{4.12}$$

We use this setup in order to compare our results with the case of Bell states, which has already

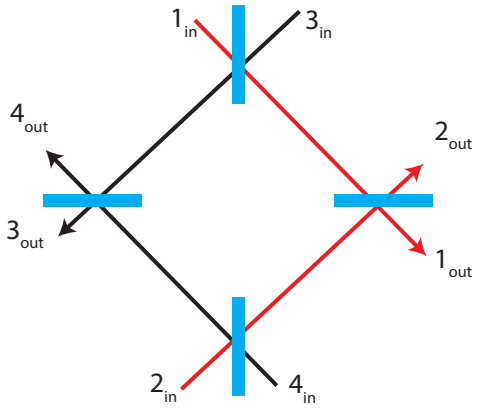

Figure 4.2: Ancillary photons are passed through the modes 3 and 4, and beam splitters are 50-50

been analyzed in section 3.2. Recall that this setup was used to obtain a 75% success probability in distinguishing between the Bell states along with an ancillary maximally entangled state.

When the four photons in (4.10) and (4.11) are passed through this setup, the final states can

be written in terms of the output operators using (4.12). This will lead to a large number of terms. Before writing out these terms, we can make some general observations of the final states using the structure of (4.10) and (4.11).

- Each term in (4.10) will have an odd number of h or v output operators, whereas the terms in (4.11) always have an even number of h's and v's.

This tells us that based on the outcome at the photodetectors, we can always tell whether the state belonged to $\{\left|\widetilde{\Psi^+}\right\rangle, \left|\widetilde{\Psi^-}\right\rangle\}$ or $\{\left|\widetilde{\Phi^+}\right\rangle, \left|\widetilde{\Phi^-}\right\rangle\}$.

More importantly, we can also conclude the following:

- Both states in (4.10) will have **identical** terms (only different coefficients). They cannot be distinguished even after introducing $|\widetilde{\gamma_1}\rangle$.

The above statement is not obvious at first glance. It can be proven by a subtle argument, described below. If $\left|\widetilde{\Psi^+}\right\rangle|\widetilde{\gamma_1}\rangle$ has term that isn't present in $\left|\widetilde{\Psi^-}\right\rangle|\widetilde{\gamma_1}\rangle$, this must mean that a cancellation has taken place in $\left|\widetilde{\Psi^-}\right\rangle|\widetilde{\gamma_1}\rangle$ when expanding the state in terms of the output operators; one that did not happen in the case of $\left|\widetilde{\Psi^+}\right\rangle|\widetilde{\gamma_1}\rangle$. It can be shown that no such cancellation can take place. Let's consider an example. Say the term $\left[h_1^{\dagger 2}h_2^\dagger v_3^\dagger\right]_{out}|0\rangle$ is not present in $\left|\widetilde{\Psi^+}\right\rangle$. Such a term can arise because of two input terms, $ae\left[h_1^\dagger v_2^\dagger h_3^\dagger h_4^\dagger\right]_{in}|0\rangle$ and $be\left[v_1^\dagger h_2^\dagger h_3^\dagger h_4^\dagger\right]_{in}|0\rangle$. Clearly, the two $\left[h_1^{\dagger 2}h_2^\dagger v_3^\dagger\right]_{out}|0\rangle$ that come out of these input terms cannot cancel irrespective of sign, since $a \neq b$. So, we have found that **any** ancillary non-maximally entangled state of the form (4.8) does not help in distinguishing between the $\left|\widetilde{\Psi^\pm}\right\rangle$ states.

We are only left to explore the effect of $|\widetilde{\gamma_1}\rangle$ on distinguishing between the remaining two states (4.11). Note that the argument discussed above does not work for the $\left|\widetilde{\Phi^\pm}\right\rangle$ states. For example, let's look at the term $\left[v_1^{\dagger 2}h_3^\dagger h_1^\dagger\right]_{out}|0\rangle$. In $\left|\widetilde{\Phi^+}\right\rangle|\widetilde{\gamma_1}\rangle$, this term can arise out of $de\left[v_1^\dagger v_2^\dagger h_3^\dagger h_4^\dagger\right]_{in}|0\rangle$ or $cf\left[h_1^\dagger h_2^\dagger v_3^\dagger h_4^\dagger\right]_{in}|0\rangle$. In $\left|\widetilde{\Phi^-}\right\rangle|\widetilde{\gamma_1}\rangle$, the possible terms are $df\left[h_1^\dagger h_2^\dagger v_3^\dagger v_4^\dagger\right]_{in}|0\rangle$ and $ce\left[v_1^\dagger v_2^\dagger h_3^\dagger h_4^\dagger\right]_{in}|0\rangle$. For specific setups, and specific values of d, e, c, and f, there is a possibility that some terms cancel out in the expansion of $\left|\widetilde{\Phi^+}\right\rangle|\widetilde{\gamma_1}\rangle$ but remain in that of $\left|\widetilde{\Phi^-}\right\rangle|\widetilde{\gamma_1}\rangle$. This is indeed what happens, as we will see.

Calculating the output states corresponding to (4.10) and (4.11) is quite difficult by hand. To prevent errors, the setup was simulated on Mathematica, and the success probabilities were calculated there too. For details of the code and calculation, please refer to the Appendix (A.1). In general, for arbitrary values of d, e, c, and f, all terms in $\left|\widetilde{\Phi^+}\right\rangle|\widetilde{\gamma_1}\rangle$ are also present in $\left|\widetilde{\Phi^-}\right\rangle|\widetilde{\gamma_1}\rangle$, only with different numerical coefficients. So there is no unambiguous discrimation between the $\left|\widetilde{\Phi^\pm}\right\rangle$ states, unless additional constraints are imposed on the parameters. A non-zero probability of unambiguous state discrimination is possible if one of four conditions are satisfied. These are: $de = cf$, $de = -cf$, $ce = df$ or $ce = -df$. Note that only one of these conditions can be imposed, as the parameters must satisfy normalization conditions as well. After placing one of these constraints, some terms selectively cancel out in one of the states, giving a non-zero success probability. Specifically for the setup in figure 4.2, it turns out that all of these four conditions are equivalent and give the same success probability.

If for example, we impose the condition $de = cf$, the sum of the absolute squared of all the terms

present exclusively in either $\left|\widetilde{\Phi^+}\right\rangle|\widetilde{\gamma_1}\rangle$ or $\left|\widetilde{\Phi^-}\right\rangle|\widetilde{\gamma_1}\rangle$ is given by

$$S = \frac{1}{2}|de + cf|^2 \tag{4.13}$$

S is plotted against e in figure 4.3 for the specific case of $c = 0.6$, and $d = 0.8$. Clearly, the maxima of the above function is $\frac{1}{2}$, when $e = d$ and $f = c$. This tells us that using an ancillary state of the exact same form as one of the non-maximally entangled pairs seems **most useful** in distinguishing between the states (see (4.11)). So, the maximum probability of unambiguous discrimination (assuming

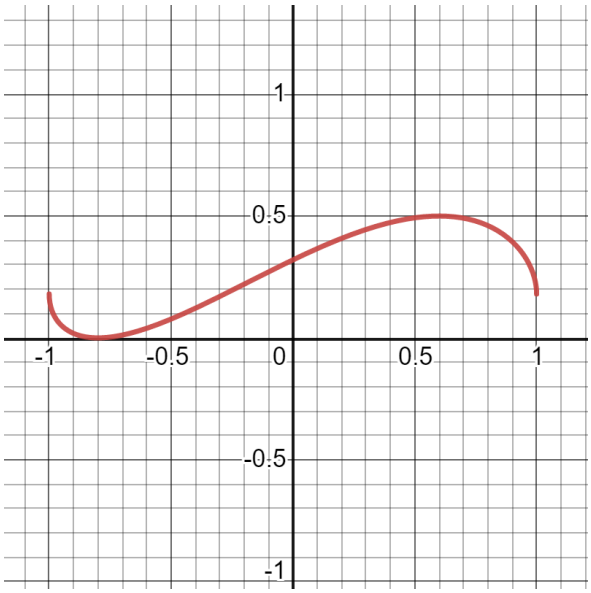

Figure 4.3: Probability S as a function of e; $d = 0.6, c = 0.8$. Maxima is at $e = d = 0.6$.

equiprobable initial states) is given by

$$\boxed{P = \frac{1}{4} \times \left[0 + 0 + \frac{1}{2}\right] = \frac{1}{8} \equiv 12.5\%} \tag{4.14}$$

To summarize, we used an ancillary non-maximally entangled state of the form (4.8). We discoved that this kind of state does not help in distinguishing between the $\left|\widetilde{\Psi^\pm}\right\rangle|\widetilde{\gamma_1}\rangle$ states irrespective of the values of e, f. However, it is useful to distinguish between the states $\left|\widetilde{\Phi^\pm}\right\rangle|\widetilde{\gamma_1}\rangle$ if the parameters e, f depend on c, d through any one of four relations: $ce = df$, $ce = -df$, $de = cf$, $de = -cf$. Irrespective of which relation is imposed, the maximum probability of unambiguous discrimination is 12.5%.

Compared to the case of Bell states, we can see that here the success probability is much lower. The reason this result leaps to 75% when $a = b$ and $c = d$ is two-fold. Firstly, the $\left|\widetilde{\Psi^\pm}\right\rangle$ states that could not be distinguished earlier, become completely distinguishable now (recall the results of section 3.2). Secondly, there are several additional terms that become unambiguous in the special case of $a = b = c = d = e = f$. These terms cancel out in $\left|\widetilde{\Phi^-}\right\rangle$ but remain in $\left|\widetilde{\Phi^+}\right\rangle$ and vice versa. As a result, the probability of success when $a = b$ and $c = d$ changes to

$$P = \frac{1}{4} \times \left[1 + 1 + \frac{1}{2} + \frac{1}{2}\right] = \frac{3}{4} \equiv 75\% \tag{4.15}$$

This result shows that distinguishing between non-maximally entangled states (a lesser resource than

the Bell states) in some cases can actually be a harder task than distinguishing between Bell states. Whether this is a general feature of all linear optical setups with ancillary entanglement is not known; this result might also be a artifact of the particular setup used. Therefore, further studies are required to generalize the claims made in this section.

4.3 Summary

This chapter addressed the question of distinguishing between Non-Maximally Entangled polarization states of two photons. The properties, uses, and experimental generation of these states were outlined. Distinguishing between the states using symmetric beam splitters is not possible. It was shown that using ancillary entanglement is only useful if the ancillary states are also partially entangled and have coefficients that depend on the specific states to be separated.

The example of one ancillary entangled pair in a specific setup proposed by Grice [Gri11] was described in detail. The most useful ancillary states were found to have exactly the same form as the NME states to be distinguished, and the maximum probability of discrimination was found to be 12.5%, a result far lower than the success obtained for the analogous case of Bell states (75%). This seems to suggest that distinguishing between partially entangled states using ancillary entanglement could be a much more difficult task, but more setups must be analyzed to substantiate this claim.

Chapter 5

GHZ states

In this chapter, we investigate the problem of distinguishing between the 3-qubit GHZ states in polarization, given by

$$\begin{aligned}
\left|\Psi_1^{\pm}\right\rangle &\equiv \frac{1}{\sqrt{2}}\left[h_1^\dagger h_2^\dagger h_3^\dagger \pm v_1^\dagger v_2^\dagger v_3^\dagger\right]_{in}|0\rangle = \frac{1}{\sqrt{2}}\left(|H,H,H\rangle \pm |V,V,V\rangle\right)\\
\left|\Psi_2^{\pm}\right\rangle &\equiv \frac{1}{\sqrt{2}}\left[h_1^\dagger h_2^\dagger v_3^\dagger \pm v_1^\dagger v_2^\dagger h_3^\dagger\right]_{in}|0\rangle = \frac{1}{\sqrt{2}}\left(|H,H,V\rangle \pm |V,V,H\rangle\right)\\
\left|\Psi_3^{\pm}\right\rangle &\equiv \frac{1}{\sqrt{2}}\left[h_1^\dagger v_2^\dagger h_3^\dagger \pm v_1^\dagger h_2^\dagger v_3^\dagger\right]_{in}|0\rangle = \frac{1}{\sqrt{2}}\left(|H,V,H\rangle \pm |V,H,V\rangle\right)\\
\left|\Psi_4^{\pm}\right\rangle &\equiv \frac{1}{\sqrt{2}}\left[v_1^\dagger h_2^\dagger h_3^\dagger \pm h_1^\dagger v_2^\dagger v_3^\dagger\right]_{in}|0\rangle = \frac{1}{\sqrt{2}}\left(|V,H,H\rangle \pm |H,V,V\rangle\right)
\end{aligned} \tag{5.1}$$

These orthogonal states form a basis for the 8-dimensional Hilbert space describing the polarization of three photons and were first studied by Greenberger, Horne, and Zelinger [GHZ89]. These form a class of entangled states for 3-qubits that is fundamentally different from another kind of states (W-states), in the sense that they cannot be transformed into each other through local operations and classical communication [DVC00]. The GHZ states have widely been used in several multipartite quantum information processes. Some examples are teleportation [KB98], quantum communication [GYW05], secret sharing [HBB99] [HHL11], and cryptography [CL04]. They have also been used to describe tests of local realism [GHSZ90]. Integral to generalized protocols for teleportation and dense coding is distinguishing between different GHZ states (GHZ-state analysis). Therefore, it is worth investigating how to do this.

The first question that we must address is, how are these states produced? One way to create GHZ entanglement is to use two Bell pairs and detect one photon in such a manner to collapse the remaining three photons into a GHZ state. This method was first demonstrated by Bouwmeester et al., [BPD$^+$99], and is presented here. Their experimental scheme is shown in figure 5.1. Here, a BBO crystal is pumped by an UV laser and produces entangled photons. For creating a GHZ state, we require the crystal to produce two Bell pairs in quick succession, giving rise to four photons. These photons travel through modes a and b, and then pass through a 50-50 beam splitter, two polarizing beam splitters and a half wave plate, before being detected by four detectors, D_1, D_2, D_3, and a trigger detector T.

The main result of the paper is the following: If the two photon pairs are indistinguishable, and all four detectors detect one photon each, then the state of the three photons reaching detectors

D_1, D_2, D_3 is a GHZ state. The idea behind this result is: if the experimental apparatus cannot distinguish between the two successive photon pairs, then one cannot tell which pair the photon reaching detector T belonged to. It turns out that erasing this information about the T photon leads to the required GHZ correlation for the remaining three photons. Note that the desired four-fold

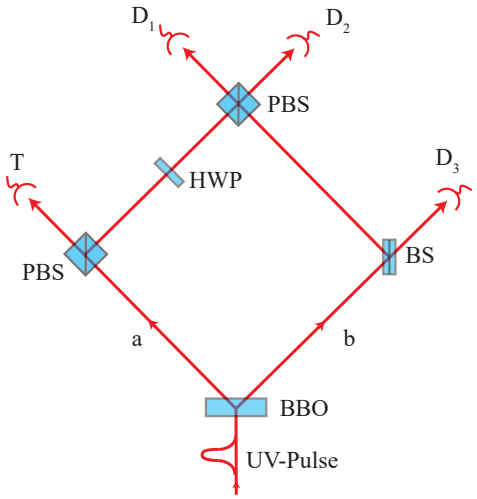

Figure 5.1: Setup to detect GHZ entanglement [BPD+99]

coincidence will not occur all the time; it is certainly possible that two photons reach one detector. However, such outcomes do not help in creating the GHZ state, as we will see. Let us study the setup in detail now. If each detector sees one photon, then a horizontally polarized photon must have reached T (because the PBS transmits $|H\rangle$ photons). This means that the other photon belonging to this entangled pair (which we'll call the companion photon) must be vertically polarized, and travels through mode b. Now, as it passes through the 50-50 beam splitter, there are two possibilities. Either it gets transmitted to detector D_3, or it gets reflected towards the PBS, where it is reflected again into D_2. So, we have realized that the companion photon of the one detected at T can reach either D_2 or D_3. Let us deal with the two cases one by one.

Consider the case where companion photon is detected at D_3. This means that the second entangled pair must have reached D_1 and D_2. We now study this second photon pair. The photon in mode a could not have been horizontally polarized, since if it was the PBS would transmit it towards T. So, the photon in mode a must be vertically polarized, and the photon in mode b must be horizontally polarized. The photon in a then passes through a HWP, where it is transformed into the state $\frac{1}{\sqrt{2}}(|H\rangle + |V\rangle)$. This photon now is equally likely to be detected at D_1 and D_2. The photon in mode b passes through the beam splitter towards D_3 with a 50% chance, and is reflected with a 50% chance towards the PBS, where it will get transmitted to D_1. If we restrict our interest to the case where each detector measures only one photon, we know that the b photon reaches D_1 (since a photon from the first pair already reached D_3), and thus the a photon must've reached D_2. This means that it must've been horizontally polarized. Therefore, we conclude that if the companion photon of T reaches D_3, then the state of the three photons at the D detectors must be $|H\rangle_1 |H\rangle_2 |V\rangle_3$.

Let us now consider the other scenario, where the vertically polarized companion photon of T reaches D_2. In this case, the photon in mode a, after passing through the HWP must reach D_1. This means that it must have been vertically polarized as well. Finally, the companion photon of the second pair, which is horizontally polarized in mode b must be transmitted by the beam splitter into D_3. Thus,

the state of the 3 photons in the D detectors in this case is clearly $|V\rangle_1 |V\rangle_2 |H\rangle_3$.

In principle, these two outcomes can be distinguishable if the time at which the detectors click can be measured exactly. In the first scenario, the two detectors T and D_3 would detect their photons together, whereas the detectors D_1 and D_2 might detect their photons slightly later, or vice versa. However, if the UV pulse is considerably shorter than the coherence time of the photons (as was in the experiment), then we can't distinguish between the above two scenarios. Therefore, the state of the three photons must have been the superposition state

$$|\Psi\rangle = \frac{1}{\sqrt{2}} \left(|H\rangle_1 |H\rangle_2 |V\rangle_3 \pm |V\rangle_1 |V\rangle_2 |H\rangle_3 \right) \tag{5.2}$$

This is how a GHZ state can be created. To figure out the exact sign in equation (5.2), an explicit calculation can be done that tracks the evolution of the states. Consider the following four-photon state, created as a result of two down-conversions.

$$|\psi\rangle = \frac{1}{2} \left(|H\rangle_a |V\rangle_b - |V\rangle_a |H\rangle_b \right) \left(|H\rangle_a^{'} |V\rangle_b^{'} - |V\rangle_a^{'} |H\rangle_b^{'} \right) \tag{5.3}$$

As discussed, individual terms $|H\rangle_a, |V\rangle_a, |H\rangle_b, |H\rangle_b$ evolve through the setup as (the same relations hold for the primed states)

$$\begin{aligned} |H\rangle_a &\rightarrow |H\rangle_T \\ |H\rangle_b &\rightarrow \frac{1}{\sqrt{2}} (|H\rangle_1 + |H\rangle_3) \\ |V\rangle_a &\rightarrow \frac{1}{\sqrt{2}} (|H\rangle_2 + |V\rangle_1) \\ |V\rangle_b &\rightarrow \frac{1}{\sqrt{2}} (|V\rangle_2 + |V\rangle_3) \end{aligned} \tag{5.4}$$

Using these relations in (5.11), we get

$$\begin{aligned} &\frac{1}{2} \left(|H\rangle_a |V\rangle_b - |V\rangle_a |H\rangle_b \right) \left(|H\rangle_a^{'} |V\rangle_b^{'} - |V\rangle_a^{'} |H\rangle_b^{'} \right) \rightarrow \\ &\frac{1}{4} \left(|H\rangle_T \sqrt{2} \, (|V\rangle_2 + |V\rangle_3) - (|H\rangle_2 + |V\rangle_1)(|H\rangle_1 + |H\rangle_3) \right) \left(|H\rangle_T^{'} \frac{1}{\sqrt{2}} (|V\rangle_2^{'} + |V\rangle_3^{'}) - \frac{1}{2} (|H\rangle_2^{'} + |V\rangle_1^{'})(|H\rangle_1^{'} + |H\rangle_3^{'}) \right) \end{aligned} \tag{5.5}$$

Collecting only those terms where one photon reaches the detector T, we get

$$-\frac{1}{4\sqrt{2}} \left(|H\rangle_T \ (|V\rangle_2 + |V\rangle_3)(|H\rangle_2^{'} + |V\rangle_1^{'})(|H\rangle_1^{'} + |H\rangle_3^{'}) + |H\rangle_T^{'} (|H\rangle_2 + |V\rangle_1)(|H\rangle_1 + |H\rangle_3)(|V\rangle_2^{'} + |V\rangle_3^{'}) \right) \tag{5.6}$$

Further, we pick those terms where there is a single photon detection at all four detectors. This gives us

$$-\frac{1}{4\sqrt{2}} \left(|H\rangle_T \ (|V\rangle_2 |V\rangle_1^{'} |H\rangle_3^{'} + |V\rangle_3 |H\rangle_2^{'} |H\rangle_1^{'}) + |H\rangle_T^{'} (|H\rangle_2 |H\rangle_1 |V\rangle_3^{'} + |V\rangle_1 |H\rangle_3 |V\rangle_2^{'} \right) \tag{5.7}$$

Till now, we've assumed that the two photon pairs are distinguishable. If this assumption is removed, then we must make no distinction between the primed and unprimed states. This gives us the final (normalized) state

$$|\psi\rangle = \frac{1}{\sqrt{2}} |H_T\rangle \left(|H\rangle_1 |H\rangle_2 |V\rangle_3 + |V\rangle_1 |V\rangle_2 |H\rangle_3 \right) \tag{5.8}$$

Thus, we have indeed produced a GHZ state. To summarize, a GHZ-type correlation is only detected

if the time delay between the production of both pairs is smaller than the coherence time of the photons (i.e., both photon pairs are indistinguishable), and if a four-fold coincidence is observed in the detectors D_1, D_2, D_3, and T. This state can be converted into any of the other seven GHZ states using local unitary operations on one of the photons.

Now that we have discussed a method for creating GHZ entanglement, we proceed to the main issue addressed in this chapter: distinguishing between the eight GHZ states. Separating states across two different sets is always possible by simply passing the above states through three polarizing beam splitters. The crucial question to ask is whether we can distinguish within one set (say $\left|\Psi_1^{\pm}\right\rangle$). Let's say we were to pass these states through a 3X3 symmetric beam splitter (known as the 'tritter'), which performs the transformation

$$\begin{pmatrix} a_1^\dagger \\ a_2^\dagger \\ a_3^\dagger \end{pmatrix}_{in} \rightarrow \begin{bmatrix} 1 & 1 & 1 \\ 1 & \omega & \omega^2 \\ 1 & \omega^2 & \omega \end{bmatrix} \begin{pmatrix} a_1^\dagger \\ a_2^\dagger \\ a_3^\dagger \end{pmatrix}_{out} \quad a \in \{h, v\} \tag{5.9}$$

where ω is the cube root of unity; $\omega^3 = 1$.
The states $\left|\Psi_1^{\pm}\right\rangle$ transform as

$$\left|\Psi_1^{\pm}\right\rangle \rightarrow \frac{1}{3\sqrt{6}} \left[(h_1^{\dagger 3} + h_2^{\dagger 3} + h_3^{\dagger 3} - h_1^\dagger h_2^\dagger h_3^\dagger) \pm (v_1^{\dagger 3} + v_2^{\dagger 3} + v_3^{\dagger 3} - 3v_1^\dagger v_2^\dagger v_3^\dagger)\right]_{out} |0\rangle \tag{5.10}$$

Clearly, both states have the same terms and can't be distinguished from each other. In fact, we don't have to calculate out the expressions to see this. Each of the four states in (5.1) contains two terms (one on either side of the $\pm$ sign) which differ in the number of h and v operators in them. This means that when we use (5.9) to write out the output states, there will be no cancellation across the $\pm$ sign. Thus, $|\Psi^+\rangle$ cannot be distinguished from $|\Psi^-\rangle$ for all the four pairs of states in (5.1).

So, we have seen that passing the GHZ states through a symmetric 3X3 beam splitter does not help with their unambiguous discrimination. In fact, the above statement holds in more general situations, as discussed below.

Result: Mixing the spatial modes of creation operators alone without changing polarization (i.e., an arbitrary configuration of beam splitters and phase shifters) cannot distinguish *within* a set of states in (5.1).

The justification for this result is as follows: All the four sets of states above have different numbers of h and v operators across the $\pm$ sign. Since the beam splitters do not change the polarization of photons, no cancellation can arise that creates a difference between $\left|\Psi_i^+\right\rangle$ and $\left|\Psi_i^-\right\rangle$. It must be noted that for the Bell states, a symmetric beam splittler was able to distinguish between two of the four states, $|\Psi^+\rangle$ and $|\Psi^-\rangle$ because both terms across the $\pm$ had only one h and v each.

The above reasoning seems to suggest that for distinguishing between the GHZ states, it might be necessary to use setups that change polarization, making use of gadgets like half-wave plates, etc. However, as a starting point, my analysis in this chapter only involves setups that don't change polarization. A future direction is to extend the results obtained in this chapter to more general setups that change polarization.

5.1 Squeezing

Motivated from the paper of Zaidi and Loock [ZvL13], a natural question to ask would be if gaussian squeezing operations can help with distinguishing between the GHZ states. Since a 3X3 beam splitter does not help at all, I decided to investigate the following two scenarios separately:

1. Passing the states through 3 single-mode squeezers directly, without a beam splitter.
2. Passing the states through a beam splitter and then single-mode squeezers

Both these possibilities are discussed below.

5.1.1 Without a beam splitter

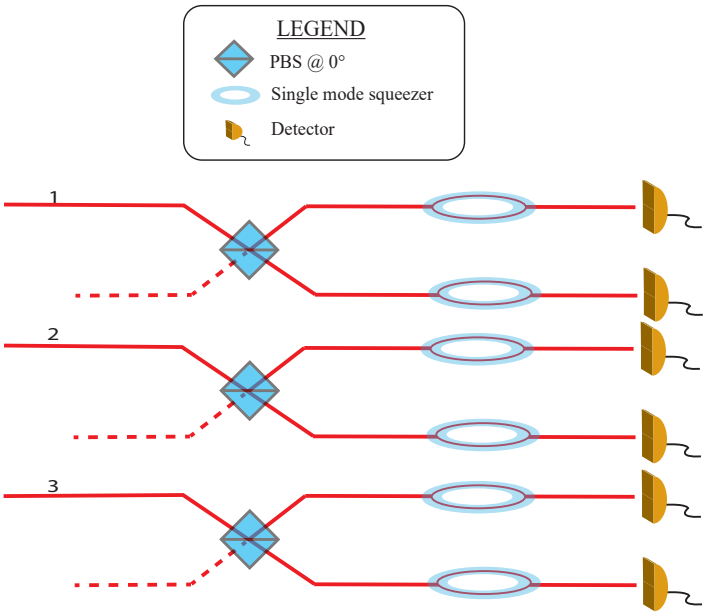

Figure 5.2: Passing the states through three polarizing beam splitters, and then single-mode squeezers

We assume that the polarizing beam splitters transmit horizontally polarized and reflect vertically polarized photons. After this operation, what will the final states be? Let us take an example. If we send in the state $|H, H, H\rangle$, then all the photons will be transmitted through the polarizing beam splitter and will be detected at the 1st, 3rd, and the 5th detector. This resultant state will be represented as $|101010\rangle$, where the ith number in the ket denotes the number of photons reaching the ith detector. Similarly, the state $|V, V, V\rangle$ will result in the opposite state after the PBS, $|010101\rangle$, since all photons will be reflected.
In this manner, the evolution of all the 8 GHZ states can be calculated to be

$$\begin{aligned}
\left|\Psi_1^{\pm}\right\rangle &= \frac{1}{\sqrt{2}}\left(|H,H,H\rangle \pm |V,V,V\rangle\right) \rightarrow \frac{1}{\sqrt{2}}\left[|101010\rangle \pm |010101\rangle\right] \\
\left|\Psi_2^{\pm}\right\rangle &= \frac{1}{\sqrt{2}}\left(|H,H,V\rangle \pm |V,V,H\rangle\right) \rightarrow \frac{1}{\sqrt{2}}\left[|101001\rangle \pm |010110\rangle\right] \\
\left|\Psi_3^{\pm}\right\rangle &= \frac{1}{\sqrt{2}}\left(|H,V,H\rangle \pm |V,H,V\rangle\right) \rightarrow \frac{1}{\sqrt{2}}\left[|100110\rangle \pm |011001\rangle\right] \\
\left|\Psi_4^{\pm}\right\rangle &= \frac{1}{\sqrt{2}}\left(|V,H,H\rangle \pm |H,V,V\rangle\right) \rightarrow \frac{1}{\sqrt{2}}\left[|011010\rangle \pm |100101\rangle\right]
\end{aligned} \tag{5.11}$$

At this point, we can distinguish between the states from different sets ($\left|\Psi_i^{\pm}\right\rangle$), but not within a set. Since squeezing adds photons in pairs, the terms in $\left|\Psi_1^{\pm}\right\rangle$ after squeezing will all be of the form $|$odd, even, odd, even, odd, even$\rangle$ or $|$even, odd, even, odd, even, odd$\rangle$. This signature does not appear in the other three states. It is obvious that each set of states has a distinct signature. Given perfect photon number resolving detectors, we can thus always distinguish *between* different sets even after squeezing.

Unfortunately, we cannot distinguish within a set. This is because each $\left|\Psi_i^{\pm}\right\rangle$ is a combination of two states with exactly opposite odd/even parity in each spatial mode (in this context, by parity, I mean the odd/even structure of the photon numbers at the detectors. For example, the state $|111110\rangle$ has the same parity as the state $|313332\rangle$, as both have the structure $|$odd, odd, odd, odd, odd, even$\rangle$. On the other hand, $|111110\rangle$ and $|200203\rangle$ have opposite parity). Now, $\left|\Psi_3^{\pm}\right\rangle$ before squeezing has the terms $|100110\rangle$ and $|011001\rangle$. After squeezing, both these states would give rise to infinite terms - but their signature would always be $|$odd, even, even, odd, odd, even$\rangle$ and $|$even, odd, odd, even, even, odd$\rangle$ respectively. So, there can never be a cancellation across the $\pm$ sign, and thus $\left|\Psi_i^{+}\right\rangle$ can never be told apart from $\left|\Psi_i^{-}\right\rangle$ using squeezing.

5.1.2 With a beam splitter

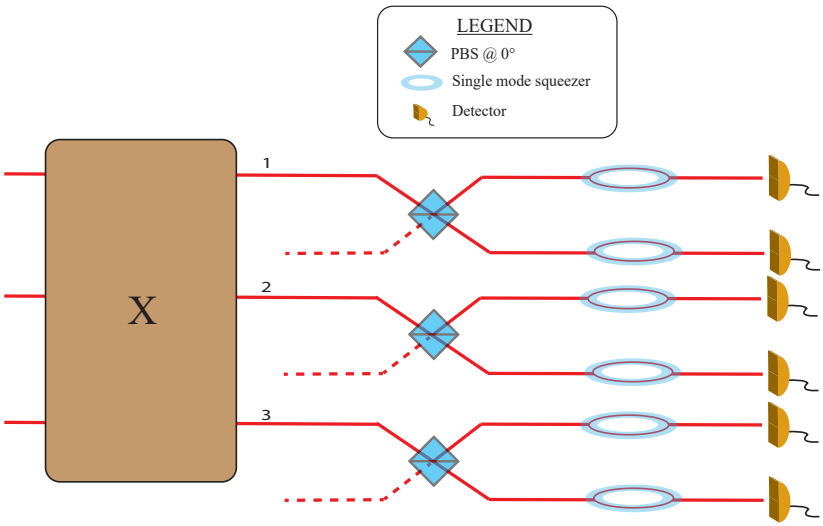

Figure 5.3: General setup with single mode squeezers

Consider the setup in figure 5.3, where X is some arbitrary mixing of spatial modes. The question we ask is: does gaussian squeezing after the unitary X help in discriminating between $\left|\Psi_i^{+}\right\rangle$ and $\left|\Psi_i^{-}\right\rangle$?

Let us take the example of $\left|\Psi_2^{\pm}\right\rangle$. After passing through any configuration of beam splitters, terms in the state can only be of the form: $h_i^\dagger h_j^\dagger v_k^\dagger \pm v_l^\dagger v_m^\dagger h_n^\dagger$ (indices can take same values). Before squeezing, these terms can never cancel each other. The question is, can there be a cancellation after squeezing?

The answer is no, because both these terms will never have the same parity after the PBSs. For example, if the state after X is $h_1^{\dagger 2} v_3^\dagger$, then the state after the PBSs is $|200001\rangle$ ($|$even,even,even,even,even,odd$\rangle$). Other 3-photon states with the same parity are: $|020001\rangle$, $|002001\rangle$, $|000201\rangle$, $|000021\rangle$ and $|000003\rangle$. If any of these states were on the other side of the $\pm$, then there **is** a possibility of cancellation after squeezing. But a close look at these terms reveals the following: since the output state must

have atleast one $h^\dagger$ operator, $|020001\rangle$ $(v_1^{\dagger 2} v_3^\dagger)$, $|000201\rangle$ $(v_2^{\dagger 2} v_3^\dagger)$ and $|000003\rangle$ $(v_3^{\dagger 3})$ can be ruled out. The remaining two possibilities can arise only because of the term on the same side of the $\pm$ sign. Therefore, terms on both sides of the $\pm$ sign can never cancel each other even after squeezing, leading to the exact same terms for both $\left|\Psi_2^+\right\rangle$ and $\left|\Psi_2^-\right\rangle$.

So, single-mode squeezing operations after **any** configuration of beam splitters (without ancillary photons) retain distinguishability across sets but do not help in distinguishing within a set. The basic reason why this is so can be traced down to the fact that GHZ states are built out of a tensor product of an odd number of Hilbert spaces, whereas squeezing always adds photons in even numbers. This is why gaussian squeezing was useful in Bell state analysis (two-qubit states) but fails to help here.

Note: The above conclusions might not generalize to setups that do change polarization; squeezing might be a useful resource in such situations.

5.2 Maximum possible success using linear optics (and no additional resources)

As discussed above, purely spatial mixing of the creation operators is not sufficient to distinguish between the GHZ states. An upper bound on the success probability of GHZ-analysis using purely linear optical elements was set by Jian-wei Pan and Anton Zelinger in their 1998 paper [PZ98]. They showed that only two of the eight states can be completely separated, also providing a simple experimental setup that implemented this 25% efficient GHZ-state analyzer.

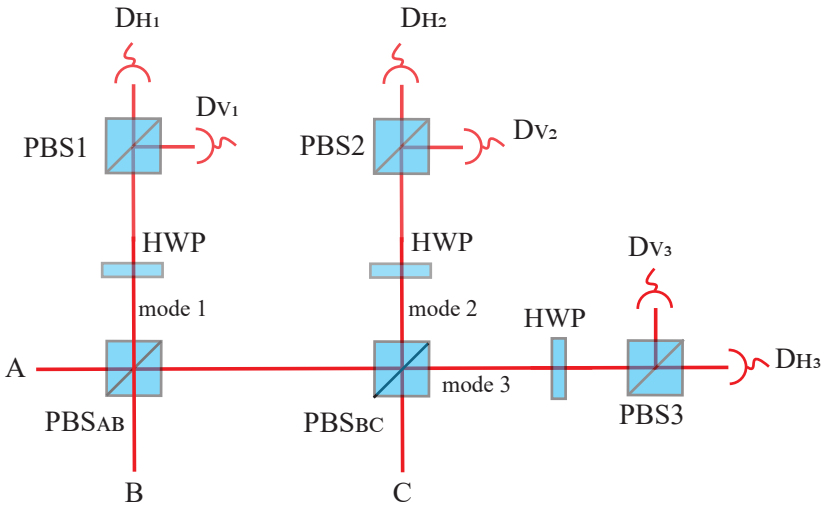

Figure 5.4: Linear optics GHZ state analysis [PZ98]

The three photons of the GHZ state pass are incident onto two polarizing beam splitters through modes A,B, and C. The PBSs transmit horizontally polarized photons. So, if the state $|H_A\rangle |H_B\rangle |V_C\rangle$ is incident onto PBSs, the photon from B passes straight through to mode 1. Further, the photon in mode A gets transmitted twice into mode 3. However, the vertically polarized photon from mode C gets reflected by PBS_{BC} into mode 3, leading to the final state $|H_1\rangle |H_3\rangle |V_3\rangle$. Calculating the

evolution of all states in (5.1) through the PBSs in a similar fashion, we get:

$$\begin{aligned}
\left|\Psi_1^{\pm}\right\rangle &\equiv \frac{1}{\sqrt{2}}\left(|H_A\rangle|H_B\rangle|H_C\rangle \pm |V_A\rangle|V_B\rangle|V_C\rangle\right) \rightarrow \frac{1}{\sqrt{2}}\left(|H_1\rangle|H_2\rangle|H_3\rangle \pm |V_1\rangle|V_2\rangle|V_3\rangle\right) \\
\left|\Psi_2^{\pm}\right\rangle &\equiv \frac{1}{\sqrt{2}}\left(|H_A\rangle|H_B\rangle|V_C\rangle \pm |V_A\rangle|V_B\rangle|H_C\rangle\right) \rightarrow \frac{1}{\sqrt{2}}\left(|H_1\rangle|H_3\rangle|V_3\rangle \pm |V_1\rangle|H_2\rangle|V_2\rangle\right) \\
\left|\Psi_3^{\pm}\right\rangle &\equiv \frac{1}{\sqrt{2}}\left(|H_A\rangle|V_B\rangle|H_C\rangle \pm |V_A\rangle|H_B\rangle|V_C\rangle\right) \rightarrow \frac{1}{\sqrt{2}}\left(|H_2\rangle|V_2\rangle|H_3\rangle \pm |H_1\rangle|V_1\rangle|V_3\rangle\right) \\
\left|\Psi_4^{\pm}\right\rangle &\equiv \frac{1}{\sqrt{2}}\left(|V_A\rangle|H_B\rangle|H_C\rangle \pm |V_A\rangle|V_B\rangle|H_C\rangle\right) \rightarrow \frac{1}{\sqrt{2}}\left(|H_1\rangle|V_1\rangle|H_2\rangle \pm |V_2\rangle|H_3\rangle|V_3\rangle\right)
\end{aligned} \tag{5.12}$$

Notice that only the states $\left|\Psi_1^{\pm}\right\rangle$ have a photon in each of the modes 1,2, and 3 after the PBSs. So, only these two states can set off detectors D_1, D_2, D_3 simultaneously. Thus, we can already tell this pair of states apart from the other six states. But how can we distinguish within these two states? The Half Wave Plates (HWP) enable us to further separate $\left|\Psi_1^{+}\right\rangle$ from $\left|\Psi_1^{-}\right\rangle$. The action of these HWPs is given by:

$$\begin{aligned}
|H_i\rangle &\rightarrow \frac{1}{\sqrt{2}}\left(|H_i\rangle + |V_i\rangle\right) \\
|V_i\rangle &\rightarrow \frac{1}{\sqrt{2}}\left(|H_i\rangle - |V_i\rangle\right)
\end{aligned} \tag{5.13}$$

where $i = \{1, 2, 3\}$. The evolution of $\left|\Psi_1^{\pm}\right\rangle$ through the HWPs is then

$$\left|\Psi_1^{\pm}\right\rangle \xrightarrow{\text{HWPs}} \frac{1}{4\sqrt{2}}\left[\left(|H_1\rangle + |V_1\rangle\right)\left(|H_2\rangle + |V_2\rangle\right)\left(|H_3\rangle + |V_3\rangle\right) \pm \left(|H_1\rangle - |V_1\rangle\right)\left(|H_2\rangle - |V_2\rangle\right)\left(|H_3\rangle - |V_3\rangle\right)\right] \tag{5.14}$$

Simplifying the above expression, we get for the two states

$$\begin{aligned}
\left|\Psi_1^{+}\right\rangle &\rightarrow \frac{1}{2}\left(|H_1\rangle|H_2\rangle|H_3\rangle + |H_1\rangle|V_2\rangle|V_3\rangle + |V_1\rangle|H_2\rangle|V_3\rangle + |V_1\rangle|V_2\rangle|H_3\rangle\right) \\
\left|\Psi_1^{-}\right\rangle &\rightarrow \frac{1}{2}\left(|V_1\rangle|V_2\rangle|V_3\rangle + |H_1\rangle|H_2\rangle|V_3\rangle + |V_1\rangle|H_2\rangle|H_3\rangle + |H_1\rangle|V_2\rangle|H_3\rangle\right)
\end{aligned} \tag{5.15}$$

Clearly, the terms in both states don't have any overlap. So, the second set of polarizing beam splitters ensure that the detector outcomes are completely different for the states $\left|\Psi_1^{+}\right\rangle$ and $\left|\Psi_1^{-}\right\rangle$. Thus, this linear optics setup can deterministically separate out 2 out of the 8 GHZ states. Teleportation with the above apparatus for state discrimination will succeed with a probability of 25%. Moreover, this setup can also be used to create GHZ entanglement. For example, if three particles, each independently belonging to a Bell pair are sent into the setup and collapsed into a GHZ state, the three remaining particles would also be described by a GHZ state.

As discussed before, we would like to enhance this probability using other resources. In the following sections, I discuss some literature and original results along this direction.

5.3 Ancillary Entanglement

In this section, we explore the possibility of distinguishing between the GHZ states using additional entanglement as a resource. Our analysis is restricted to polarization-preserving setups; those that don't contain wave-plates. More general setups will be investigated in the future. We first consider using only ancillary Bell states and then move on to exploring other kinds of states.

5.3.1 Ancillary Bell pairs

Let us assume that we're provided with an ancillary Bell state of the form

$$\left|\Phi^+_{Bell}\right\rangle \equiv \frac{1}{\sqrt{2}}\left[h_4^\dagger h_5^\dagger + v_4^\dagger v_5^\dagger\right]_{in}|0\rangle = \frac{1}{\sqrt{2}}\left(|H,H\rangle + |V,V\rangle\right) \tag{5.16}$$

Our task is to distinguish between the states

$$\left|\Psi^\pm_1\right\rangle\left|\Phi^+_{Bell}\right\rangle \equiv \frac{1}{2}\left[\left(h_1^\dagger h_2^\dagger h_3^\dagger \pm v_1^\dagger v_2^\dagger v_3^\dagger\right)\left(h_4^\dagger h_5^\dagger + v_4^\dagger v_5^\dagger\right)\right]_{in}|0\rangle \tag{5.17}$$

The output state depends on the particular unitary mapping connecting the input to output modes. Without discussing a specific experimental setup, we will first try to make general statements about discriminating between the above states.

It is useful to classify the four input terms in (5.17) according to the number of h and v operators they contain. The term with 3 $h^\dagger$ operators and 2 $v^\dagger$ operators will be represented as $[3,2]$, and so on. This 'bracket representation' is useful for two reasons:

- For **any** setup that does not change the polarization of the photons, the above classification will remain the same for all the output terms that result out of an input term. For instance, we can be sure that a $[5,0]$ input term will give rise to output terms all of which will be $[5,0]$ (i.e, contain only horizontally polarized photons) as well.
- Two terms with different bracket representations do not interact with each other and can never cancel. Therefore, this gives us a convenient way to compare the final output terms.

For the terms in (5.17), we have four possible brackets: $[3,2],[2,3],[5,0],[0,5]$. Since each input term has a unique bracket, there can never be cancellations between two input terms. Essentially, the four input terms don't interact with each other even when the state is expanded in terms of the output operators. The state $\left|\Psi^+_1\right\rangle\left|\Phi^+_{Bell}\right\rangle$ cannot have unique terms that are absent in $\left|\Psi^-_1\right\rangle\left|\Phi^+_{Bell}\right\rangle$ and vice versa.

Therefore, using the ancillary Bell state $\left|\Phi^+_{Bell}\right\rangle$ does not help in distinguishing between $\left|\Psi^\pm_1\right\rangle$. What about the states $\left|\Psi^\pm_2\right\rangle, \left|\Psi^\pm_3\right\rangle, \left|\Psi^\pm_4\right\rangle$? Can $\left|\Phi^+_{Bell}\right\rangle$ help distinguish between these states? Firstly, notice that these states are identical in their bracket representations:

$$\begin{aligned}
\left|\Psi^\pm_2\right\rangle &= \frac{1}{\sqrt{2}}\left[h_1^\dagger h_2^\dagger v_3^\dagger \pm v_1^\dagger v_2^\dagger h_3^\dagger\right]_{in}|0\rangle \equiv \frac{1}{\sqrt{2}}\left([2,1]\pm[1,2]\right)|0\rangle \\
\left|\Psi^\pm_3\right\rangle &= \frac{1}{\sqrt{2}}\left[h_1^\dagger v_2^\dagger h_3^\dagger \pm v_1^\dagger h_2^\dagger v_3^\dagger\right]_{in}|0\rangle \equiv \frac{1}{\sqrt{2}}\left([2,1]\pm[1,2]\right)|0\rangle \\
\left|\Psi^\pm_4\right\rangle &= \frac{1}{\sqrt{2}}\left[v_1^\dagger h_2^\dagger h_3^\dagger \pm h_1^\dagger v_2^\dagger v_3^\dagger\right]_{in}|0\rangle \equiv \frac{1}{\sqrt{2}}\left([2,1]\pm[1,2]\right)|0\rangle
\end{aligned} \tag{5.18}$$

For this reason, the states $\left|\Psi^\pm_2\right\rangle, \left|\Psi^\pm_3\right\rangle, \left|\Psi^\pm_4\right\rangle$ will be collectively referred to as $|\Psi_i\rangle$, $i=2,3,4$.

$$\begin{aligned}
\left|\Psi^\pm_i\right\rangle\left|\Phi^+_{Bell}\right\rangle &\equiv \frac{1}{2}\left[\left([2,1]\pm[1,2]\right)\left([2,0]+[0,2]\right)\right]_{in}|0\rangle \\
&\equiv \frac{1}{2}\left[\left([4,1]+[2,3]\right)\pm\left([3,2]+[1,4]\right)\right]_{in}|0\rangle
\end{aligned} \tag{5.19}$$

When two brackets $[a,b]$ and $[c,d]$ multiply, the result is simply $[a+c,b+d]$, since the number of $h^\dagger$ and $v^\dagger$ operators just add up. In the above equation, all the four terms have different bracket

representations. Clearly then, they don't interact with each other, and $\left|\Phi^+_{Bell}\right\rangle$ does not help in distinguishing between the states $|\Psi_i\rangle$ as well. Had there been a [2,3] term on both sides of the $\pm$ sign, then there would be a chance of discrimination because when the state is expanded in terms of the output operators, some cancellations can happen differently for $\left|\Psi^+_i\right\rangle$ and $\left|\Psi^-_i\right\rangle$

Therefore, using a Bell state of the form $\left|\Phi^+_{Bell}\right\rangle$ in a polarization-preserving setting does not help in discriminating between the GHZ states. Further, it turns out that **none** of the four Bell states help us as ancillaries to distinguish between the GHZ states. The case for the ancillary state $\left|\Psi^+_{Bell}\right\rangle$ is shown below - clearly, no cancellation can take place.

$$\begin{aligned}\left|\Psi^\pm_1\right\rangle\left|\Psi^+_{Bell}\right\rangle &\equiv \frac{1}{2}\left[\left([3,0]\pm[0,3]\right)\left([1,1]+[1,1]\right)\right]_{in}|0\rangle \\ &\equiv \frac{1}{2}\left[\left([4,1]\right)\pm\left([1,4]\right)\right]_{in}|0\rangle\end{aligned} \tag{5.20}$$

$$\begin{aligned}\left|\Psi^\pm_i\right\rangle\left|\Psi^+_{Bell}\right\rangle &\equiv \frac{1}{2}\left[\left([2,1]\pm[1,2]\right)\left([1,1]+[1,1]\right)\right]_{in}|0\rangle \\ &\equiv \frac{1}{2}\left[\left([3,2]\right)\pm\left([2,3]\right)\right]_{in}|0\rangle\end{aligned} \tag{5.21}$$

So, it seems like using one Bell pair is not useful. The next question one could ask is: what if we use more Bell states? Consider discriminating between

$$\begin{aligned}\left|\Psi^\pm_1\right\rangle\left|\Phi^+_{Bell}\right\rangle\left|\Phi^+_{Bell}\right\rangle &= \frac{1}{2\sqrt{2}}\left[\left(h_1^\dagger h_2^\dagger h_3^\dagger \pm v_1^\dagger v_2^\dagger v_3^\dagger\right)\left(h_4^\dagger h_5^\dagger + v_4^\dagger v_5^\dagger\right)\left(h_6^\dagger h_7^\dagger + v_6^\dagger v_7^\dagger\right)\right]_{in}|0\rangle \\ &\equiv \frac{1}{2\sqrt{2}}\left[\left([3,0]\pm[0,3]\right)\left([2,0]+[0,2]\right)\left([2,0]+[0,2]\right)\right]|0\rangle \\ &\equiv \frac{1}{2\sqrt{2}}\left[\left([3,0]\pm[0,3]\right)\left([4,0]+2[2,2]+[0,4]\right)\right]|0\rangle \\ &\equiv \frac{1}{2\sqrt{2}}\left[\left([7,0]+2[5,2]+[3,4]\right)\pm\left([4,3]+2[2,5]+[0,7]\right)\right]|0\rangle\end{aligned} \tag{5.22}$$

Clearly, the output states will yield identical detector outcomes, and we cannot separate one state from another.

Unsurprisingly, the above result can be extended to any number of ancillary Bell states. Suppose we possess the following (unnormalized) ancillary state

$$\begin{aligned}|\beta\rangle &= \left|\Phi^+_{Bell}\right\rangle^{\otimes k}\left|\Phi^-_{Bell}\right\rangle^{\otimes l}\left|\Psi^+_{Bell}\right\rangle^{\otimes m}\left|\Psi^-_{Bell}\right\rangle^{\otimes n} \\ &\equiv \left[\left([2,0]+[0,2]\right)^k\left([2,0]-[0,2]\right)^l\left([1,1]+[1,1]\right)^m\left([1,1]-[1,1]\right)^n\right]_{in}|0\rangle\end{aligned} \tag{5.23}$$

Consider the evolution of this state through a general setup. Once expanded in terms of the output operators, there are only two possibilities. Either all terms are [odd,odd], or all terms are [even,even]. This feature of Bell ancillaries renders them useless to discriminate between GHZ states. Since GHZ states are three-photon states, the number of creation operators must be odd. Therefore, a GHZ state always has terms of the form [even, odd] or [odd, even]. For instance, consider the states

$$\begin{aligned}\left|\Psi^\pm_1\right\rangle|\beta\rangle &\to \left[\left(h_1^\dagger h_2^\dagger h_3^\dagger \pm v_1^\dagger v_2^\dagger v_3^\dagger\right)_{in}|0\rangle\right]\otimes|\beta\rangle \\ &\equiv \left[\left([3,0]\pm[0,3]\right)\left([\text{even,even}]\text{ or }[\text{odd,odd}]\right)\right]|0\rangle\end{aligned} \tag{5.24}$$

$$\begin{aligned}[3,0][\text{odd,odd}] &\rightarrow [\text{even,odd}] \\ [0,3][\text{odd,odd}] &\rightarrow [\text{odd,even}]\end{aligned} \tag{5.25}$$

Clearly, no term from [3,0] [even,even] (or [3,0] [odd,odd]) can match with [0,3] [even,even] (or [0,3] [odd,odd]). Therefore, the ancillary state $|\beta\rangle$ does not help in distinguishing between the states $\left|\Psi_1^{\pm}\right\rangle$. For the same reason, we can't hope to separate the states $\left|\Psi_i^{\pm}\right\rangle$ as well.

Therefore, any number of ancillary Bell pairs in a polarization-preserving linear optical setup do not help with distinguishing between the GHZ states.

5.3.2 One ancillary GHZ state

In this section, we investigate using ancillary 3-photon states of the same form as the GHZ states itself. We assume that the particular ancillary state used (called $|\gamma_1\rangle$) is just the $\left|\Psi_1^{+}\right\rangle$ state in (4.1). Therefore, the goal is now to distinguish between the states

$$\begin{aligned}\left|\Psi_1^{\pm}\right\rangle|\gamma_1\rangle &\equiv \frac{1}{2}\left[(h_1^\dagger h_2^\dagger h_3^\dagger \pm v_1^\dagger v_2^\dagger v_3^\dagger)(h_4^\dagger h_5^\dagger h_6^\dagger + v_4^\dagger v_5^\dagger v_6^\dagger)\right]_{in}|0\rangle \\ \left|\Psi_2^{\pm}\right\rangle|\gamma_1\rangle &\equiv \frac{1}{2}\left[(h_1^\dagger h_2^\dagger v_3^\dagger \pm v_1^\dagger v_2^\dagger h_3^\dagger)(h_4^\dagger h_5^\dagger h_6^\dagger + v_4^\dagger v_5^\dagger v_6^\dagger)\right]_{in}|0\rangle \\ \left|\Psi_3^{\pm}\right\rangle|\gamma_1\rangle &\equiv \frac{1}{2}\left[(h_1^\dagger v_2^\dagger h_3^\dagger \pm v_1^\dagger h_2^\dagger v_3^\dagger)(h_4^\dagger h_5^\dagger h_6^\dagger + v_4^\dagger v_5^\dagger v_6^\dagger)\right]_{in}|0\rangle \\ \left|\Psi_4^{\pm}\right\rangle|\gamma_1\rangle &\equiv \frac{1}{2}\left[(v_1^\dagger h_2^\dagger h_3^\dagger \pm h_1^\dagger v_2^\dagger v_3^\dagger)(h_4^\dagger h_5^\dagger h_6^\dagger + v_4^\dagger v_5^\dagger v_6^\dagger)\right]_{in}|0\rangle\end{aligned} \tag{5.26}$$

The choice of this ancillary state makes it impossible to distinguish within the sets $\left|\Psi_2^{\pm}\right\rangle|\gamma_1\rangle, \left|\Psi_3^{\pm}\right\rangle|\gamma_1\rangle, \left|\Psi_4^{\pm}\right\rangle|\gamma_1\rangle$ (i.e, $\left|\Psi_i^{\pm}\right\rangle|\gamma_1\rangle$). To see why, let's consider the example of $\left|\Psi_2^{\pm}\right\rangle|\gamma_1\rangle$.

$$\begin{aligned}\left|\Psi_2^{\pm}\right\rangle|\gamma_1\rangle &\equiv \frac{1}{2}\left[([2,1] \pm [1,2])\,([3,0]+[0,3])\right]|0\rangle \\ &\equiv \frac{1}{2}\left[([5,1]+[2,4]) \pm ([1,5]+[4,2])\right]|0\rangle\end{aligned} \tag{5.27}$$

Once this state is expanded in terms of the output operators, terms on either side of the $\pm$ sign have different bracket representations and can never cancel each other. Therefore, $\left|\Psi_2^{+}\right\rangle|\gamma_1\rangle$ and $\left|\Psi_2^{-}\right\rangle|\gamma_1\rangle$ will always have the same terms (modulo sign).

To investigate whether we can distinguish between $\left|\Psi_1^{\pm}\right\rangle$, we must look at the evolution of the states

$$\begin{aligned}\left|\Psi_1^{+}\right\rangle|\gamma_1\rangle &\equiv \frac{1}{2}\left[(h_1^\dagger h_2^\dagger h_3^\dagger + v_1^\dagger v_2^\dagger v_3^\dagger)(h_4^\dagger h_5^\dagger h_6^\dagger + v_4^\dagger v_5^\dagger v_6^\dagger)\right]_{in}|0\rangle \\ \left|\Psi_1^{-}\right\rangle|\gamma_1\rangle &\equiv \frac{1}{2}\left[(h_1^\dagger h_2^\dagger h_3^\dagger - v_1^\dagger v_2^\dagger v_3^\dagger)(h_4^\dagger h_5^\dagger h_6^\dagger + v_4^\dagger v_5^\dagger v_6^\dagger)\right]_{in}|0\rangle\end{aligned} \tag{5.28}$$

Note that the bracket argument no longer rules out unambiguous discrimination here. In (5.28), the four terms have the brackets [6,0], [0,6], [3,3] and [3,3]. There are two [3,3] terms, which are added in $\left|\Psi_1^{+}\right\rangle$ and subtracted in $\left|\Psi_1^{-}\right\rangle$. Therefore, unique cancellations may take place in one of the states and not the other. The amount of this unambiguous discrimination will certainly depend on the particular setup used.

Similarily, using another type of ancillary state $|\gamma_i\rangle$ (denoting an ancillary of the form $|\Psi_2\rangle, |\Psi_3\rangle$, or

$|\Psi_4\rangle$) can potentially help us separate the states $|\Psi_i\rangle$ but not $|\Psi_1\rangle$, as shown below.

$$\begin{aligned} \left|\Psi_1^{\pm}\right\rangle|\gamma_i\rangle &\equiv \frac{1}{2}\left[([3,0]+[0,3])\left([2,1]\pm[1,2]\right)\right]|0\rangle \\ &\equiv \frac{1}{2}\left[([5,1]+[4,2])\pm([1,5]+[2,4])\right]|0\rangle \end{aligned} \tag{5.29}$$

$$\begin{aligned} \left|\Psi_i^{\pm}\right\rangle|\gamma_i\rangle &\equiv \frac{1}{2}\left[([2,1]+[1,2])\left([2,1]\pm[1,2]\right)\right]|0\rangle \\ &\equiv \frac{1}{2}\left[([4,2]+\mathbf{[3,3]})\pm(\mathbf{[3,3]}+[2,4])\right]|0\rangle \end{aligned} \tag{5.30}$$

Our next task is to analyze some setups and try to calculate the amount of unambiguous discrimination of the GHZ states through these setups. A natural way to combine the six photons might be the setup illustrated in figure 5.5. The beam 'tritters' need not be symmetric, X_1 and X_2 denote some arbitrary unitary mixing of the spatial modes {1,2,4} and {3,5,6}. Let us analyze the states in (5.28). We only study the evolution of the terms $h_1^\dagger h_2^\dagger h_3^\dagger v_4^\dagger v_5^\dagger v_6^\dagger$ and $v_1^\dagger v_2^\dagger v_3^\dagger h_4^\dagger h_5^\dagger h_6^\dagger$, as the other two terms ([6,0],[0,6]) are common (with sign) to both states anyway. The question we ask is: can there be a cancellation between these terms in either $\left|\Psi_1^+\right\rangle$ or $\left|\Psi_1^-\right\rangle$ when expanded in terms of the output operators?

Consider for the moment only the $v^\dagger$ operators. Because of the way the modes are mixed, we can say that $v_1^\dagger v_2^\dagger v_3^\dagger$ when evolved into the output state will contain two v operators in modes {1,2,4}. Similarily, the output corresponding to the term $v_4^\dagger v_5^\dagger v_6^\dagger$ will have two v operators in modes {3,5,6}. Since these two sets have no overlap, we directly see that the output terms corresponding to $h_1^\dagger h_2^\dagger h_3^\dagger v_4^\dagger v_5^\dagger v_6^\dagger$ and $v_1^\dagger v_2^\dagger v_3^\dagger h_4^\dagger h_5^\dagger h_6^\dagger$ can never cancel with each other.

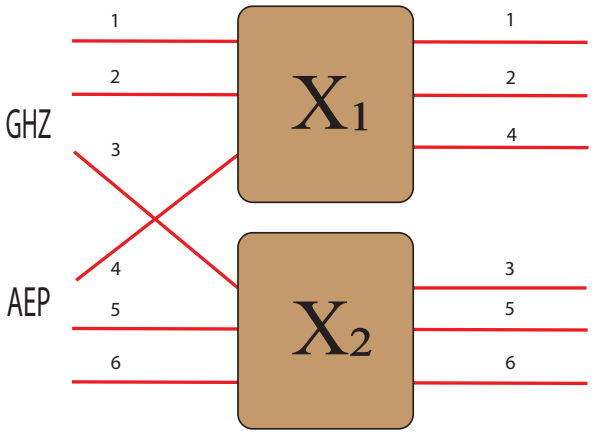

Figure 5.5: A particular setup with Ancillary Entangled Photons (AEP)

Thus, we can conclude that the setup used does not help us distinguish between the states in (5.28). An identical argument can be used to show that the setup in figure 5.6 also is of no use. In fact, The above analysis carries forward to the [3,3] terms in (5.30) as well. Terms on both sides of the $\pm$ sign never have the same set of h (or v) operators, and can never cancel. Thus, the setups in figures 5.5 and 5.6 are not useful for separating these states too.

Since using 3×3 unitaries does not seem to help us, we next consider a setup (figure 5.7) made up of 50-50 beam splitters only. The transformation of creation operators through this setup is given

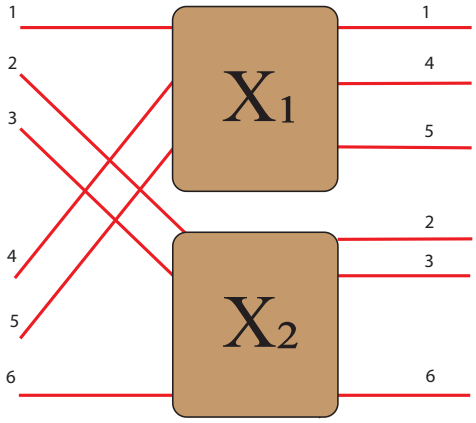

Figure 5.6: A similar setup with Ancillary Entangled Photons (AEP)

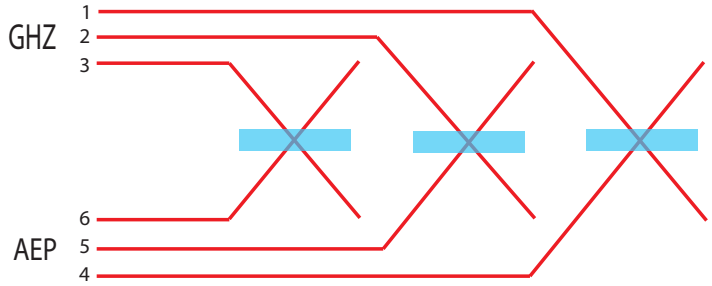

Figure 5.7: A particular setup with Ancillary Entangled Photons (AEP) (beam splitters are 50-50)

by:

$$\begin{pmatrix} a_1^\dagger \\ a_2^\dagger \\ . \\ . \\ . \\ a_6^\dagger \end{pmatrix}_{in} \rightarrow \frac{1}{\sqrt{2}} \begin{bmatrix} 1 & 0 & 0 & i & 0 & 0 \\ 0 & 1 & 0 & 0 & i & 0 \\ 0 & 0 & 1 & 0 & 0 & i \\ i & 0 & 0 & 1 & 0 & 0 \\ 0 & i & 0 & 0 & 1 & 0 \\ 0 & 0 & i & 0 & 0 & 1 \end{bmatrix} \begin{pmatrix} a_1^\dagger \\ a_2^\dagger \\ . \\ . \\ . \\ a_6^\dagger \end{pmatrix}_{out} \tag{5.31}$$

This transformation matrix reflects that fact that our setup is essentially just three beam splitters. After passing through the setup, the states in (5.28) are given in figures 5.8 and 5.9.

Clearly, some unambiguous discrimination is possible, as many terms that are present in $\left|\Psi_1^+\right\rangle|\gamma_1\rangle$ are not present in $\left|\Psi_1^-\right\rangle|\gamma_1\rangle$ and vice versa. In fact, there are eights sets of four terms that are completely different in each state. Thus, there are a total of $32 \times 2 = 64$ distinct terms that can unambiguously identify one state from the other. The coefficient of each of these terms is either $\frac{1}{8}i$ (for $\left|\Psi_1^+\right\rangle|\gamma_1\rangle$) or $\frac{1}{8}$ (for $\left|\Psi_1^-\right\rangle|\gamma_1\rangle$). Since the ancillary $|\gamma_1\rangle$ cannot help with separating the states $\left|\Psi_i^\pm\right\rangle$, the total success probability is

$$\boxed{P = \frac{1}{8}\left[0+0+0+32\times|i/8|^2+32\times|1/8|^2\right] = \frac{1}{8}} \tag{5.32}$$

Therefore, ancillary entangled photons **do** help in distinguishing within a set of the GHZ states. For the setup in figure 5.7, using the ancillary state $|\gamma_1\rangle$ gives unambiguous outputs for the states $\left|\Psi_1^\pm\right\rangle|\gamma_1\rangle$ 50% of the time, resulting in an overall success probability of $\frac{1}{8} \equiv 12.5\%$. However, the success probability obtained is very low, even lesser than the highest we can achieve without any ancillaries. Two questions that naturally arise after the above result are:

$$
\begin{aligned}
&-\frac{1}{16}\,i\,h1^2\,h2^2\,h3^2-\frac{1}{16}\,i\,h2^2\,h3^2\,h4^2-\frac{1}{16}\,i\,h1^2\,h3^2\,h5^2-\frac{1}{16}\,i\,h3^2\,h4^2\,h5^2-\\
&\frac{1}{16}\,i\,h1^2\,h2^2\,h6^2-\frac{1}{16}\,i\,h2^2\,h4^2\,h6^2-\frac{1}{16}\,i\,h1^2\,h5^2\,h6^2-\frac{1}{16}\,i\,h4^2\,h5^2\,h6^2-\\
&\frac{1}{8}\,i\,h1\,h2\,h3\,v1\,v2\,v3+\frac{1}{8}\,i\,h3\,h4\,h5\,v1\,v2\,v3+\frac{1}{8}\,i\,h2\,h4\,h6\,v1\,v2\,v3+\frac{1}{8}\,i\,h1\,h5\,h6\,v1\,v2\,v3-\\
&\frac{1}{16}\,i\,v1^2\,v2^2\,v3^2-\frac{1}{8}\,i\,h2\,h3\,h4\,v2\,v3\,v4-\frac{1}{8}\,i\,h1\,h3\,h5\,v2\,v3\,v4-\frac{1}{8}\,i\,h1\,h2\,h6\,v2\,v3\,v4+\\
&\frac{1}{8}\,i\,h4\,h5\,h6\,v2\,v3\,v4-\frac{1}{16}\,i\,v2^2\,v3^2\,v4^2-\frac{1}{8}\,i\,h2\,h3\,h4\,v1\,v3\,v5-\frac{1}{8}\,i\,h1\,h3\,h5\,v1\,v3\,v5-\\
&\frac{1}{8}\,i\,h1\,h2\,h6\,v1\,v3\,v5+\frac{1}{8}\,i\,h4\,h5\,h6\,v1\,v3\,v5+\frac{1}{8}\,i\,h1\,h2\,h3\,v3\,v4\,v5-\frac{1}{8}\,i\,h3\,h4\,h5\,v3\,v4\,v5-\\
&\frac{1}{8}\,i\,h2\,h4\,h6\,v3\,v4\,v5-\frac{1}{8}\,i\,h1\,h5\,h6\,v3\,v4\,v5-\frac{1}{16}\,i\,v1^2\,v3^2\,v5^2-\frac{1}{16}\,i\,v3^2\,v4^2\,v5^2-\\
&\frac{1}{8}\,i\,h2\,h3\,h4\,v1\,v2\,v6-\frac{1}{8}\,i\,h1\,h3\,h5\,v1\,v2\,v6-\frac{1}{8}\,i\,h1\,h2\,h6\,v1\,v2\,v6+\frac{1}{8}\,i\,h4\,h5\,h6\,v1\,v2\,v6+\\
&\frac{1}{8}\,i\,h1\,h2\,h3\,v2\,v4\,v6-\frac{1}{8}\,i\,h3\,h4\,h5\,v2\,v4\,v6-\frac{1}{8}\,i\,h2\,h4\,h6\,v2\,v4\,v6-\frac{1}{8}\,i\,h1\,h5\,h6\,v2\,v4\,v6+\\
&\frac{1}{8}\,i\,h1\,h2\,h3\,v1\,v5\,v6-\frac{1}{8}\,i\,h3\,h4\,h5\,v1\,v5\,v6-\frac{1}{8}\,i\,h2\,h4\,h6\,v1\,v5\,v6-\frac{1}{8}\,i\,h1\,h5\,h6\,v1\,v5\,v6+\\
&\frac{1}{8}\,i\,h2\,h3\,h4\,v4\,v5\,v6+\frac{1}{8}\,i\,h1\,h3\,h5\,v4\,v5\,v6+\frac{1}{8}\,i\,h1\,h2\,h6\,v4\,v5\,v6-\frac{1}{8}\,i\,h4\,h5\,h6\,v4\,v5\,v6-\\
&\frac{1}{16}\,i\,v1^2\,v2^2\,v6^2-\frac{1}{16}\,i\,v2^2\,v4^2\,v6^2-\frac{1}{16}\,i\,v1^2\,v5^2\,v6^2-\frac{1}{16}\,i\,v4^2\,v5^2\,v6^2
\end{aligned}
$$

Figure 5.8: $\left|\Psi_1^+\right\rangle|\gamma_1\rangle$ after passing through the setup

$$
\begin{aligned}
&-\frac{1}{16}\,i\,h1^2\,h2^2\,h3^2-\frac{1}{16}\,i\,h2^2\,h3^2\,h4^2-\frac{1}{16}\,i\,h1^2\,h3^2\,h5^2-\frac{1}{16}\,i\,h3^2\,h4^2\,h5^2-\frac{1}{16}\,i\,h1^2\,h2^2\,h6^2-\\
&\frac{1}{16}\,i\,h2^2\,h4^2\,h6^2-\frac{1}{16}\,i\,h1^2\,h5^2\,h6^2-\frac{1}{16}\,i\,h4^2\,h5^2\,h6^2+\frac{1}{8}\,h2\,h3\,h4\,v1\,v2\,v3+\frac{1}{8}\,h1\,h3\,h5\,v1\,v2\,v3+\\
&\frac{1}{8}\,h1\,h2\,h6\,v1\,v2\,v3-\frac{1}{8}\,h4\,h5\,h6\,v1\,v2\,v3+\frac{1}{16}\,i\,v1^2\,v2^2\,v3^2-\frac{1}{8}\,h1\,h2\,h3\,v2\,v3\,v4+\\
&\frac{1}{8}\,h3\,h4\,h5\,v2\,v3\,v4+\frac{1}{8}\,h2\,h4\,h6\,v2\,v3\,v4+\frac{1}{8}\,h1\,h5\,h6\,v2\,v3\,v4+\frac{1}{16}\,i\,v2^2\,v3^2\,v4^2-\\
&\frac{1}{8}\,h1\,h2\,h3\,v1\,v3\,v5+\frac{1}{8}\,h3\,h4\,h5\,v1\,v3\,v5+\frac{1}{8}\,h2\,h4\,h6\,v1\,v3\,v5+\frac{1}{8}\,h1\,h5\,h6\,v1\,v3\,v5-\\
&\frac{1}{8}\,h2\,h3\,h4\,v3\,v4\,v5-\frac{1}{8}\,h1\,h3\,h5\,v3\,v4\,v5-\frac{1}{8}\,h1\,h2\,h6\,v3\,v4\,v5+\frac{1}{8}\,h4\,h5\,h6\,v3\,v4\,v5+\\
&\frac{1}{16}\,i\,v1^2\,v3^2\,v5^2+\frac{1}{16}\,i\,v3^2\,v4^2\,v5^2-\frac{1}{8}\,h1\,h2\,h3\,v1\,v2\,v6+\frac{1}{8}\,h3\,h4\,h5\,v1\,v2\,v6+\frac{1}{8}\,h2\,h4\,h6\,v1\,v2\,v6+\\
&\frac{1}{8}\,h1\,h5\,h6\,v1\,v2\,v6-\frac{1}{8}\,h2\,h3\,h4\,v2\,v4\,v6-\frac{1}{8}\,h1\,h3\,h5\,v2\,v4\,v6-\frac{1}{8}\,h1\,h2\,h6\,v2\,v4\,v6+\\
&\frac{1}{8}\,h4\,h5\,h6\,v2\,v4\,v6-\frac{1}{8}\,h2\,h3\,h4\,v1\,v5\,v6-\frac{1}{8}\,h1\,h3\,h5\,v1\,v5\,v6-\frac{1}{8}\,h1\,h2\,h6\,v1\,v5\,v6+\\
&\frac{1}{8}\,h4\,h5\,h6\,v1\,v5\,v6+\frac{1}{8}\,h1\,h2\,h3\,v4\,v5\,v6-\frac{1}{8}\,h3\,h4\,h5\,v4\,v5\,v6-\frac{1}{8}\,h2\,h4\,h6\,v4\,v5\,v6-\\
&\frac{1}{8}\,h1\,h5\,h6\,v4\,v5\,v6+\frac{1}{16}\,i\,v1^2\,v2^2\,v6^2+\frac{1}{16}\,i\,v2^2\,v4^2\,v6^2+\frac{1}{16}\,i\,v1^2\,v5^2\,v6^2+\frac{1}{16}\,i\,v4^2\,v5^2\,v6^2
\end{aligned}
$$

Figure 5.9: $\left|\Psi_1^-\right\rangle|\gamma_1\rangle$ after passing through the setup

- Are there other setups with six photons that give a better success probability? What is the maximum achievable success probability with one ancillary 3-photon state?
- Since one ancillary pair leads to a non-zero probability of discrimination, we can expect that using more number of ancillary pairs will yield better success. Can we quantify this? Which ancillary states are most useful?

The next few sections will address these questions. It turns out that in this setup, using any of the $|\gamma_i\rangle's$ as ancillaries also yields a probability of 12.5%. However, note that in general, $|\gamma_i\rangle$ might be a

more favorable ancillary.

$$
\begin{aligned}
|\psi_1\rangle &\equiv \frac{1}{\sqrt{2}}([3,0]+[0,3]) \equiv \frac{1}{\sqrt{2}}(h^\dagger h^\dagger h^\dagger + v^\dagger v^\dagger v^\dagger)\,|0\rangle \\
|\psi_2\rangle &\to \frac{1}{\sqrt{2}}([2,1]+[1,2]) \equiv \frac{1}{\sqrt{2}}(h^\dagger h^\dagger v^\dagger + v^\dagger v^\dagger h^\dagger)\,|0\rangle \\
|\psi_3\rangle &\to \frac{1}{\sqrt{2}}([2,1]+[1,2]) \equiv \frac{1}{\sqrt{2}}(h^\dagger v^\dagger h^\dagger + v^\dagger h^\dagger v^\dagger)\,|0\rangle \\
|\psi_4\rangle &\to \frac{1}{\sqrt{2}}([2,1]+[1,2]) \equiv \frac{1}{\sqrt{2}}(v^\dagger h^\dagger h^\dagger + h^\dagger v^\dagger v^\dagger)\,|0\rangle
\end{aligned}
\tag{5.33}
$$

Using $|\gamma_1\rangle$ can only help us separate the states $\left|\Psi_1^{\pm}\right\rangle$, but $|\gamma_i\rangle$ might help create differences between three sets of states: $\left|\Psi_2^{\pm}\right\rangle$, $\left|\Psi_3^{\pm}\right\rangle$, and $\left|\Psi_4^{\pm}\right\rangle$. Indeed, the above probability of 12.5% can be surpassed by using $|\gamma_i\rangle$ in other setups. For example, consider the setup in figure 5.10 with general beam splitters characterized by parameters θ_1, θ_2 and θ_3. The unitary transformation corresponding to this

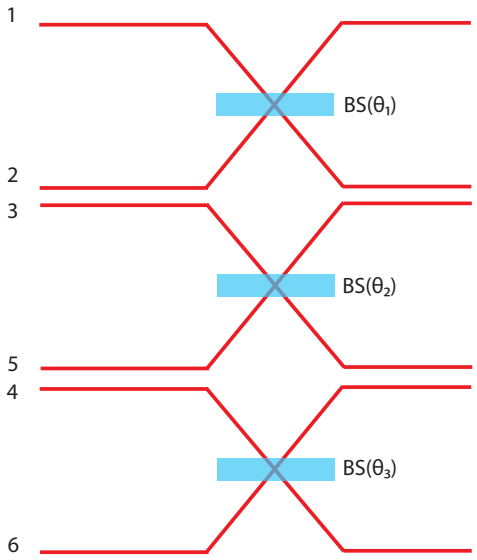

Figure 5.10: GHZ photons are sent through modes 1,2, and 3, and ancillary photons through modes 4,5,6

setup is

$$
\begin{pmatrix} a_1^\dagger \\ a_2^\dagger \\ . \\ . \\ . \\ a_6^\dagger \end{pmatrix}_{in}
\to \frac{1}{\sqrt{2}}
\begin{bmatrix}
\sin\theta_1 & 0 & i\cos\theta_1 & 0 & 0 & 0 \\
0 & \sin\theta_2 & 0 & 0 & i\cos\theta_2 & 0 \\
i\cos\theta_1 & 0 & \sin\theta_1 & 0 & 0 & 0 \\
0 & 0 & 0 & \sin\theta_3 & 0 & i\cos\theta_3 \\
0 & i\cos\theta_2 & 0 & 0 & \sin\theta_2 & 0 \\
0 & 0 & 0 & i\cos\theta_3 & 0 & \sin\theta_3
\end{bmatrix}
\begin{pmatrix} a_1^\dagger \\ a_2^\dagger \\ . \\ . \\ . \\ a_6^\dagger \end{pmatrix}_{out}
\tag{5.34}
$$

This setup was simulated on Mathematica. Collecting the coefficients of all the unambiguous outcomes and adding their absolute squares yields the success probability Using an ancillary of the form $|\gamma_2\rangle$ can help distinguish between the states $\left|\psi_2^{\pm}\right\rangle|\gamma_2\rangle$ and $\left|\psi_4^{\pm}\right\rangle|\gamma_2\rangle$, and the success probability turns out to be (for details, see A.2)

$$
\begin{aligned}
P(\theta_1,\theta_2,\theta_3) &= \frac{1}{8}|\sin(2\theta_1)\sin(2\theta_2)\sin(2\theta_3)|^2 + \frac{1}{8}|\sin(2\theta_1)\sin(2\theta_2)\sin(2\theta_3)|^2 \\
&= \frac{1}{4}|\sin(2\theta_1)\sin(2\theta_2)\sin(2\theta_3)|^2 \le \frac{1}{4}
\end{aligned}
\tag{5.35}
$$

In this setup, it is clear from (5.35) that symmetric beam splitters are most efficient to distinguish between the states; setting $\theta_1 = \theta_2 = \theta_3 = \pi/4$ yields the maximum success probability is 25%.

Many other setups were investigated, but none surpassed the 25% threshold. This seems to suggest that using an ancillary GHZ state in a polarization-preserving setup is no better than using polarization-changing setups and no additional resources.

5.3.3 Bound on success probability for identical ancillary $|\gamma_1\rangle$ states

Before we analyze general ancillary states, we can place certain bounds on the success rate if only the state $|\gamma_1\rangle$ is used as an ancillary. This is briefly discussed here. The states we analyzed before are

$$\begin{aligned}\left|\Psi_1^+\right\rangle|\gamma_1\rangle &\equiv \frac{1}{2}\left[(h_1^\dagger h_2^\dagger h_3^\dagger h_4^\dagger h_5^\dagger h_6^\dagger + h_1^\dagger h_2^\dagger h_3^\dagger v_4^\dagger v_5^\dagger v_6^\dagger + v_1^\dagger v_2^\dagger v_3^\dagger h_4^\dagger h_5^\dagger h_6^\dagger + v_1^\dagger v_2^\dagger v_3^\dagger v_4^\dagger v_5^\dagger v_6^\dagger)\right]_{in}|0\rangle \\ \left|\Psi_1^-\right\rangle|\gamma_1\rangle &\equiv \frac{1}{2}\left[(h_1^\dagger h_2^\dagger h_3^\dagger h_4^\dagger h_5^\dagger h_6^\dagger + h_1^\dagger h_2^\dagger h_3^\dagger v_4^\dagger v_5^\dagger v_6^\dagger - v_1^\dagger v_2^\dagger v_3^\dagger h_4^\dagger h_5^\dagger h_6^\dagger - v_1^\dagger v_2^\dagger v_3^\dagger v_4^\dagger v_5^\dagger v_6^\dagger)\right]_{in}|0\rangle\end{aligned} \tag{5.36}$$

Each of the four terms in both states have a norm of 1/4. Once expanded through the output operators, each term will give rise to many more terms. However, since our transformations are unitary, they will not change the norm of the states. Thus, the sum of the norms of all the terms that arise out of $(h_1^\dagger h_2^\dagger h_3^\dagger h_4^\dagger h_5^\dagger h_6^\dagger)|0\rangle$ will still be 1/4. This crucial fact helps us place a bound on the success probability without talking about a specific unitary mapping.

In (5.36), the [6,0] and [0,6] terms don't help in unambiguous discrimination. The two [3,3] terms however are combined differently in both states. Let us consider the extreme case (which will yield the highest probability) where the output states of $h_1^\dagger h_2^\dagger h_3^\dagger v_4^\dagger v_5^\dagger v_6^\dagger + v_1^\dagger v_2^\dagger v_3^\dagger h_4^\dagger h_5^\dagger h_6^\dagger$ and $h_1^\dagger h_2^\dagger h_3^\dagger v_4^\dagger v_5^\dagger v_6^\dagger - v_1^\dagger v_2^\dagger v_3^\dagger h_4^\dagger h_5^\dagger h_6^\dagger$ have no overlap. This means that the output states corresponding to these terms are orthogonal and have completely different detector outcomes. What does this imply for the success probability?

The [3,3] terms make up 50% of all terms in both states. This implies that if the initial state was $\left|\Psi_1^+\right\rangle$ or $\left|\Psi_1^-\right\rangle$, then 50% of the time, the outcome at the detectors can unambiguously identify the GHZ state. If the initial state was any other GHZ state $|\Psi_i\rangle$, then $|\gamma_1\rangle$ does not help in distinguishing between $\left|\Psi_i^\pm\right\rangle$. Therefore, the maximum possible success probability (for equiprobable initial GHZ states) is

$$P_1 = \frac{1}{8}\left[\frac{2}{4} + \frac{2}{4}\right] = \frac{1}{8} \equiv 12.5\% \tag{5.37}$$

Thus, the maximum possible success probability is itself 12.5%! This was attained in the setup discussed earlier. Therefore, we can be sure that using $|\gamma_1\rangle$ as ancillary, a higher success probability cannot be achieved, and our earlier setup is an optimal one.

This result can be generalized to any number of identical ancillary $|\gamma_1\rangle$ states. If for example, we

have two ancillary GHZ states of the form $|\gamma_1\rangle$, then we have to distinguish between the states

$$\begin{aligned}\left|\Psi_1^{\pm}\right\rangle|\gamma_1\rangle|\gamma_1\rangle &\equiv \frac{1}{2\sqrt{2}}\left[(h_1^\dagger h_2^\dagger h_3^\dagger \pm v_1^\dagger v_2^\dagger v_3^\dagger)(h_4^\dagger h_5^\dagger h_6^\dagger + v_4^\dagger v_5^\dagger v_6^\dagger)(h_7^\dagger h_8^\dagger h_9^\dagger + v_7^\dagger v_8^\dagger v_9^\dagger)\right]_{in}|0\rangle \\ &\equiv \frac{1}{2\sqrt{2}}\left[([3,0]\pm[0,3])([3,0]+[0,3])([3,0]+[0,3])\right]_{in}|0\rangle \\ &\equiv \frac{1}{2\sqrt{2}}\left[([3,0]\pm[0,3])([6,0]+2[3,3]+[0,6])\right]_{in}|0\rangle \\ &\equiv \frac{1}{2\sqrt{2}}\left[([9,0]+2[6,3]+[3,6])\pm([0,9]+2[3,6]+[6,3])\right]_{in}|0\rangle\end{aligned} \tag{5.38}$$

Of the eight terms above, three are [6,3], three are [3,6], and there are one each of [9,0] and [0,9]. If we suppose that the [3,6] and the [6,3] terms combine to form orthogonal states at the outputs, then 6 out of the 8 terms will yield unambiguous outcomes at the detectors. A similar calculation like above yields a success probability of

$$P_2 = \frac{1}{8}\left[\frac{6}{8}+\frac{6}{8}\right] = \frac{3}{16} \equiv 18.75\% \tag{5.39}$$

Extending this calculation to N ancillary 3-photon states, we obtain the following result.

$$P_N = \frac{1}{8}\left[2\times\left(\frac{2^{N+1}-2}{2^{N+1}}\right)\right] = \frac{1}{4}\left[\frac{2^N-1}{2^N}\right] = \frac{1}{4}\left[1-2^{-N}\right] \tag{5.40}$$

Therefore, the success probability exponentially approaches the value $\frac{1}{4}$. This result is expected, because we know that ancillaries of the form $|\gamma_1\rangle$ cannot help in distinguishing within the sets $\left|\Psi_2^{\pm}\right\rangle$,$\left|\Psi_3^{\pm}\right\rangle$, and $\left|\Psi_4^{\pm}\right\rangle$. So, the most we can hope for is perfect discrimination between the states $\left|\Psi_1^{+}\right\rangle$ and $\left|\Psi_1^{-}\right\rangle$, and this is what we observe as $N\to\infty$.
It must be noted that these are 'hard' bounds. They certainly cannot be surpassed, but it is unclear whether they can be reached either. We haven't found setups that saturate this bound even for $N=2$. In the next section, we will generalize the above discussion to include other types of ancillary states.

5.3.4 Bounds on success probability for general ancillary states

If we confine ourselves to a total of 6 photons, our best bet is to use the ancillary $|\gamma_i\rangle$. As discussed in (5.29) and (5.30), this does not help us with separating $\left|\Psi_1^{\pm}\right\rangle$, but it does help with $\left|\Psi_i^{\pm}\right\rangle$:

$$\begin{aligned}\left|\Psi_i^{\pm}\right\rangle|\gamma_i\rangle &\equiv \frac{1}{2}\left[([2,1]\pm[1,2])\,([2,1]+[1,2])\right]|0\rangle \\ &\equiv \frac{1}{2}\left[([4,2]+\mathbf{[3,3]})\pm(\mathbf{[3,3]}+[2,4])\right]|0\rangle\end{aligned} \tag{5.41}$$

The maximum possible success would be achieved if a setup can perfectly separate the [3,3] terms in $\left|\Psi_i^{+}\right\rangle$ and $\left|\Psi_i^{-}\right\rangle$ for **each of i = 2,3,4**. In this extreme case, two of the four terms in $\left|\Psi_i^{+}\right\rangle$ and $\left|\Psi_i^{-}\right\rangle$ are orthogonal with completely different outcomes. Thus, this places a bound on success probability if we're restricted to 6 photons:

$$P = \frac{1}{8}\left[0+3\times(2/4+2/4)\right] = \frac{3}{8} \equiv 37.5\% \tag{5.42}$$

Therefore, for six photon setups (that don't change the polarization of photons), one can never achieve a success probability of beyond 37.5%.

A similar calculation can be performed if additional ancillary states are used. By analyzing the terms with the same bracket representation and assuming (in the extreme case) that they completely cancel in both the states, we can obtain the highest possible success probability of discrimination for a given number of ancillary used. This calculation was performed on Mathematica (see A.2), and the results are listed in the table below. Only ancillary states built out of Bell and GHZ states were investigated, as these are relatively easier to produce than four-photon entangled states and above. The first column lists the total number of photons used (GHZ photons and the ancillaries). For a given number of photons, all possible ancillary states which are a product of Bell and GHZ states were analyzed, and the state listed in column two is the one which yields the highest bound on the success probability. The states $|\phi^+\rangle$ and $|\gamma_i\rangle$ seem to serve best as ancillaries. The maximum probability

Number of photons	Best Ancillary	Success Probability
6	$\|\gamma_i\rangle$	37.5%
8	$\|\gamma_i\rangle \|\phi^+\rangle$	62.5%
9	$\|\gamma_i\rangle \|\gamma_i\rangle$	56.5%
10	$\|\gamma_i\rangle \|\phi^+\rangle \|\phi^+\rangle$	78.125%
12	$\|\gamma_i\rangle \|\phi^+\rangle \|\phi^+\rangle \|\phi^+\rangle$	87.5%
13	$\|\gamma_1\rangle \|\gamma_i\rangle \|\phi^+\rangle \|\phi^+\rangle$	89.0625%
14	$\|\gamma_i\rangle \|\phi^+\rangle \|\phi^+\rangle \|\phi^+\rangle \|\phi^+\rangle$	92.969%

Table 5.1: Maximum success probability of GHZ state discrimination for polarization-preserving setups as a function of (total) photon number

increases with photon number, approaching 100% for large values. This result is intuitive, and in line with Grice's result for the Bell states [Gri11]. However, it must be noted that it is unclear whether these bounds are attainable. Specfiic experimental setups that yield these success probabilities have also not been discovered; this is a work in progress.

5.4 Hyperentanglement

In section 3.4, we saw that the Bell states can be completely distinguished in a linear optical setting if they are also entangled in a second degree of freedom. We could ask an analogous question for the GHZ states as well. It so happens that the GHZ states can also be perfectly separated out if they are entangled in two degrees of freedom. An experimental setup for achieving this was first proposed in 2013 by Song *et al.* [SSL13], and is discussed below. Consider the GHZ states,

$$\begin{aligned}
\left|\Psi_1^{\pm}\right\rangle &\equiv \frac{1}{\sqrt{2}}\left(|H\rangle|H\rangle|H\rangle \pm |V\rangle|V\rangle|V\rangle\right)\\
\left|\Psi_2^{\pm}\right\rangle &\equiv \frac{1}{\sqrt{2}}\left(|V\rangle|H\rangle|H\rangle \pm |H\rangle|V\rangle|V\rangle\right)\\
\left|\Psi_3^{\pm}\right\rangle &\equiv \frac{1}{\sqrt{2}}\left(|H\rangle|V\rangle|H\rangle \pm |V\rangle|H\rangle|V\rangle\right)\\
\left|\Psi_4^{\pm}\right\rangle &\equiv \frac{1}{\sqrt{2}}\left(|H\rangle|H\rangle|V\rangle \pm |V\rangle|V\rangle|H\rangle\right)
\end{aligned} \tag{5.43}$$

which are also entangled in path/momentum degrees of freedom in GHZ-like states as follows:

$$
\begin{aligned}
\left|\Psi_1^{\pm}\right\rangle_m &\equiv \frac{1}{\sqrt{2}}\left(|L_1\rangle|L_2\rangle|L_3\rangle \pm |R_1\rangle|R_2\rangle|R_3\rangle\right) \\
\left|\Psi_2^{\pm}\right\rangle_m &\equiv \frac{1}{\sqrt{2}}\left(|R_1\rangle|L_2\rangle|L_3\rangle \pm |L_1\rangle|R_2\rangle|R_3\rangle\right) \\
\left|\Psi_3^{\pm}\right\rangle_m &\equiv \frac{1}{\sqrt{2}}\left(|L_1\rangle|R_2\rangle|L_3\rangle \pm |R_1\rangle|L_2\rangle|R_3\rangle\right) \\
\left|\Psi_4^{\pm}\right\rangle_m &\equiv \frac{1}{\sqrt{2}}\left(|L_1\rangle|L_2\rangle|R_3\rangle \pm |R_1\rangle|R_2\rangle|L_3\rangle\right)
\end{aligned}
\tag{5.44}
$$

$|L\rangle$ and $|R\rangle$ denote two different paths for a photon, see figure 5.11. Each 'L'-shaped arm independently operates on one photon, and consists of two polarizing beam splitters, two half-wave plates (these devices are central to distinguishing between GHZ states, as we shall see), and four detectors. The paper demostrates how to distinguish between the eight states (a fixed entangled state in the momentum degree of freedom) of the form:

$$
|\Psi\rangle = |\Psi\rangle_p \otimes \left|\Psi_1^{+}\right\rangle_m \tag{5.45}
$$

where $|\Psi\rangle_p$ denotes one of the polarization entangled states in (5.43). Since there are a total of 12

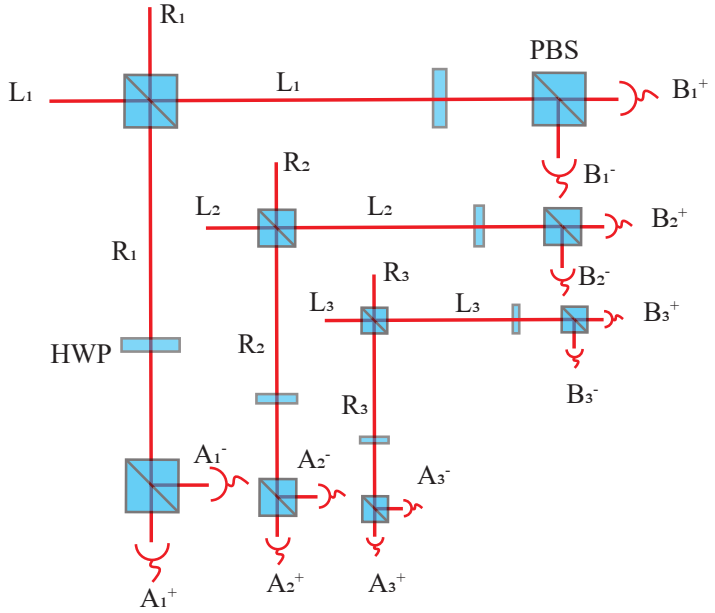

Figure 5.11: Hyperentangled GHZ state analysis [SSL13]. PBS: polarizing beam splitter, HWP: Half wave plate

detectors, the number of possible outcomes at the detectors is $\binom{12}{3} = 220$. Each of the states in (5.45) leads to 8 distinct outcomes at the detectors after passing through the setup, and thus we have a total of 64 coincidence outcomes, a number far lesser than the total number of possibilities. The evolution

State	Detector signatures
$\|\Psi^+\rangle_1 \otimes \|\Psi_1^+\rangle_m$	$A_1^+A_2^+A_3^+$, $B_1^+B_2^+B_3^+$, $A_1^+A_2^-A_3^-$, $B_1^+B_2^-B_3^-$, $A_1^-A_2^-A_3^+$, $B_1^-B_2^-B_3^+$, $A_1^-A_2^+A_3^-$, $B_1^-B_2^+B_3^-$
$\|\Psi^-\rangle_1 \otimes \|\Psi_1^+\rangle_m$	$A_1^-A_2^-A_3^-$, $B_1^-B_2^-B_3^-$, $A_1^-A_2^+A_3^+$, $B_1^-B_2^+B_3^+$, $A_1^+A_2^-A_3^+$, $B_1^+B_2^-B_3^+$, $A_1^+A_2^+A_3^-$, $B_1^+B_2^+B_3^-$
$\|\Psi^+\rangle_2 \otimes \|\Psi_1^+\rangle_m$	$B_1^+A_2^+A_3^+$, $A_1^+B_2^+B_3^+$, $B_1^+A_2^-A_3^-$, $A_1^+B_2^-B_3^-$, $B_1^-A_2^+A_3^-$, $A_1^-B_2^+B_3^-$, $B_1^-A_2^-A_3^+$, $A_1^-B_2^-B_3^+$
$\|\Psi^-\rangle_2 \otimes \|\Psi_1^+\rangle_m$	$B_1^-A_2^-A_3^-$, $A_1^-B_2^-B_3^-$, $B_1^-A_2^+A_3^+$, $A_1^-B_2^+B_3^+$, $B_1^+A_2^-A_3^+$, $A_1^+B_2^-B_3^+$, $B_1^+A_2^+A_3^-$, $A_1^+B_2^+B_3^-$
$\|\Psi^+\rangle_3 \otimes \|\Psi_1^+\rangle_m$	$A_1^+B_2^+A_3^+$, $B_1^+A_2^+B_3^+$, $A_1^+B_2^-A_3^-$, $B_1^+A_2^-B_3^-$, $A_1^-B_2^+A_3^-$, $B_1^-A_2^+B_3^-$, $A_1^-B_2^-A_3^+$, $B_1^-A_2^-B_3^+$
$\|\Psi^-\rangle_3 \otimes \|\Psi_1^+\rangle_m$	$A_1^-B_2^-A_3^-$, $B_1^-A_2^-B_3^-$, $A_1^-B_2^+A_3^+$, $B_1^-A_2^+B_3^+$, $A_1^+B_2^-A_3^+$, $B_1^+A_2^-B_3^+$, $A_1^+B_2^+A_3^-$, $B_1^+A_2^+B_3^-$
$\|\Psi^+\rangle_4 \otimes \|\Psi_1^+\rangle_m$	$A_1^+A_2^+B_3^+$, $B_1^+B_2^+A_3^+$, $A_1^+A_2^-B_3^-$, $B_1^+B_2^-A_3^-$, $A_1^-A_2^-B_3^+$, $B_1^-B_2^-A_3^+$, $A_1^-A_2^+B_3^-$, $B_1^-B_2^+A_3^-$
$\|\Psi^-\rangle_4 \otimes \|\Psi_1^+\rangle_m$	$A_1^-A_2^-B_3^-$, $B_1^-B_2^-A_3^-$, $A_1^-A_2^+B_3^+$, $B_1^-B_2^+A_3^+$, $A_1^+A_2^-B_3^+$, $B_1^+B_2^-A_3^+$, $A_1^+A_2^+B_3^-$, $B_1^+B_2^+A_3^-$

Table 5.2: Possible detector signatures for each of the eight hyperentangled GHZ states

of $|\Psi^+\rangle_1 \otimes |\Psi_1^+\rangle_m$ is worked out below, as an example.

$$
\begin{aligned}
|\Psi\rangle = |\Psi^+\rangle_1 \otimes |\Psi_1^+\rangle_m &= \frac{1}{2}\left(|HHH\rangle + |VVV\rangle\right)\left(|L_1L_2L_3\rangle + |R_1R_2R_3\rangle\right) \\
&\xrightarrow{PBS} |HHH\rangle\left(|L_1L_2L_3\rangle + |R_1R_2R_3\rangle\right) + |VVV\rangle\left(|R_1R_2R_3\rangle + |L_1L_2L_3\rangle\right) \\
&\xrightarrow{HWP} \left(\frac{|H\rangle + |V\rangle}{\sqrt{2}}\right)^{\otimes 3}\left(|L_1L_2L_3\rangle + |R_1R_2R_3\rangle\right) + \left(\frac{|H\rangle - |V\rangle}{\sqrt{2}}\right)^{\otimes 3}\left(|R_1R_2R_3\rangle + |L_1L_2L_3\rangle\right) \\
&= \frac{1}{2\sqrt{2}}[\left(|HHH\rangle + |HVV\rangle + |VVH\rangle + |VHV\rangle\right)|L_1L_2L_3\rangle \\
&\quad + \left(|HHH\rangle + |HVV\rangle + |VVH\rangle + |VHV\rangle\right)]|R_1R_2R_3\rangle
\end{aligned}
$$

In accordance with the above output state, the detectors that can fire are: $A_1^+A_2^+A_3^+$, $B_1^+B_2^+B_3^+$, $A_1^+A_2^-A_3^-$, $B_1^+B_2^-B_3^-$, $A_1^-A_2^-A_3^+$, $B_1^-B_2^-B_3^+$, $A_1^-A_2^+A_3^-$, $B_1^-B_2^+B_3^-$. This set of outcomes occurs only for the state $|\Psi^+\rangle_1 \otimes |\Psi_1^+\rangle_m$, and can be used to uniquely identify this state. Similarily, all other states also have mutually exclusive outcomes, and are tabulated in table 5.2 (taken from [SSL13]). Thus, the eight hyperentangled GHZ states can be completely distinguished using this setup. The authors were also able to provide a natural extention of this setup to distinguish between N-photon GHZ-like entangled states. The setup simply requires N identical 'L-shaped' arms, and a total of $4N$ detectors. Each arm is built exactly like in figure 5.11. Complementary to this example, one can also use polarization entanglement to distinguish between momentum-entangled states. These results possibly can be used for multipartite generalizations of quantum information protocols like superdense coding, etc.

As discussed previously, a crucial reason why these states become completely separated once we involve two degrees of freedom is simply the number of choices available at the detectors. If we're

restricted to a single degree of freedom, there aren't sufficient number of outcomes at the detectors that render all the states unambiguous. In the current scenario, the total number of outcomes at the detectors ($\binom{4N}{N}$) always exceeds the number required ($O(2^N)$).

5.5 Summary

This chapter began by describing the GHZ states, their production and applications. The bound for success probability of GHZ state measurements using linear optics is 25%. Unlike in the case of BSM, it was shown that gaussian squeezing operations in general are not useful to separate the GHZ states. Since squeezing adds photons in pairs, this turns out to be incompatible with the GHZ states, which are made out of three (an odd number of) photons.

A large portion of the chapter dealt with ancillary entanglement as a resource in polarization preserving setups. It was shown that using only Bell states as ancillaries is not sufficient, they must be used along with GHZ states as well. For a single ancillary state, various 6 photon setups were discussed. Although the maximum possible success was shown to be 37.5%, no setups achieving success beyond 25% could be found. This suggests that polarization changing devices (like wave plates) may be crucial to better success, as a single GHZ state an ancillary does not seem to give any advantage over polarization changing setups without ancillary photons.

Moreover, it was shown that if N ancillaries of the form $|\Psi_1\rangle$ are used, the success probability cannot exceed $\frac{1}{4}\left[1-2^{-N}\right]$. When different kinds of ancillaries are used, a closed-form expression for the bound on success probability could not be obtained. However, bounds were numerically calculated up to $N = 14$, and the success probability in general increases with photon number and approaches unity. At $N = 14$, the bound was found to be around 93%. Whether these bounds can be saturated for any N is uncertain but is believed to be unlikely. Moreover, the states of the form $|\Psi_i\rangle$ and $|\Phi^{\pm}\rangle$ were found to be most useful as ancillaries.

Like in the case of Bell states, hyperentangled GHZ states can be completely distinguished using linear optics. This result is useful for generalizations of dense coding for multipartite systems.

Chapter 6

Conclusion and Future Directions

Linear Optics Quantum Computing (LOQC) is a promising route for the implementation of a practical quantum computer. Most quantum information protocols contain a step where one party must perform a measurement of two or more particles onto a basis of orthogonal entangled states (for example, a Bell measurement, or a GHZ measurement, etc.). This thesis addressed the problem of distinguishing between orthogonal entangled states of photons using linear optical setups. We explored three kinds of states: Bell states and Non-Maximally Entangled (NME) states of two-photons, and the three-photon GHZ states.

Chapters 2 and 3 discussed existing literature regarding Bell State Measurements. We saw that a perfect Bell state analyzer cannot be implemented using linear optics [LCS99], and the best one can do without ancillary photons is to distinguish between two of the four Bell states [CL01]. Applying gaussian squeezing operations on the Bell states allows us to surpass this 50% bound, but not by much, as the maximum success probability is around 64.3% [ZvL13]. Further, ancillary entangled photons can be used to better distinguish the Bell states. Using $2^N - 2$ ancillary photons yields a success probability of $1 - 1/2^N$ [Gri11]. Although non-linear optical gadgets allow for a perfect Bell state measurement [KKS01], these are quite inefficient as per today's technology. Another important resource for Bell state analysis is hyperentanglement, or entanglement in multiple degrees of freedom of the photon. Bell states entangled in two degrees of freedom can be perfectly distinguished using linear optics. Several setups have been proposed to distinguish between various kinds of hyperentangled photons [KW98] [SHKW06] [BVMDM07] [KLL$^+$19] [BWK08], and some of these setups were discussed in the text. Hyperentangled Bell states can can help achieve perfect superdense coding, but are not a useful resource for teleportation.

In this thesis, we attempted to extend some of the above ideas to the case of distinguishing between the NME and the GHZ states. We showed that Bell states in general are not useful as ancillaries for distinguishing between the NME states; one must only use partially entangled states. Further, the form of the ancillaries must depend on the particular NME states to be distinguished. We took a particular example of setup with one ancillary entangled pair and illustrated that the maximum success probability achievable (12.5%) is much lower than the analogous scenario for Bell states, which yielded a success of 75%. Coming to the GHZ states, only two of the eight states can be distinguished using linear optics [PZ98]. We focused on ancillary entanglement as a resource to enhance this probability in polarization preserving setups. We were able to place bounds on the success achievable as a function of number of photons used. We observed that $|\Psi_i\rangle$ and $|\Phi^{\pm}\rangle$ were the most useful ancillaries, and the maximum success probability steadily increases with photon number, approaching 93% for

$N = 14$.

These results further the understanding of multi-photon state discrimination, and could be applied to quantum information protocols that involve GHZ or partially entangled states. However, this work is only in its preliminary stages. Quite a number of questions are open and need more study. Some directions yet to be explored are given below.

In our discussion of non-maximally entangled states, we observed that additional ancillaries must be non-maximally entangled in order to be of help in distinguishing between the states. We plan on generalizing this result to n pairs of ancillary photons and compare this with the corresponding scenario for Bell states. Another important question to study might be distinguishing between these states using entanglement in two degrees of freedom. What resources might be required for a complete discrimination of a set of orthogonal non-maximally entangled states? It is also worth exploring how useful squeezing operations are for this purpose, and study any possible relation between the squeezing parameter and the states to be distinguished.

With regard to GHZ states, we would like to derive better bounds on the success probability as a function of number of photons. Moreover, all the setups analyzed were polarization-preserving. We are currently studying more general setups free from this restriction. The aim is to place bounds on the success probability for such setups, and compare these bounds to that placed by Grice for Bell states. We also wish to study the other class of three-qubit entangled states, the W states, and see if a similar scenario holds for distinguishing between them using linear optics. More importantly, we would like to gain some intuition for how to design a setup for distinguishing between a set of states. Deveoping a general method that describes how to separate a given set of states using linear optics could be a useful result with many applications.

In a broader sense, we would like to understand in more detail the restrictions LOQC places on quantum information protocols, and the challenges of practical implementations of LOQC. We also wish to contrast the results obtained in this thesis to linear optics for continuous variables. Lastly, we are also exploring Boson sampling and measurement-based quantum computing in LOQC.

Bibliography

[AP02] Pankaj Agrawal and Arun K Pati. Probabilistic quantum teleportation. *Physics Letters A*, 305(1-2):12–17, 2002.

[BBC+93] Charles H Bennett, Gilles Brassard, Claude Crépeau, Richard Jozsa, Asher Peres, and William K Wootters. Teleporting an unknown quantum state via dual classical and einstein-podolsky-rosen channels. *Physical review letters*, 70(13):1895, 1993.

[BBPS96] Charles H Bennett, Herbert J Bernstein, Sandu Popescu, and Benjamin Schumacher. Concentrating partial entanglement by local operations. *Physical Review A*, 53(4):2046, 1996.

[BPD+99] Dik Bouwmeester, Jian-Wei Pan, Matthew Daniell, Harald Weinfurter, and Anton Zeilinger. Observation of three-photon greenberger-horne-zeilinger entanglement. *Physical Review Letters*, 82(7):1345, 1999.

[BPM+97] Dik Bouwmeester, Jian-Wei Pan, Klaus Mattle, Manfred Eibl, Harald Weinfurter, and Anton Zeilinger. Experimental quantum teleportation. *Nature*, 390(6660):575–579, 1997.

[Bra05] Samuel L Braunstein. Squeezing as an irreducible resource. *Physical Review A*, 71(5):055801, 2005.

[BVMDM07] M Barbieri, G Vallone, P Mataloni, and F De Martini. Complete and deterministic discrimination of polarization bell states assisted by momentum entanglement. *Physical Review A*, 75(4):042317, 2007.

[BW92] Charles H Bennett and Stephen J Wiesner. Communication via one-and two-particle operators on einstein-podolsky-rosen states. *Physical review letters*, 69(20):2881, 1992.

[BWK08] Julio T Barreiro, Tzu-Chieh Wei, and Paul G Kwiat. Beating the channel capacity limit for linear photonic superdense coding. *Nature physics*, 4(4):282–286, 2008.

[CL01] John Calsamiglia and Norbert Lütkenhaus. Maximum efficiency of a linear-optical bell-state analyzer. *Applied Physics B*, 72(1):67–71, 2001.

[CL04] Kai Chen and Hoi-Kwong Lo. Multi-partite quantum cryptographic protocols with noisy ghz states. *arXiv preprint quant-ph/0404133*, 2004.

[DVC00] Wolfgang Dür, Guifre Vidal, and J Ignacio Cirac. Three qubits can be entangled in two inequivalent ways. *Physical Review A*, 62(6):062314, 2000.

[Ebe93] Philippe H Eberhard. Background level and counter efficiencies required for a loophole-free einstein-podolsky-rosen experiment. *Physical Review A*, 47(2):R747, 1993.

[GHSZ90] Daniel M Greenberger, Michael A Horne, Abner Shimony, and Anton Zeilinger. Bell's theorem without inequalities. *American Journal of Physics*, 58(12):1131–1143, 1990.

[GHZ89] Daniel M Greenberger, Michael A Horne, and Anton Zeilinger. Going beyond bell's theorem. In *Bell's theorem, quantum theory and conceptions of the universe*, pages 69–72. Springer, 1989.

[GKK05] Christopher Gerry, Peter Knight, and Peter L Knight. *Introductory quantum optics*. Cambridge university press, 2005.

[GR05] Berry Groisman and Benni Reznik. Implementing nonlocal gates with nonmaximally entangled states. *Physical Review A*, 71(3):032322, 2005.

[Gri11] Warren P Grice. Arbitrarily complete bell-state measurement using only linear optical elements. *Physical Review A*, 84(4):042331, 2011.

[GYW05] Ting Gao, Feng-Li Yan, and Zhi-Xi Wang. Deterministic secure direct communication using ghz states and swapping quantum entanglement. *Journal of Physics A: Mathematical and General*, 38(25):5761, 2005.

[HBB99] Mark Hillery, Vladimír Bužek, and André Berthiaume. Quantum secret sharing. *Physical Review A*, 59(3):1829, 1999.

[HHL11] Tzonelih Hwang, Cheng-Chieh Hwang, and Chuan-Ming Li. Multiparty quantum secret sharing based on ghz states. *Physica Scripta*, 83(4):045004, 2011.

[KB98] Anders Karlsson and Mohamed Bourennane. Quantum teleportation using three-particle entanglement. *Physical Review A*, 58(6):4394, 1998.

[KG19] Thomas Kilmer and Saikat Guha. Boosting linear-optical bell measurement success probability with predetection squeezing and imperfect photon-number-resolving detectors. *Physical Review A*, 99(3):032302, 2019.

[KKS01] Yoon-Ho Kim, Sergei P Kulik, and Yanhua Shih. Quantum teleportation of a polarization state with a complete bell state measurement. *Physical Review Letters*, 86(7):1370, 2001.

[KLL+19] Ling-Jun Kong, Yongnan Li, Rui Liu, Wen-Rong Qi, Qiang Wang, Zhou-Xiang Wang, Shuang-Yin Huang, Yu Si, Chenghou Tu, Wei Hu, et al. Complete measurement and multiplexing of orbital angular momentum bell states. *Physical Review A*, 100(2):023822, 2019.

[KLM01] Emanuel Knill, Raymond Laflamme, and Gerald J Milburn. A scheme for efficient quantum computation with linear optics. *nature*, 409(6816):46–52, 2001.

[KW98] Paul G Kwiat and Harald Weinfurter. Embedded bell-state analysis. *Physical Review A*, 58(4):R2623, 1998.

[LCS99] N Lütkenhaus, J Calsamiglia, and K-A Suominen. Bell measurements for teleportation. *Physical Review A*, 59(5):3295, 1999.

[LDL+06] Xi-Han Li, Fu-Guo Deng, Chun-Yan Li, Yu-Jie Liang, Ping Zhou, and Hong-Yu Zhou. Deterministic secure quantum communication without maximally entangled states. *arXiv preprint quant-ph/0606007*, 2006.

[MG08] Joanna Modławska and Andrzej Grudka. Nonmaximally entangled states can be better for multiple linear optical teleportation. *Physical review letters*, 100(11):110503, 2008.

[MVWZ01] Alois Mair, Alipasha Vaziri, Gregor Weihs, and Anton Zeilinger. Entanglement of the orbital angular momentum states of photons. *Nature*, 412(6844):313–316, 2001.

[MWKZ96] Klaus Mattle, Harald Weinfurter, Paul G Kwiat, and Anton Zeilinger. Dense coding in experimental quantum communication. *Physical Review Letters*, 76(25):4656, 1996.

[PZ98] Jian-wei Pan and Anton Zeilinger. Greenberger-horne-zeilinger-state analyzer. *Physical Review A*, 57(3):2208, 1998.

[RZBB94] Michael Reck, Anton Zeilinger, Herbert J Bernstein, and Philip Bertani. Experimental realization of any discrete unitary operator. *Physical review letters*, 73(1):58, 1994.

[SHKW06] Carsten Schuck, Gerhard Huber, Christian Kurtsiefer, and Harald Weinfurter. Complete deterministic linear optics bell state analysis. *Physical review letters*, 96(19):190501, 2006.

[SSL13] Yu-Bo Sheng Siyu Song, Ye Cao and Gui-Lu Long. Complete greenberger–horne–zeilinger state analyzer using hyperentanglement. *Quantum Information Processing*, 12(1):381–393, 2013.

[TBMM95] Justin R Torgerson, David Branning, Carlos H Monken, and Leonard Mandel. Experimental demonstration of the violation of local realism without bell inequalities. *Physics Letters A*, 204(5-6):323–328, 1995.

[VT05] Franck Vidal and Abderrahmane Tadjeddine. Sum-frequency generation spectroscopy of interfaces. *Reports on Progress in Physics*, 68(5):1095, 2005.

[WJEK99] Andrew G White, Daniel FV James, Philippe H Eberhard, and Paul G Kwiat. Nonmaximally entangled states: production, characterization, and utilization. *Physical review letters*, 83(16):3103, 1999.

[WPM03] SP Walborn, S Pádua, and CH Monken. Hyperentanglement-assisted bell-state analysis. *Physical Review A*, 68(4):042313, 2003.

[WSH17] Brian P Williams, Ronald J Sadlier, and Travis S Humble. Superdense coding over optical fiber links with complete bell-state measurements. *Physical review letters*, 118(5):050501, 2017.

[XLG01] Peng Xue, Chuan-Feng Li, and Guang-Can Guo. Efficient quantum-key-distribution scheme with nonmaximally entangled states. *Physical Review A*, 64(3):032305, 2001.

[ZvL13] Hussain A Zaidi and Peter van Loock. Beating the one-half limit of ancilla-free linear optics bell measurements. *Physical review letters*, 110(26):260501, 2013.

Appendix A

Mathematica Simulations

In this appendix, I will describe the code I used (in Mathematica) to obtain some of the results given in chapters 4 and 5, regarding state discrimination using ancillary entanglement. The first section will discuss distinguishing between non-maximally entangled states, and the second section will discuss results regarding the GHZ states.

A.1 Non-maximally entangled states

Recall that the task in section 4.2 was to distinguish between the states

$$\begin{aligned} \left|\widetilde{\Phi^+}\right\rangle|\widetilde{\gamma_1}\rangle &= \left[(c\ h_1^\dagger h_2^\dagger + d\ v_1^\dagger v_2^\dagger)(e\ h_3^\dagger h_4^\dagger + f\ v_3^\dagger v_4^\dagger)\right]_{in}|0\rangle \\ \left|\widetilde{\Phi^-}\right\rangle|\widetilde{\gamma_1}\rangle &= \left[(d\ h_1^\dagger h_2^\dagger - c\ v_1^\dagger v_2^\dagger)(e\ h_3^\dagger h_4^\dagger + f\ v_3^\dagger v_4^\dagger)\right]_{in}|0\rangle \end{aligned} \tag{A.1}$$

In the simulation, the input creation operators are represented by lowercase letters, and the output creation operators with uppercase letters. The block below relates the two sets of operators through the unitary U.

```
vars= {h1, h2, h3, h4, v1, v2, v3, v4};
Vec1 = {{h1}, {h2}, {h3}, {h4}}; Vec2 = {{v1}, {v2}, {v3}, {v4}};
U = 1/2*{{1,I,I,-1},{I,1,-1,I},{I,-1,1,I},{-1,I,I,1}};
Vec3 = U . Vec1;  Vec4 = U . Vec2;
H1 = Vec3[[1]][[1]]; H2 = Vec3[[2]][[1]]; H3 = Vec3[[3]][[1]]; H4 =
   Vec3[[4]][[1]];
V1 = Vec4[[1]][[1]]; V2 = Vec4[[2]][[1]]; V3 = Vec4[[3]][[1]]; V4 =
   Vec4[[4]][[1]];
```

To find the final states after evolving through the setup, one can simply use the commands

```
phiplus = ExpandAll[(c H1 H2 + d V1 V2) ( e H3 H4 + f V3 V4 )];
phiminus = ExpandAll[(d H1 H2 - c V1 V2) ( e H3 H4 + f V3 V4 )];
```

The figures A.1 and A.2 display the outputs of the above commands: the states $\left|\widetilde{\Phi^+}\right\rangle|\widetilde{\gamma_1}\rangle$ and $\left|\widetilde{\Phi^-}\right\rangle|\widetilde{\gamma_1}\rangle$ after passing through the setup. Note that all operators in the images that follow are creation operators, the daggers on top of the operators are not shown.

We would like to compare these two large expressions. Firstly, we can list out the different terms

$$\frac{1}{16} c\, e\, h1^4 + \frac{1}{8} c\, e\, h1^2\, h2^2 + \frac{1}{16} c\, e\, h2^4 + \frac{1}{8} c\, e\, h1^2\, h3^2 - \frac{1}{8} c\, e\, h2^2\, h3^2 + \frac{1}{16} c\, e\, h3^4 + \frac{1}{2} c\, e\, h1\, h2\, h3\, h4 -$$
$$\frac{1}{8} c\, e\, h1^2\, h4^2 + \frac{1}{8} c\, e\, h2^2\, h4^2 + \frac{1}{8} c\, e\, h3^2\, h4^2 + \frac{1}{16} c\, e\, h4^4 + \frac{1}{16} d\, e\, h1^2\, v1^2 + \frac{1}{16} c\, f\, h1^2\, v1^2 +$$
$$\frac{1}{16} d\, e\, h2^2\, v1^2 + \frac{1}{16} c\, f\, h2^2\, v1^2 - \frac{1}{8} i\, d\, e\, h1\, h3\, v1^2 + \frac{1}{8} i\, c\, f\, h1\, h3\, v1^2 - \frac{1}{16} d\, e\, h3^2\, v1^2 -$$
$$\frac{1}{16} c\, f\, h3^2\, v1^2 - \frac{1}{8} i\, d\, e\, h2\, h4\, v1^2 + \frac{1}{8} i\, c\, f\, h2\, h4\, v1^2 - \frac{1}{16} d\, e\, h4^2\, v1^2 - \frac{1}{16} c\, f\, h4^2\, v1^2 +$$
$$\frac{1}{16} d\, f\, v1^4 + \frac{1}{16} d\, e\, h1^2\, v2^2 + \frac{1}{16} c\, f\, h1^2\, v2^2 + \frac{1}{16} d\, e\, h2^2\, v2^2 + \frac{1}{16} c\, f\, h2^2\, v2^2 - \frac{1}{8} i\, d\, e\, h1\, h3\, v2^2 +$$
$$\frac{1}{8} i\, c\, f\, h1\, h3\, v2^2 - \frac{1}{16} d\, e\, h3^2\, v2^2 - \frac{1}{16} c\, f\, h3^2\, v2^2 - \frac{1}{8} i\, d\, e\, h2\, h4\, v2^2 + \frac{1}{8} i\, c\, f\, h2\, h4\, v2^2 -$$
$$\frac{1}{16} d\, e\, h4^2\, v2^2 - \frac{1}{16} c\, f\, h4^2\, v2^2 + \frac{1}{8} d\, f\, v1^2\, v2^2 + \frac{1}{16} d\, f\, v2^4 + \frac{1}{8} i\, d\, e\, h1^2\, v1\, v3 - \frac{1}{8} i\, c\, f\, h1^2\, v1\, v3 +$$
$$\frac{1}{8} i\, d\, e\, h2^2\, v1\, v3 - \frac{1}{8} i\, c\, f\, h2^2\, v1\, v3 + \frac{1}{4} d\, e\, h1\, h3\, v1\, v3 + \frac{1}{4} c\, f\, h1\, h3\, v1\, v3 - \frac{1}{8} i\, d\, e\, h3^2\, v1\, v3 +$$
$$\frac{1}{8} i\, c\, f\, h3^2\, v1\, v3 + \frac{1}{4} d\, e\, h2\, h4\, v1\, v3 + \frac{1}{4} c\, f\, h2\, h4\, v1\, v3 - \frac{1}{8} i\, d\, e\, h4^2\, v1\, v3 + \frac{1}{8} i\, c\, f\, h4^2\, v1\, v3 -$$
$$\frac{1}{16} d\, e\, h1^2\, v3^2 - \frac{1}{16} c\, f\, h1^2\, v3^2 - \frac{1}{16} d\, e\, h2^2\, v3^2 - \frac{1}{16} c\, f\, h2^2\, v3^2 + \frac{1}{8} i\, d\, e\, h1\, h3\, v3^2 - \frac{1}{8} i\, c\, f\, h1\, h3\, v3^2 +$$
$$\frac{1}{16} d\, e\, h3^2\, v3^2 + \frac{1}{16} c\, f\, h3^2\, v3^2 + \frac{1}{8} i\, d\, e\, h2\, h4\, v3^2 - \frac{1}{8} i\, c\, f\, h2\, h4\, v3^2 + \frac{1}{16} d\, e\, h4^2\, v3^2 +$$
$$\frac{1}{16} c\, f\, h4^2\, v3^2 + \frac{1}{8} d\, f\, v1^2\, v3^2 - \frac{1}{8} d\, f\, v2^2\, v3^2 + \frac{1}{16} d\, f\, v3^4 + \frac{1}{8} i\, d\, e\, h1^2\, v2\, v4 - \frac{1}{8} i\, c\, f\, h1^2\, v2\, v4 +$$
$$\frac{1}{8} i\, d\, e\, h2^2\, v2\, v4 - \frac{1}{8} i\, c\, f\, h2^2\, v2\, v4 + \frac{1}{4} d\, e\, h1\, h3\, v2\, v4 + \frac{1}{4} c\, f\, h1\, h3\, v2\, v4 - \frac{1}{8} i\, d\, e\, h3^2\, v2\, v4 +$$
$$\frac{1}{8} i\, c\, f\, h3^2\, v2\, v4 + \frac{1}{4} d\, e\, h2\, h4\, v2\, v4 + \frac{1}{4} c\, f\, h2\, h4\, v2\, v4 - \frac{1}{8} i\, d\, e\, h4^2\, v2\, v4 + \frac{1}{8} i\, c\, f\, h4^2\, v2\, v4 +$$
$$\frac{1}{2} d\, f\, v1\, v2\, v3\, v4 - \frac{1}{16} d\, e\, h1^2\, v4^2 - \frac{1}{16} c\, f\, h1^2\, v4^2 - \frac{1}{16} d\, e\, h2^2\, v4^2 - \frac{1}{16} c\, f\, h2^2\, v4^2 + \frac{1}{8} i\, d\, e\, h1\, h3\, v4^2 -$$
$$\frac{1}{8} i\, c\, f\, h1\, h3\, v4^2 + \frac{1}{16} d\, e\, h3^2\, v4^2 + \frac{1}{16} c\, f\, h3^2\, v4^2 + \frac{1}{8} i\, d\, e\, h2\, h4\, v4^2 - \frac{1}{8} i\, c\, f\, h2\, h4\, v4^2 +$$
$$\frac{1}{16} d\, e\, h4^2\, v4^2 + \frac{1}{16} c\, f\, h4^2\, v4^2 - \frac{1}{8} d\, f\, v1^2\, v4^2 + \frac{1}{8} d\, f\, v2^2\, v4^2 + \frac{1}{8} d\, f\, v3^2\, v4^2 + \frac{1}{16} d\, f\, v4^4$$

Figure A.1: $\left|\widetilde{\Phi^+}\right\rangle |\widetilde{\gamma_1}\rangle$ after passing through the setup

separately without their coefficients, to know what detector outcomes are possible. To do this, one uses

```
v = List@@Expand[Collect[phiplus, vars, 1 &]]
```

This command collects only the parts of the state which contain elements from the list vars. The result of this outcome is shown in figure A.3). The same list is obtained for both states, confirming that all terms in $\left|\widetilde{\Phi^+}\right\rangle |\widetilde{\gamma_1}\rangle$ are also present in $\left|\widetilde{\Phi^-}\right\rangle |\widetilde{\gamma_1}\rangle$, only with different coefficients (so there is no unambiguous discrimation between the $\left|\widetilde{\Phi^\pm}\right\rangle$ states at the moment).

```
In[1]:= List@@Expand[Collect[phiplus,vars,1 &]] = = List@@Expand[
    Collect[phiminus,vars,1 &]];
Out[1]= True
```

In figure A.3, note that the number of h and v operators is always even, as we would expect from (4.11). To check if some discrimination is possible, we must look at the coefficients of these outcomes. Since we will be calculating probabilities, it is more useful to list down the absolute squared of the coefficients. However, note that this is not enough! We must take into account the relation

$$\begin{aligned} a^{\dagger n} |0\rangle &= \sqrt{n!}\, |n\rangle \\ \implies \langle 0|\, a^n a^{\dagger n} |0\rangle &= n! \end{aligned} \tag{A.2}$$

So, we must include this factor of $n!$ while calculating probabilities of outcomes. The block of code below takes this into account, and creates a list normlist1 containing the probabilites of all the outcomes in figure A.3, in order.

$$\frac{1}{16} d\,e\,h1^4 + \frac{1}{8} d\,e\,h1^2\,h2^2 + \frac{1}{16} d\,e\,h2^4 + \frac{1}{8} d\,e\,h1^2\,h3^2 - \frac{1}{8} d\,e\,h2^2\,h3^2 + \frac{1}{16} d\,e\,h3^4 + \frac{1}{2} d\,e\,h1\,h2\,h3\,h4 -$$
$$\frac{1}{8} d\,e\,h1^2\,h4^2 + \frac{1}{8} d\,e\,h2^2\,h4^2 + \frac{1}{8} d\,e\,h3^2\,h4^2 + \frac{1}{16} d\,e\,h4^4 - \frac{1}{16} c\,e\,h1^2\,v1^2 + \frac{1}{16} d\,f\,h1^2\,v1^2 -$$
$$\frac{1}{16} c\,e\,h2^2\,v1^2 + \frac{1}{16} d\,f\,h2^2\,v1^2 + \frac{1}{8} i\,c\,e\,h1\,h3\,v1^2 + \frac{1}{8} i\,d\,f\,h1\,h3\,v1^2 + \frac{1}{16} c\,e\,h3^2\,v1^2 -$$
$$\frac{1}{16} d\,f\,h3^2\,v1^2 + \frac{1}{8} i\,c\,e\,h2\,h4\,v1^2 + \frac{1}{8} i\,d\,f\,h2\,h4\,v1^2 + \frac{1}{16} c\,e\,h4^2\,v1^2 - \frac{1}{16} d\,f\,h4^2\,v1^2 -$$
$$\frac{1}{16} c\,f\,v1^4 - \frac{1}{16} c\,e\,h1^2\,v2^2 + \frac{1}{16} d\,f\,h1^2\,v2^2 - \frac{1}{16} c\,e\,h2^2\,v2^2 + \frac{1}{16} d\,f\,h2^2\,v2^2 + \frac{1}{8} i\,c\,e\,h1\,h3\,v2^2 +$$
$$\frac{1}{8} i\,d\,f\,h1\,h3\,v2^2 + \frac{1}{16} c\,e\,h3^2\,v2^2 - \frac{1}{16} d\,f\,h3^2\,v2^2 + \frac{1}{8} i\,c\,e\,h2\,h4\,v2^2 + \frac{1}{8} i\,d\,f\,h2\,h4\,v2^2 +$$
$$\frac{1}{16} c\,e\,h4^2\,v2^2 - \frac{1}{16} d\,f\,h4^2\,v2^2 - \frac{1}{8} c\,f\,v1^2\,v2^2 - \frac{1}{16} c\,f\,v2^4 - \frac{1}{8} i\,c\,e\,h1^2\,v1\,v3 - \frac{1}{8} i\,d\,f\,h1^2\,v1\,v3 -$$
$$\frac{1}{8} i\,c\,e\,h2^2\,v1\,v3 - \frac{1}{8} i\,d\,f\,h2^2\,v1\,v3 - \frac{1}{4} c\,e\,h1\,h3\,v1\,v3 + \frac{1}{4} d\,f\,h1\,h3\,v1\,v3 + \frac{1}{8} i\,c\,e\,h3^2\,v1\,v3 +$$
$$\frac{1}{8} i\,d\,f\,h3^2\,v1\,v3 - \frac{1}{4} c\,e\,h2\,h4\,v1\,v3 + \frac{1}{4} d\,f\,h2\,h4\,v1\,v3 + \frac{1}{8} i\,c\,e\,h4^2\,v1\,v3 + \frac{1}{8} i\,d\,f\,h4^2\,v1\,v3 +$$
$$\frac{1}{16} c\,e\,h1^2\,v3^2 - \frac{1}{16} d\,f\,h1^2\,v3^2 + \frac{1}{16} c\,e\,h2^2\,v3^2 - \frac{1}{16} d\,f\,h2^2\,v3^2 - \frac{1}{8} i\,c\,e\,h1\,h3\,v3^2 - \frac{1}{8} i\,d\,f\,h1\,h3\,v3^2 -$$
$$\frac{1}{16} c\,e\,h3^2\,v3^2 + \frac{1}{16} d\,f\,h3^2\,v3^2 - \frac{1}{8} i\,c\,e\,h2\,h4\,v3^2 - \frac{1}{8} i\,d\,f\,h2\,h4\,v3^2 - \frac{1}{16} c\,e\,h4^2\,v3^2 +$$
$$\frac{1}{16} d\,f\,h4^2\,v3^2 - \frac{1}{8} c\,f\,v1^2\,v3^2 + \frac{1}{8} c\,f\,v2^2\,v3^2 - \frac{1}{16} c\,f\,v3^4 - \frac{1}{8} i\,c\,e\,h1^2\,v2\,v4 - \frac{1}{8} i\,d\,f\,h1^2\,v2\,v4 -$$
$$\frac{1}{8} i\,c\,e\,h2^2\,v2\,v4 - \frac{1}{8} i\,d\,f\,h2^2\,v2\,v4 - \frac{1}{4} c\,e\,h1\,h3\,v2\,v4 + \frac{1}{4} d\,f\,h1\,h3\,v2\,v4 + \frac{1}{8} i\,c\,e\,h3^2\,v2\,v4 +$$
$$\frac{1}{8} i\,d\,f\,h3^2\,v2\,v4 - \frac{1}{4} c\,e\,h2\,h4\,v2\,v4 + \frac{1}{4} d\,f\,h2\,h4\,v2\,v4 + \frac{1}{8} i\,c\,e\,h4^2\,v2\,v4 + \frac{1}{8} i\,d\,f\,h4^2\,v2\,v4 -$$
$$\frac{1}{2} c\,f\,v1\,v2\,v3\,v4 + \frac{1}{16} c\,e\,h1^2\,v4^2 - \frac{1}{16} d\,f\,h1^2\,v4^2 + \frac{1}{16} c\,e\,h2^2\,v4^2 - \frac{1}{16} d\,f\,h2^2\,v4^2 - \frac{1}{8} i\,c\,e\,h1\,h3\,v4^2 -$$
$$\frac{1}{8} i\,d\,f\,h1\,h3\,v4^2 - \frac{1}{16} c\,e\,h3^2\,v4^2 + \frac{1}{16} d\,f\,h3^2\,v4^2 - \frac{1}{8} i\,c\,e\,h2\,h4\,v4^2 - \frac{1}{8} i\,d\,f\,h2\,h4\,v4^2 -$$
$$\frac{1}{16} c\,e\,h4^2\,v4^2 + \frac{1}{16} d\,f\,h4^2\,v4^2 + \frac{1}{8} c\,f\,v1^2\,v4^2 - \frac{1}{8} c\,f\,v2^2\,v4^2 - \frac{1}{8} c\,f\,v3^2\,v4^2 - \frac{1}{16} c\,f\,v4^4$$

Figure A.2: $\left|\widetilde{\Phi^-}\right\rangle |\widetilde{\gamma_1}\rangle$ at the end of the setup

$$\{h1^4,\ h1^2\,h2^2,\ h2^4,\ h1^2\,h3^2,\ h2^2\,h3^2,\ h3^4,\ h1\,h2\,h3\,h4,\ h1^2\,h4^2,\ h2^2\,h4^2,\ h3^2\,h4^2,\ h4^4,\ h1^2\,v1^2,$$
$$h2^2\,v1^2,\ h1\,h3\,v1^2,\ h3^2\,v1^2,\ h2\,h4\,v1^2,\ h4^2\,v1^2,\ v1^4,\ h1^2\,v2^2,\ h2^2\,v2^2,\ h1\,h3\,v2^2,\ h3^2\,v2^2,$$
$$h2\,h4\,v2^2,\ h4^2\,v2^2,\ v1^2\,v2^2,\ v2^4,\ h1^2\,v1\,v3,\ h2^2\,v1\,v3,\ h1\,h3\,v1\,v3,\ h3^2\,v1\,v3,\ h2\,h4\,v1\,v3,$$
$$h4^2\,v1\,v3,\ h1^2\,v3^2,\ h2^2\,v3^2,\ h1\,h3\,v3^2,\ h3^2\,v3^2,\ h2\,h4\,v3^2,\ h4^2\,v3^2,\ v1^2\,v3^2,\ v2^2\,v3^2,$$
$$v3^4,\ h1^2\,v2\,v4,\ h2^2\,v2\,v4,\ h1\,h3\,v2\,v4,\ h3^2\,v2\,v4,\ h2\,h4\,v2\,v4,\ h4^2\,v2\,v4,\ v1\,v2\,v3\,v4,$$
$$h1^2\,v4^2,\ h2^2\,v4^2,\ h1\,h3\,v4^2,\ h3^2\,v4^2,\ h2\,h4\,v4^2,\ h4^2\,v4^2,\ v1^2\,v4^2,\ v2^2\,v4^2,\ v3^2\,v4^2,\ v4^4\}$$

Figure A.3: List of various outcomes for $\left|\widetilde{\Phi^\pm}\right\rangle |\widetilde{\gamma_1}\rangle$

```
list1 = Which[Length[v]==0,0,Length[v]!=0,Abs[(Coefficient[phiplus
    ,#]&/@v)]^2]; i=1;
While[i<= Length[v],{check= Cases[v[[i]], _?NumericQ, -1];list1[[i]]=
   Which[Length[check]==1,list1[[i]]*Factorial[check[[1]]],Length[
   check]==2,list1[[i]]*4,Length[check]==0,list1[[i]]];i++;}]
normlist1=list1;
```

Identical commands can be written for phiminus. This list for both the states is given in figures A.4 and A.5. The numbers in both these figures add to one (as expected) if the normalization conditions, $|c|^2 + |d|^2 = 1$ and $|e|^2 + |f|^2 = 1$ are valid. To check this, one can use the FullSimplify command:

```
In[1]:= FullSimplify[Total[normlist1],{c*Conjugate[c]+d*Conjugate[d]
    == 1, f*Conjugate[f]+e*Conjugate[e] = = 1}]
Out[1]= 1
```

Had we not accounted for (A.2), the above total would not have added to 1. To reiterate, figure A.3 shows the possible outcomes at the detectors, and figures A.4 and A.5 show the probabilities of

$$\Big\{\frac{3}{32}\,\text{Abs}[c\,e]^2,\ \frac{1}{16}\,\text{Abs}[c\,e]^2,\ \frac{3}{32}\,\text{Abs}[c\,e]^2,\ \frac{1}{16}\,\text{Abs}[c\,e]^2,\ \frac{1}{16}\,\text{Abs}[c\,e]^2,\ \frac{3}{32}\,\text{Abs}[c\,e]^2,\ \frac{1}{4}\,\text{Abs}[c\,e]^2,$$
$$\frac{1}{16}\,\text{Abs}[c\,e]^2,\ \frac{1}{16}\,\text{Abs}[c\,e]^2,\ \frac{1}{16}\,\text{Abs}[c\,e]^2,\ \frac{3}{32}\,\text{Abs}[c\,e]^2,\ 4\,\text{Abs}\Big[\frac{d\,e}{16}+\frac{c\,f}{16}\Big]^2,\ 4\,\text{Abs}\Big[\frac{d\,e}{16}+\frac{c\,f}{16}\Big]^2,$$
$$2\,\text{Abs}\Big[-\frac{1}{8}\,i\,d\,e+\frac{i\,c\,f}{8}\Big]^2,\ 4\,\text{Abs}\Big[-\frac{d\,e}{16}-\frac{c\,f}{16}\Big]^2,\ 2\,\text{Abs}\Big[-\frac{1}{8}\,i\,d\,e+\frac{i\,c\,f}{8}\Big]^2,\ 4\,\text{Abs}\Big[-\frac{d\,e}{16}-\frac{c\,f}{16}\Big]^2,$$
$$\frac{3}{32}\,\text{Abs}[d\,f]^2,\ 4\,\text{Abs}\Big[\frac{d\,e}{16}+\frac{c\,f}{16}\Big]^2,\ 4\,\text{Abs}\Big[\frac{d\,e}{16}+\frac{c\,f}{16}\Big]^2,\ 2\,\text{Abs}\Big[-\frac{1}{8}\,i\,d\,e+\frac{i\,c\,f}{8}\Big]^2,\ 4\,\text{Abs}\Big[-\frac{d\,e}{16}-\frac{c\,f}{16}\Big]^2,$$
$$2\,\text{Abs}\Big[-\frac{1}{8}\,i\,d\,e+\frac{i\,c\,f}{8}\Big]^2,\ 4\,\text{Abs}\Big[-\frac{d\,e}{16}-\frac{c\,f}{16}\Big]^2,\ \frac{1}{16}\,\text{Abs}[d\,f]^2,\ \frac{3}{32}\,\text{Abs}[d\,f]^2,\ 2\,\text{Abs}\Big[\frac{i\,d\,e}{8}-\frac{i\,c\,f}{8}\Big]^2,$$
$$2\,\text{Abs}\Big[\frac{i\,d\,e}{8}-\frac{i\,c\,f}{8}\Big]^2,\ \text{Abs}\Big[\frac{d\,e}{4}+\frac{c\,f}{4}\Big]^2,\ 2\,\text{Abs}\Big[-\frac{1}{8}\,i\,d\,e+\frac{i\,c\,f}{8}\Big]^2,\ \text{Abs}\Big[\frac{d\,e}{4}+\frac{c\,f}{4}\Big]^2,\ 2\,\text{Abs}\Big[-\frac{1}{8}\,i\,d\,e+\frac{i\,c\,f}{8}\Big]^2,$$
$$4\,\text{Abs}\Big[-\frac{d\,e}{16}-\frac{c\,f}{16}\Big]^2,\ 4\,\text{Abs}\Big[-\frac{d\,e}{16}-\frac{c\,f}{16}\Big]^2,\ 2\,\text{Abs}\Big[\frac{i\,d\,e}{8}-\frac{i\,c\,f}{8}\Big]^2,\ 4\,\text{Abs}\Big[\frac{d\,e}{16}+\frac{c\,f}{16}\Big]^2,\ 2\,\text{Abs}\Big[\frac{i\,d\,e}{8}-\frac{i\,c\,f}{8}\Big]^2,$$
$$4\,\text{Abs}\Big[\frac{d\,e}{16}+\frac{c\,f}{16}\Big]^2,\ \frac{1}{16}\,\text{Abs}[d\,f]^2,\ \frac{1}{16}\,\text{Abs}[d\,f]^2,\ \frac{3}{32}\,\text{Abs}[d\,f]^2,\ 2\,\text{Abs}\Big[\frac{i\,d\,e}{8}-\frac{i\,c\,f}{8}\Big]^2,$$
$$2\,\text{Abs}\Big[\frac{i\,d\,e}{8}-\frac{i\,c\,f}{8}\Big]^2,\ \text{Abs}\Big[\frac{d\,e}{4}+\frac{c\,f}{4}\Big]^2,\ 2\,\text{Abs}\Big[-\frac{1}{8}\,i\,d\,e+\frac{i\,c\,f}{8}\Big]^2,\ \text{Abs}\Big[\frac{d\,e}{4}+\frac{c\,f}{4}\Big]^2,\ 2\,\text{Abs}\Big[-\frac{1}{8}\,i\,d\,e+\frac{i\,c\,f}{8}\Big]^2,$$
$$\frac{1}{4}\,\text{Abs}[d\,f]^2,\ 4\,\text{Abs}\Big[-\frac{d\,e}{16}-\frac{c\,f}{16}\Big]^2,\ 4\,\text{Abs}\Big[-\frac{d\,e}{16}-\frac{c\,f}{16}\Big]^2,\ 2\,\text{Abs}\Big[\frac{i\,d\,e}{8}-\frac{i\,c\,f}{8}\Big]^2,\ 4\,\text{Abs}\Big[\frac{d\,e}{16}+\frac{c\,f}{16}\Big]^2,$$
$$2\,\text{Abs}\Big[\frac{i\,d\,e}{8}-\frac{i\,c\,f}{8}\Big]^2,\ 4\,\text{Abs}\Big[\frac{d\,e}{16}+\frac{c\,f}{16}\Big]^2,\ \frac{1}{16}\,\text{Abs}[d\,f]^2,\ \frac{1}{16}\,\text{Abs}[d\,f]^2,\ \frac{1}{16}\,\text{Abs}[d\,f]^2,\ \frac{3}{32}\,\text{Abs}[d\,f]^2\Big\}$$

Figure A.4: $\left|\widetilde{\Phi^+}\right\rangle|\widetilde{\gamma_1}\rangle$: Probabilities of various outcomes

$$\Big\{\frac{3}{32}\,\text{Abs}[d\,e]^2,\ \frac{1}{16}\,\text{Abs}[d\,e]^2,\ \frac{3}{32}\,\text{Abs}[d\,e]^2,\ \frac{1}{16}\,\text{Abs}[d\,e]^2,\ \frac{1}{16}\,\text{Abs}[d\,e]^2,\ \frac{3}{32}\,\text{Abs}[d\,e]^2,\ \frac{1}{4}\,\text{Abs}[d\,e]^2,$$
$$\frac{1}{16}\,\text{Abs}[d\,e]^2,\ \frac{1}{16}\,\text{Abs}[d\,e]^2,\ \frac{1}{16}\,\text{Abs}[d\,e]^2,\ \frac{3}{32}\,\text{Abs}[d\,e]^2,\ 4\,\text{Abs}\Big[-\frac{c\,e}{16}+\frac{d\,f}{16}\Big]^2,\ 4\,\text{Abs}\Big[-\frac{c\,e}{16}+\frac{d\,f}{16}\Big]^2,$$
$$2\,\text{Abs}\Big[\frac{i\,c\,e}{8}+\frac{i\,d\,f}{8}\Big]^2,\ 4\,\text{Abs}\Big[\frac{c\,e}{16}-\frac{d\,f}{16}\Big]^2,\ 2\,\text{Abs}\Big[\frac{i\,c\,e}{8}+\frac{i\,d\,f}{8}\Big]^2,\ 4\,\text{Abs}\Big[\frac{c\,e}{16}-\frac{d\,f}{16}\Big]^2,\ \frac{3}{32}\,\text{Abs}[c\,f]^2,$$
$$4\,\text{Abs}\Big[-\frac{c\,e}{16}+\frac{d\,f}{16}\Big]^2,\ 4\,\text{Abs}\Big[-\frac{c\,e}{16}+\frac{d\,f}{16}\Big]^2,\ 2\,\text{Abs}\Big[\frac{i\,c\,e}{8}+\frac{i\,d\,f}{8}\Big]^2,\ 4\,\text{Abs}\Big[\frac{c\,e}{16}-\frac{d\,f}{16}\Big]^2,\ 2\,\text{Abs}\Big[\frac{i\,c\,e}{8}+\frac{i\,d\,f}{8}\Big]^2,$$
$$4\,\text{Abs}\Big[\frac{c\,e}{16}-\frac{d\,f}{16}\Big]^2,\ \frac{1}{16}\,\text{Abs}[c\,f]^2,\ \frac{3}{32}\,\text{Abs}[c\,f]^2,\ 2\,\text{Abs}\Big[-\frac{1}{8}\,i\,c\,e-\frac{i\,d\,f}{8}\Big]^2,\ 2\,\text{Abs}\Big[-\frac{1}{8}\,i\,c\,e-\frac{i\,d\,f}{8}\Big]^2,$$
$$\text{Abs}\Big[-\frac{c\,e}{4}+\frac{d\,f}{4}\Big]^2,\ 2\,\text{Abs}\Big[\frac{i\,c\,e}{8}+\frac{i\,d\,f}{8}\Big]^2,\ \text{Abs}\Big[-\frac{c\,e}{4}+\frac{d\,f}{4}\Big]^2,\ 2\,\text{Abs}\Big[\frac{i\,c\,e}{8}+\frac{i\,d\,f}{8}\Big]^2,\ 4\,\text{Abs}\Big[\frac{c\,e}{16}-\frac{d\,f}{16}\Big]^2,$$
$$4\,\text{Abs}\Big[\frac{c\,e}{16}-\frac{d\,f}{16}\Big]^2,\ 2\,\text{Abs}\Big[-\frac{1}{8}\,i\,c\,e-\frac{i\,d\,f}{8}\Big]^2,\ 4\,\text{Abs}\Big[-\frac{c\,e}{16}+\frac{d\,f}{16}\Big]^2,\ 2\,\text{Abs}\Big[-\frac{1}{8}\,i\,c\,e-\frac{i\,d\,f}{8}\Big]^2,$$
$$4\,\text{Abs}\Big[-\frac{c\,e}{16}+\frac{d\,f}{16}\Big]^2,\ \frac{1}{16}\,\text{Abs}[c\,f]^2,\ \frac{1}{16}\,\text{Abs}[c\,f]^2,\ \frac{3}{32}\,\text{Abs}[c\,f]^2,\ 2\,\text{Abs}\Big[-\frac{1}{8}\,i\,c\,e-\frac{i\,d\,f}{8}\Big]^2,$$
$$2\,\text{Abs}\Big[-\frac{1}{8}\,i\,c\,e-\frac{i\,d\,f}{8}\Big]^2,\ \text{Abs}\Big[-\frac{c\,e}{4}+\frac{d\,f}{4}\Big]^2,\ 2\,\text{Abs}\Big[\frac{i\,c\,e}{8}+\frac{i\,d\,f}{8}\Big]^2,\ \text{Abs}\Big[-\frac{c\,e}{4}+\frac{d\,f}{4}\Big]^2,\ 2\,\text{Abs}\Big[\frac{i\,c\,e}{8}+\frac{i\,d\,f}{8}\Big]^2,$$
$$\frac{1}{4}\,\text{Abs}[c\,f]^2,\ 4\,\text{Abs}\Big[\frac{c\,e}{16}-\frac{d\,f}{16}\Big]^2,\ 4\,\text{Abs}\Big[\frac{c\,e}{16}-\frac{d\,f}{16}\Big]^2,\ 2\,\text{Abs}\Big[-\frac{1}{8}\,i\,c\,e-\frac{i\,d\,f}{8}\Big]^2,\ 4\,\text{Abs}\Big[-\frac{c\,e}{16}+\frac{d\,f}{16}\Big]^2,$$
$$2\,\text{Abs}\Big[-\frac{1}{8}\,i\,c\,e-\frac{i\,d\,f}{8}\Big]^2,\ 4\,\text{Abs}\Big[-\frac{c\,e}{16}+\frac{d\,f}{16}\Big]^2,\ \frac{1}{16}\,\text{Abs}[c\,f]^2,\ \frac{1}{16}\,\text{Abs}[c\,f]^2,\ \frac{1}{16}\,\text{Abs}[c\,f]^2,\ \frac{3}{32}\,\text{Abs}[c\,f]^2\Big\}$$

Figure A.5: $\left|\widetilde{\Phi^-}\right\rangle|\widetilde{\gamma_1}\rangle$: Probabilities of various outcomes

obtaining these corresponding outcomes for $\left|\widetilde{\Phi^+}\right\rangle|\widetilde{\gamma_1}\rangle$ and $\left|\widetilde{\Phi^-}\right\rangle|\widetilde{\gamma_1}\rangle$ respectively.

From figure A.4, it is clear that some of the coefficients can be put to 0 by satisfying either $de = cf$ or $de = -cf$. Making these coefficients vanish removes the corresponding terms (in figure A.3) in the expansion of the state $\left|\widetilde{\Phi^+}\right\rangle|\widetilde{\gamma_1}\rangle$. However, the corresponding terms in $\left|\widetilde{\Phi^-}\right\rangle|\widetilde{\gamma_1}\rangle$ do not vanish and still remain. Thus, we have achieved partial unambiguous discrimination of the states $\left|\widetilde{\Phi^\pm}\right\rangle|\widetilde{\gamma_1}\rangle$. Likewise, certain terms in $\left|\widetilde{\Phi^-}\right\rangle|\widetilde{\gamma_1}\rangle$ can be set to zero using the conditions $ce = df$ or $ce = -df$, without removing the terms in $\left|\widetilde{\Phi^+}\right\rangle|\widetilde{\gamma_1}\rangle$. These would also lead to some partial discrimination of the two states.

In this particular setup, all the above four constraints are equivalent. So, without loss of gener-

ality, we will impose $ce = df$. The zeroes in the figure A.6 denote the absence of terms in the state

$$\left\{\frac{3}{32}\text{Abs[d e]}^2,\ \frac{1}{16}\text{Abs[d e]}^2,\ \frac{3}{32}\text{Abs[d e]}^2,\ \frac{1}{16}\text{Abs[d e]}^2,\ \frac{1}{16}\text{Abs[d e]}^2,\ \frac{3}{32}\text{Abs[d e]}^2,\ \frac{1}{4}\text{Abs[d e]}^2,\right.$$
$$\frac{1}{16}\text{Abs[d e]}^2,\ \frac{1}{16}\text{Abs[d e]}^2,\ \frac{1}{16}\text{Abs[d e]}^2,\ \frac{3}{32}\text{Abs[d e]}^2,\ 0,\ 0,\ \frac{1}{8}\text{Abs[d f]}^2,\ 0,\ \frac{1}{8}\text{Abs[d f]}^2,\ 0,$$
$$\frac{3}{32}\text{Abs[c f]}^2,\ 0,\ 0,\ \frac{1}{8}\text{Abs[d f]}^2,\ 0,\ \frac{1}{8}\text{Abs[d f]}^2,\ 0,\ \frac{1}{16}\text{Abs[c f]}^2,\ \frac{3}{32}\text{Abs[c f]}^2,\ \frac{1}{8}\text{Abs[d f]}^2,$$
$$\frac{1}{8}\text{Abs[d f]}^2,\ 0,\ \frac{1}{8}\text{Abs[d f]}^2,\ 0,\ \frac{1}{8}\text{Abs[d f]}^2,\ 0,\ 0,\ \frac{1}{8}\text{Abs[d f]}^2,\ 0,\ \frac{1}{8}\text{Abs[d f]}^2,\ 0,\ \frac{1}{16}\text{Abs[c f]}^2,$$
$$\frac{1}{16}\text{Abs[c f]}^2,\ \frac{3}{32}\text{Abs[c f]}^2,\ \frac{1}{8}\text{Abs[d f]}^2,\ \frac{1}{8}\text{Abs[d f]}^2,\ 0,\ \frac{1}{8}\text{Abs[d f]}^2,\ 0,\ \frac{1}{8}\text{Abs[d f]}^2,\ \frac{1}{4}\text{Abs[c f]}^2,$$
$$\left.0,\ 0,\ \frac{1}{8}\text{Abs[d f]}^2,\ 0,\ \frac{1}{8}\text{Abs[d f]}^2,\ 0,\ \frac{1}{16}\text{Abs[c f]}^2,\ \frac{1}{16}\text{Abs[c f]}^2,\ \frac{1}{16}\text{Abs[c f]}^2,\ \frac{3}{32}\text{Abs[c f]}^2\right\}$$

Figure A.6: $\left|\widetilde{\Phi^-}\right\rangle|\widetilde{\gamma_1}\rangle$: Probabilities after imposing $ce = df$

$\left|\widetilde{\Phi^-}\right\rangle|\widetilde{\gamma_1}\rangle$. In order to calculate the success probability of discrimination, one simply has to calculate the probability of obtaining these relevant outcomes for the state $\left|\widetilde{\Phi^+}\right\rangle|\widetilde{\gamma_1}\rangle$. That is, we must add the numbers in figure A.4 for $\left|\widetilde{\Phi^+}\right\rangle|\widetilde{\gamma_1}\rangle$ that are present precisely in the positions where $\left|\widetilde{\Phi^-}\right\rangle|\widetilde{\gamma_1}\rangle$ has a 0. The code below achieves this, by first using the Position command to make a list of all the locations where normlist2 has a zero. Then, the quantity dd is constructed by just adding the relevant terms needed from normlist1.

```
In[1]:=
i=1;While[i<=Length[normlist1],{normlist1[[i]] = normlist1[[i]]/.c e
    -> d f;i++}]
i=1;While[i<=Length[normlist2],{normlist2[[i]] = normlist2[[i]]/.c e
    -> d f;i++}]
cc=Position[normlist2,0] ;
i=1;dd=0;
While[i<= Length[cc], {dd = dd +normlist1[[cc[[i]][[1]]]];i++ }]
FullSimplify[dd,{Abs[c]^2+Abs[d]^2 == 1,Abs[f]^2+Abs[e]^2 == 1}]

Out[1]= 1/2 Abs [d e + c f]^2
```

Upon simplifying the final result subject to the normalization conditions, we get

$$S = \frac{1}{2}|de + cf|^2 \tag{A.3}$$

This was precisely the result quoted in (4.13). Had we used any of the other constraints, we would have gotten the results

$$\begin{aligned}(ce \to -df) &\implies S = \frac{1}{2}|de - cf|^2\\ (de \to cf) &\implies S = \frac{1}{2}|ce + df|^2\\ (de \to -cf) &\implies S = \frac{1}{2}|ce - df|^2\end{aligned} \tag{A.4}$$

Clearly using any of the four constraints would give us the same maximum probability of discrimination, 12.5%.

A.2 GHZ states

In this section, I will describe the two types of codes. The first code discusses GHZ state discrimination using ancillary entanglement in a **particular** setup, and the second will discuss bounds on the success probability of discrimination for **general** polarization-preserving setups. The codes for the former were used to obtain the results in (5.32) and (5.35), and the latter were used to derive the table 5.1.

This approach outlined below can be adapted and used to calculate success probabilities of discrimination between any set of states, through a specified setup. To begin with, the unitary corresponding to the setup must be defined. Instead of typing out the whole matrix, one can define a function that outputs a beam splitter matrix of the required dimension, as shown below.

```
setupdimension = 6; beg = IdentityMatrix[setupdimension];
beamsplitter[a_, b_,theta_] := { beg1 = beg;
  beg1[[a, a]] =  Sin[theta]; beg1[[b, b]] = Sin[theta];
  beg1[[a, b]] = I*Cos[theta];   beg1[[b, a]] =I*Cos[theta];
  beg1}
```

This function is useful to create unitaries corresponding to setups containing multiple beam splitters. The function Wholeunitary defined below takes in a list of modes to be connected by the beam splitters and generates the corresponding unitary by matrix multiplication.

```
Wholeunitary[locations_, numberofbs_] := { A = beg;
  For[i = 1, i <= numberofbs, i++, A = A . Flatten[beamsplitter[
   locations[[i]][[1]], locations[[i]][[2]],locations[[i]][[3]]],
   1]]; A}
bsarray ={{1,4,Pi/4}, {2,5, Pi/4}, {3,6,Pi/4}};
U = Flatten[Wholeunitary[bsarray, Length[bsarray]],1];
(* bsarray1 ={{1,3,\[Theta]1}, {2,5, \[Theta]2}, {4,6, \[Theta]3}}; U
    = Flatten[Wholeunitary[bsarray1, Length[bsarray1]],1]; *)
```

The setups shown in figure 5.7 and 5.10 are correspond to bsarray and bsarray1. The input and output operators can be related in the same way as discussed in the previous section. Let us first discuss the result of (5.32), where the ancillary $|\gamma_1\rangle$ was used to distinguish between the states $|\Psi^{\pm}\rangle$. The final states after evolving through the setup are

```
ghz1plus = ExpandAll[1/2 (H1 H2 H3 + V1 V2 V3) (H4 H5 H6 + V4 V5 V6)
   ];
ghz1minus = ExpandAll[1/2 (H1 H2 H3 - V1 V2 V3)(H4 H5 H6 + V4 V5 V6)
   ];
```

The procedure to calculate success probabilities is similar to A.1, with a simpler code, as there are no parameters to optimize. If we want to quantify how useful the ancillary $|\gamma_1\rangle$ is to distinguish between the states $|\Psi^{\pm}\rangle$, we must identify those terms that are uniquely present in either ghz1plus or ghz1minus. This is done using a combination of the Complement and the Intersection command, applied to both expressions. Once this is done, we simply calculate the absolute squared sum of the relevant coefficients.

```
In[]:=
uniqueterms =  Complement[Union[ghz1plus, ghz1minus], Intersection[
   ghz1plus, ghz1minus]];
```

```
v = List@@Expand[Collect[uniqueterms, vars, 1 &]];
sum = Which[Length[v]==0,0,Length[v]!=0,Abs[Coefficient[uniqueterms
    ,#]&/@v]^2];
Simplify[Total[sum]]

Out[] = 1
```

To check if $|\gamma_1\rangle$ helps distinguish between the other sets of GHZ states, the same block above can be used. In those cases, the v list turns out to be empty. Therefore, the total success probability of discrimination is thus $\frac{1}{8}[0+0+0+1] \equiv 12.5\%$.

We now discuss the result in (5.35). Here, we used the ancillary $|\gamma_2\rangle$, and studied the evolution of the states $\left|\Psi_2^{\pm}\right\rangle|\gamma_2\rangle$, $\left|\Psi_3^{\pm}\right\rangle|\gamma_2\rangle$, and $\left|\Psi_4^{\pm}\right\rangle|\gamma_2\rangle$ through the setup 5.10. A small caveat at this stage: if we want to confirm if the setup is unitary, the usual UnitaryMatrixQ command does not work. We must impose constraints on the θ parameters, like shown below:

```
In[]:= Simplify[U . ConjugateTranspose[U], {Element[\[Theta]1,Reals],
    Element[\[Theta]2,Reals],Element[\[Theta]3,Reals]}] ==
    IdentityMatrix[6]

Out[] = True
```

The final states can be expanded as:

```
ghz2plus = ExpandAll[1/2 (H1 H2 V3 + V1 V2 H3) (H4 H5 V6 + V4 V5 H6)
    ];
ghz2minus = ExpandAll[1/2 (H1 H2 V3 - V1 V2 H3)(H4 H5 V6 + V4 V5 H6)
    ];

ghz3plus = ExpandAll[1/2 (H1 V2 H3 + V1 H2 V3) (H4 H5 V6 + V4 V5 H6)
    ];
ghz3minus = ExpandAll[1/2 (H1 V2 H3 - V1 H2 V3)(H4 H5 V6 + V4 V5 H6)
    ];

ghz4plus = ExpandAll[1/2 (V1 H2 H3 + H1 V2 V3) (H4 H5 V6 + V4 V5 H6)
    ];
ghz4minus = ExpandAll[1/2 (V1 H2 H3 - H1 V2 V3)(H4 H5 V6 + V4 V5 H6)
    ];
```

We calculate the success probability using exactly the same block of code discussed earlier. It turns out that the sum calculated for $\left|\Psi_3^{\pm}\right\rangle|\gamma_2\rangle$ is zero, but both $\left|\Psi_2^{\pm}\right\rangle|\gamma_2\rangle$ and $\left|\Psi_4^{\pm}\right\rangle|\gamma_2\rangle$ give the same sum of $\frac{1}{8}|\sin(2\theta_1)\sin(2\theta_2)\sin(2\theta_3)|^2$ (taking into account equiprobable initial GHZ states). Therefore, the total probability of discrimination is

$$P_s = 2 \times \frac{1}{8}|\sin(2\theta_1)\sin(2\theta_2)\sin(2\theta_3)|^2 = \frac{1}{4}|\sin(2\theta_1)\sin(2\theta_2)\sin(2\theta_3)|^2 \leq \frac{1}{4} \tag{A.5}$$

We next discuss how to place upper bounds on the success probability of discrimination without considering a specific setup. Let us say we want to distinguish between two states $|\Psi^+\rangle$, and $|\Psi^-\rangle$, using an ancillary $|\beta\rangle$. The idea, as discussed in the main text, is to classify terms in the total state $|\Psi^{\pm}\rangle|\beta\rangle$

based on the number of $h^\dagger$ and $v^\dagger$ operators they have, and then assume that two equivalent terms on either side of the $\pm$ sign combine to produce two mutually exclusive sets of outcomes for both states.

In our analysis, we use two types of ancillaries: Bell states ($|\Psi\rangle$ and $|\Phi\rangle$) and the GHZ states ($|\gamma_1\rangle$ and $|\gamma_i\rangle$). We first define them as sets just containing their bracket representations i.e. the number of $h^\dagger$ and $v^\dagger$ operators.

```
gamma1 = {{3, 0}, {0, 3}}; gammai = {{2, 1}, {1, 2}};
phiplus = {{2, 0}, {0, 2}}; psiplus = {{1, 1}, {1, 1}};
```

In order to combine different terms, we define the functions join and fullmultiply.

```
join[A_, B_] := {A[[1]] + B[[1]], A[[2]] + B[[2]]};
fullmultiply[A_, B_] := {abcd = List[];
  For[i = 1, i <= Length[A], i++, For[j = 1, j <= Length[B], j++,
    AppendTo[abcd, join[A[[i]], B[[j]]]]]; Sequence @@ abcd}
```

Join simply simulates multiplying two brackets, by creating a third bracket with element-wise sum of the two initial brackets. The fullmultiply function simulates multiplying two terms, each having multiple brackets, by constructing a set with all possible bracket multiplications.

Let us take the example of distinguishing between the GHZ states, using an ancillary state $|\beta\rangle = |\gamma_i\rangle |\Phi\rangle |\Phi\rangle$ (product state of a GHZ state of the type $[2,1] \pm [1,2]$ with two Bell states of type $[2,0] \pm [0,2]$). We first define and expand out this ancillary.

```
In[]:=
A2 ={gammai,phiplus,phiplus}; n = Length[A2];
While[Length[A2] > 1, c = fullmultiply[A2[[1]], A2[[2]]];
 A2 = Drop[A2, 1]; A2[[1]] = c;]
A1 = Flatten[A2, 1]

Out[]= {{6,1},{4,3},{4,3},{2,5},{5,2},{3,4},{3,4},{1,6}}
```

Next, we locate terms which are common in $\left|\Psi_1^+\right\rangle |\beta\rangle$ and $\left|\Psi_1^-\right\rangle |\beta\rangle$. To do this, we calculate the Intersection between a [3,0] term multiplied with $|\beta\rangle$ and a [0,3] term multiplied with $|\beta\rangle$. A similar procedure is carried out for $\left|\Psi_i^+\right\rangle |\beta\rangle$ and $\left|\Psi_i^-\right\rangle |\beta\rangle$.

```
In[]:=
XX = Intersection[fullmultiply[{{0, 3}}, A1], fullmultiply[{{3, 0}},
   A1]]
YY = Intersection[fullmultiply[{{2, 1}}, A1], fullmultiply[{{1, 2}},
   A1]]

Out[]=
{{4,6},{5,5},{6,4}}
{{3,7},{4,6},{5,5},{6,4},{7,3}}
```

Once we have these lists, we simply must count how many times each of the elements of these lists are present in the products $[3,0]|\beta\rangle$ and $[0,3]|\beta\rangle$, and $[2,1]|\beta\rangle$ and $[1,2]|\beta\rangle$. If for example, the element [4,6] is present only once in $[3,0]|\beta\rangle$ and $[0,3]|\beta\rangle$, then assuming perfect cancellation (for an upper bound on the success probability), the [4,6] terms on both sides of the $\pm$ sign must combine to give two completely different terms for both states, leading to a contribution of $(4/2^{n+1})$ to the success

probability (excluding the 1/8 overall factor). Here, n is the number of ancillary states; the 2^{n+1} factor in the denominator comes as a result of their normalization.

Similarily, we can calculate the success probability of distinguishing between the $\left|\Psi_i^{\pm}\right\rangle$ states using $|\beta\rangle$. The complete code is given below:

```
In[]:=
aa = Which [Length[XX] > 1,
   Total[Table[(2/
        2^(n + 1)) *(Count[fullmultiply[{{0, 3}}, A1], XX[[b]]] +
        Count[fullmultiply[{{3, 0}}, A1], XX[[b]]]), {b, Length[XX
   ]}]],
   Length[XX] ==
    1, (2/2^(n + 1)) *(Count[fullmultiply[{{0, 3}}, A1], XX[[1]]] +
      Count[fullmultiply[{{3, 0}}, A1], XX[[1]]]), Length[XX] == 0,
   0];

bb = Which [Length[YY] > 1,
   Total[Table[(6/
        2^(n + 1)) *(Count[fullmultiply[{{2, 1}}, A1], YY[[a]]] +
        Count[fullmultiply[{{1, 2}}, A1], YY[[a]]]), {a, Length[YY
   ]}]],
   Length[YY] ==
    1, (6/2^(n + 1)) *(Count[fullmultiply[{{2, 1}}, A1], YY[[1]]] +
      Count[fullmultiply[{{1, 2}}, A1], YY[[1]]]), Length[YY] == 0,
   0];
success = 12.5*(aa + bb)

Out[]= 78.125
```

As reported in the table, the upper bound on the success probability using the ancillary state $|\gamma_i\rangle |\Phi\rangle |\Phi\rangle$ turns out to be 78.125%.